BIOENGINEERING AND CHARACTERIZATION OF AN ONCOLYTIC VACCINIA VIRUS FOR TUMOR LOCALIZED LENTIVIRUS PRODUCTION

JAAHNAVI DAVE

Thesis submitted to the University of Ottawa in partial fulfillment of the requirements for the degree of Doctor of Philosophy in Microbiology and Immunology

Department of Biochemistry, Microbiology and Immunology
Faculty of Medicine
University of Ottawa

Abstract

Oncolytic viruses (OVs) are multi-mechanistic, tumor-selective therapeutics that lyse cancer cells while stimulating anti-tumor immunity. However, one limitation of OVs as monotherapies is their inability to infect and eliminate every tumor cell. Since infected tumor cells ultimately undergo lysis, arming OVs with transgenes that promote bystander effects by targeting uninfected cells within the tumor microenvironment, including other tumor cells or immune cells, can enhance therapeutic efficacy. One extensively engineered OV platform is vaccinia virus (VV), owing to its large transgene capacity and favorable safety profile. In parallel, retrovirus-derived virus-like-particles (VLPs) and lentiviral vectors have emerged as versatile therapeutic delivery systems. VLPs transiently deliver proteins, whereas lentiviral vectors mediate stable gene delivery with clinical applications including immune cell engineering, such as CAR-T cell generation.

My thesis focuses on the development of retrovirus-derived therapeutic delivery platforms that could be integrated with oncolytic VV to enable localized transient or stable manipulation within tumors. I optimized and established a VLP platform for transient protein delivery, with an emphasis on genome editing of oncogenes. Next, I engineered VV to encode the components required for production of a self-inactivating lentivirus vector, creating a “virus within a virus”. I inserted three transgenes: the lentivirus packaging component (Gag-Pol), the vesicular stomatitis virus glycoprotein pseudotyping envelope (VSV-G) and a lentiviral vector genome containing a gene-of-interest. Infection of producer cells with engineered VV enabled the production of transduction-competent lentivirus particles, thereby establishing a proof-of-concept for this hybrid system.

The findings from this thesis establish retrovirus-derived therapeutic delivery platforms, including CRISPR-Cas9 loaded VLPs and a VV-lentiviral hybrid system, providing a versatile strategy for next-generation viral cancer therapies, with potential for direct tumor-targeting or localized *in vivo* immune cell engineering, including the generation and reprogramming of therapeutic immune cells, such as CAR-T cells, within the tumor microenvironment.

Table of Contents

Acknowledgements

"Surround yourself with good people because your life will progress in the general direction of people around you"— When I first came across this quote by Warren Buffett, it immediately reminded me of the cordial and amicable atmosphere fostered by the Cancer Research Program at the Ottawa Hospital Research Institute (OHRI). My time here was nothing short of phenomenal, and a huge shout-out goes to all of my lab members — past and present.

It is a tremendous privilege to pursue a Doctorate of Philosophy degree, and first and foremost, I extend my deepest gratitude to my supervisors- Dr. John Bell and Dr. Carolina Ilkow- for allowing me to pursue this PhD in their research labs. Dr. Bell, I cannot thank you enough for inviting me to interview with your impressive research group and taking a chance on me. The academic world is never easy, but you saw my potential and encouraged me to develop scientific independence. I am very appreciative that you were truly always available to meet with me despite your intensive and demanding schedule, and it has been an incredible honour to pursue my graduate studies under your supervision. Dr. Ilkow- thank you for always allowing me to poke my head into your office to discuss exciting pieces of data, failed experiments and, of course, many great outfits! I will forever remember my interview with you, which began with a scientific discussion, and ended with our shared love of style- something I genuinely appreciate sharing with you. I also wanted to thank you both for allowing our group to eat some tasty sweet treats during our weekly lab meetings… my teeth may have suffered as a consequence but it was totally worth it! 😉

I would also like to thank my thesis advisory committee members- Dr. Jean-Simon Diallo, Dr. Harry Atkins and Dr. Douglas Gray- for keeping me in check and on track to completing my

doctoral studies in a timely manner, and for challenging me with some thought-provoking questions throughout my studies.

During my time at OHRI, I met many wonderful individuals who became my support system, and brought camaraderie both in lab and out. Emily Brown- you were the first friend I ever made here, and you became a pillar of support throughout my PhD journey. I always looked forward to our parking lot picnic lunches and Subway sandwich runs. Sarah Tucker- I will always enjoy cracking jokes with you, teasing one another with crazy nicknames, matching outfits and our many conversations about science and life. Dr. Abera Surendran- thank you for fueling my thesis writing journey with the most delicious tubs of your authentic home-made ice-cream, countless coffee shop visits and movie and bookstore dates. Dr. Taylor Jamieson-Datzkiw- I will always appreciate our nature walks, countless early morning TC conversations and catch-up phone call sessions (also shout-out to Dr. David Datzkiw and Sisi!). You girls shaped my time in the lab when I first arrived, and as you moved on to pursue some amazing new chapters, I was fortunate to meet many more amazing lab members. My dearest friend Priya Bharadwa- thank you for baking me the most delicious strawberry flavoured birthday cakes and for taking our much needed walks around campus when we needed breaks from the benchside, and for your calming presence. I am so glad to share a love for science with you! To my sweet friend Samantha Jang- I will always cherish taking our mirror selfies and of course, sneaking snacks away from lab meeting to enjoy munching on them at our desks! Monire Jamalkhah- you are an absolutely phenomenal PhD candidate and friend, and I cannot wait to see the amazing contributions that you make to research (drive that CAR! 😉). To my other sweet friend Tamara Synek- (aka baby Monire), thanks for always sending me all the kindest and most supportive messages throughout my graduate studies! Rida

Gill- your amazing baking expertise and our shared crazy and joy-filled memories will always make me smile, and thank you for always checking in on me! Khushi Rathod- it was so nice to share culture and love for science with you! Sydney Vallati- thanks for teaching me how to skate, and I look forward to seeing what you accomplish with the TIL project! Dr. Mathieu Crupi- your friendship was instrumental in helping me complete my PhD. You never once failed to see my potential. Your constant source of encouragement pushed me to excel to the best of my abilities. Thank you for always reading over my work, and providing me with critical and thoughtful feedback, and for always being there to support me. Dr. Zaid Taha- thank you for answering my late-night panicked calls, laughing at whale jokes with me and appreciating my eclectic fashion sense. I also want to thank you both for encouraging my earring making hobby by providing me with lovely beads. Dr. Stephen Boulton – it was such a pleasure getting to know you and working on the neutrophil project along your side. I truly wanted to learn flow cytometry and how to handle mice, and you gave me those opportunities through this project. I also hope you appreciated my countless sassy remarks! Dr. Joanna Poutu Paumier- or should I say “Crazy JoJo”, your energy always lit up the room, and I am forever appreciative of your compliments to my outfits. Dr. Duncan Mackenzie- you are quite the gentle giant with a fantastic sense of humor, and I am glad you joined our lab! Dr. Peivand Sadat Mousavi- thanks for being my lab bench buddy (and slowly taking over my space!). Julia Petryk- our “mouse whisperer”- thanks for being the absolutely coolest lab manager out there, picking out delicious lab meeting treats, and for helping me furnish my apartment with awesome vintage finds! To the lab boys, Siddharth Singh and Timothy Lee- I am really glad to have met you and will always remember sneaking up on you for good laugh, especially when you would least expect it. Dylan Thomas- it was great to have a fellow fashion loving Montrealer in grad school! Jack Whelan- it has been a pleasure to work along your side

over the past few years! Bradley Austin and Kemal Alper Onsu- thank you for your smooth operations and keeping the lab running. Ricardo Marius- thank you for your wisdom and calm presence during stressful times- you truly kept me grounded. Thanks for always supporting me (figuratively… and quite literally when we skated on the Rideau canal)! XiaoHong (Annie) He- your kind soul and bright morning energy made early tissue culture days something to look forward to, and I am so glad our cells were incubator buddies! Olivia Makinson- thanks for all the fun car rides and for visiting sunflowers with me! Carole Dore – thank you for being such an organized floor-wide lab manager, always available to address our concerns. Dr. Rebecca Auer- it has been an incredible honour to be a trainee at the OHRI under your leadership. During your time as director of the cancer center, you never missed a chance to attend and engage in trainee WIPs, and your constant encouragement and support of the Cancer Research Program Trainee Committee is what allowed us to host many great activities, including the Café Scientifique and ice skating while enjoying Beavertails on the Rideau canal. I would also like to thank the OHRI Research Day organizing committee- for 6 years I was a part of the wonderful team that got together and organized this annual event showcasing the talented research being conducted at the OHRI. I also enjoyed my time as a member on the cancer research program trainee committee. A special thanks to BioCanRx for funding countless conference travel awards, and to FRQS for funding my doctoral studies.

To the Bell and Ilkow Lab alumni- you are not forgotten! Dr. Ragunath Singaravelu- you are a phenomenal scientist and thanks for being my (slightly chaotic 😉) mentor when I first joined the lab. Dr. Nikolas Tim Martin- you taught me many of the molecular biology techniques which became the foundation for my thesis work. Thank you for always looking over my cloning designs

over coffee chats. Dr. Serge Neault- thanks for checking in on me during the PhD process! Neil Moodie (aka Big homie)- thanks for sharing both the love and frustration of picking plaques with me! To the students I had the wonderful opportunity of mentoring: Wagma Safi, Claudia Santos, Jamie Asselin and Nils Nordstrom- it was a pleasure to have you in the lab and watch you grow as scientists. Wagma- it was a great having you continue grad studies in the lab! Patty- I am so grateful to have met you and Dave during my time as a student at the OHRI. Your loving nature and heartfelt messages of encouragement for my all TAC meetings and evaluations always made my days brighter. Your weekly drives home meant so much to me! Dr. Nooshin Movahed – a very special thanks for your guidance in electron microscopy and helping me generate some of the most exciting data in my thesis!

To my absolutely amazing and supportive friends who cheered me on every single step of the way, Hanna Swail, Gurleen Litt, Kelsey Vickers, Vima Priyank Patel, Rachelle Hynes, Meera Kanagalingham, Irene Kaloyannis, Sandra Zaki, Foram Vyas, Maya Rajan - I am SO fortunate to have you girls by my side. You were always a phone call away whether I needed to vent or share my exciting data with you. Your interest in my work, scientifically stimulating questions, fun-filled trips and constant source of support mean the world to me. We have experienced some of life's biggest milestones together, and as I wrap up this degree, I look forward to seeing what life has in store for us.

Dr. Denis-Claude Roy- you allowed me to pursue a summer internship in your research group, and this was my first exposure to the world of cancer immunotherapy. Thank you for that opportunity, and for your continuous support throughout my graduate journey.

Lastly, a very special thanks goes to my family. To my brother Varun, you provided a pillar of support, interesting movie and book recommendations, and stimulated my intellectual growth. Thanks for always approving my conference poster colors and their matching outfits, and for always answering my calls when I needed. Mama- you always encouraged me to pursue science with style, made countless fashionable outfits and matching accessories that I proudly wore to the lab. You encouraged a sense of creativity and individuality, which I fostered through fashion. You always provided me with your delicious home-cooked meals whenever I needed. Deddy (Dr. Dave) - thank you for the countless conversations about my data and sharing the excitement of novel results. Thank you for truly always answering my phone calls, whether they were calls of stress or calls of excitement. As my PhD journey approaches an end, I look forward to joining you in carrying the title of Dr. Dave.

List of figures

Chapter 1

Chapter 2

Chapter 3

List of tables

List of abbreviations

AAV: Adeno-associated virus
ADA: Adenosine deaminase
APCs: Antigen presenting cells
BCMA: B-cell maturation antigen
BFP: Blue fluorescent protein
CAR: Chimeric antigen receptor
Cas9: CRISPR-associated protein 9
CD: Cytosine deaminase
CEV: Cell-associated enveloped virus
CHO: Chinese hamster ovary
CMV: Cytomegalovirus
CRISPR: Clustered regularly interspaced short palindromic repeats
crRNA: CRISPR RNA
CTLA-4: Cytotoxic T-lymphocyte associated protein 4
DAMP: Danger associated molecular pattern
dCas9: deactivated Cas9
DMEM: Dulbecco's Modified Eagles medium
E6-AP: E6-associated protein
EEV: Extracellular enveloped virus
eGFP: enhanced Green fluorescent protein
FBS: Fetal bovine serum
FPV: Fowlpox virus
5-FC: 5-fluorocytosine
5-FU: 5-fluorourcail
GOI: Gene-of-interest
GM-CSF: Granulocyte macrophage colony stimulating factor
HDR: Homology directed repair
HERV: Human endogenous retrovirus
HIV-1: Human Immunodeficiency virus-1
HPV: Human papilloma virus
HSV: Herpes simplex virus
IBT: Immune checkpoint blockade therapy
IEV: Intracellular enveloped virus
IFN: Interferon
IL-10: Interleukin-10
IMV: Intracellular mature virus
Kb: Kilobase
LV: Lentivirus
mCherry: monomeric Cherry
MFI: Mean fluorescence intensity
MHC: Major histocompatibility complex
MLV: Murine leukemia virus
MPA: Mycophenolic acid

NCS: Newborn calf serum
NHEJ: Non-homologous end joining
NK: Natural killer cells
NLuc: NanoLuciferase
ORF: Open-reading frame
OV: Oncolytic virus
PAM: Protospacer adjacent motif
PAMP: Pathogen associated molecular pattern
PBS: Phosphate buffer saline
PCR: Polymerase chain reaction
PD-1: Programmed cell death protein 1
PD-L1: Programmed cell death protein ligand 1
PGK: Phosphoglycerate kinase
Rb: Retinoblastoma
REV: Reticuloendotheliosis virus
RFP: Red fluorescent protein
RNP: Ribonucleoprotein
RSV: Rous sarcoma virus
ScFv: single chain variable fragment
SFM: Serum free media
sgRNA: Single guide RNA
SCID: Severe combined immunodeficiency
TAAs: Tumor-associated antigen
TCR: T-cell receptor
TGF-β: Transforming growth factor beta
TK: Thymidine kinase
TME: Tumor microenvironment
tracrRNA: trans-activating CRISPR RNA
T-regs: Regulatory T-cells
VLPs: Virus-like-particles
VSV-G: Vesicular stomatitis virus glycoprotein
VV: Vaccinia virus
WR: Western Reserve

Thesis Preface

This thesis describes the work that I performed in the Bell and Ilkow labs as a PhD candidate. Chapter 1 provides a broad overview of cancer biology, oncolytic viruses and their application in cancer therapy, as well as the use of retroviral particles in a therapeutic context. Chapter 2 details the results based on development of a retroviral VLP platform for transient protein delivery, with an emphasis on CRISPR-Cas9-mediated oncogene targeting. Chapter 3 is focused on the bio-engineering and characterization of a novel oncolytic VV platform, designed to encode lentiviral vector components for stable gene delivery in target cells. Chapter 4 presents a general summary of the data and a discussion of potential therapeutic applications for the developed VLP and VV-lentivirus platforms. Lastly, Chapter 5 outlines the materials and methods used to conduct the studies featured in this thesis.

Chapter 1: Introduction

1. General introduction

1.1 Cancer and immune evasion strategies

On a global scale, cancer remains one of the leading causes of death, accounting for nearly 10 million deaths (reported in 2023)[1]. In Canada, cancer similarly represents a major public health challenge, placing substantial burden on both the healthcare system and the economy, with two out of five Canadians diagnosed in their lifetime, and one in four Canadians predicted to die as a consequence of the disease[2]. Cancer arises through the complex interplay of genetic mutations, environmental influences, and viral factors, resulting in the uncontrolled proliferation of malignant cells[3]. One of the key features of cancers is their ability to evade the host's immune system through a multi-faceted process known as immune-editing, which occurs in three distinct phases, known as the "three Es" model: (1) elimination, where the immune system detects and destroys precancerous and malignant cells, (2) equilibrium, where tumor cell proliferation is arrested but tumor cells are present, and editing and selection occurs and (3) escape, where tumors progressively grow and overcome immune responses[4,5]. This process allows tumors to evade immune surveillance and destruction, complicating therapeutic interventions, and contributing to suboptimal patient outcomes.

One primary mechanism of evasion is tumor-induced immune suppression, resulting in the formation of a "cold" tumor microenvironment (TME) **(Figure 1).** Tumor cells secrete cytokines such as interleukin-10 (IL-10), which blocks T-cell activation and fosters an anti-inflammatory state by inhibiting pro-inflammatory cytokine production from macrophages and dendritic cells, and transforming growth factor-beta (TGF-β), which restricts the activation and growth of T-cells

and natural killer (NK) cells[6]. Tumors also attract regulatory immune cells, including regulatory T-cells (T-regs), which are involved in preventing autoimmunity but in tumors suppress effector T-cell activity[6]. Myeloid derived suppressor cells (MDSCs) also inhibit T-cell activity by multiple mechanisms. For example, they express arginase which suppresses CD4+ and CD8+ cells by blocking uptake of arginine, an amino acid essential for T-cell activation[7]. Further, crosstalk among MDSCs and macrophages can promote polarization of macrophages towards their pro-tumor (M2) phenotype[8].

Another mechanism by which tumor cells evade immune detection is by exploitation of checkpoint pathways. Immune checkpoint molecules normally function to regulate immune responses by transmitting inhibitory signals that prevent over-activation. However, tumors can co-opt these pathways to suppress anti-tumor immunity. For example, overexpression of programmed cell death protein 1 (PD-1) on immune cells and one of its cognate ligands (PD-L1) on tumors inhibits T-cell activation and proliferation. In addition to the PD-1/PD-L1 axis, other immune checkpoints such as cytotoxic T-lymphocyte-associated antigen-4 (CTLA-4), expressed on activated T-cells, play a critical role in regulating T-cell responses. T-cell activation depends on three distinct signals. Signal one is initiated through binding of the T-cell receptor (TCR) to an antigen presented by major histocompatibility complex (MHC) molecules on antigen presenting cells (APCs). A second signal, known as co-stimulation, is mediated by interaction of CD28 on T-cells with its ligands CD80 and CD86 on APCs. Lastly, signal three is provided through cytokine-driven signaling[9]. CTLA-4 competes with CD28 for binding to CD80 and CD86, but does so with higher affinity, thereby transmitting inhibitory signals that attenuate T-cell activation[10]. Although the

coordination of CTLA-4 and CD28 signaling is essential for maintaining immune homeostasis, this balance is frequently skewed towards immunosuppression in cancer.

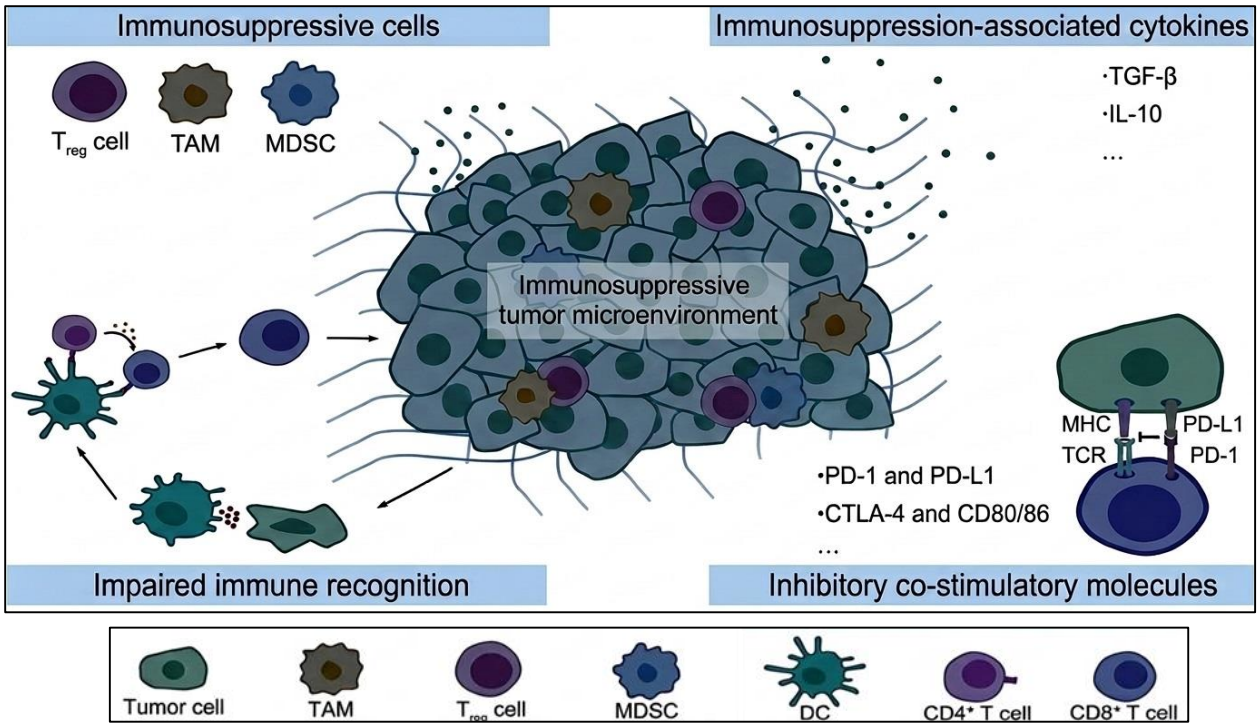

Figure 1: The immunosuppressive tumor microenvironment. The TME is dominated by immunosuppressive cell populations, including T-regs and MDSCs. Tumors secrete cytokines such as IL-10 and TGF-β, promoting M2-like tumor-associated macrophages (TAMs). Tumor cells can also co-opt immune checkpoint pathways such as the PD-1/PD-L1 axis and CTLA-4/CD80/CD86 binding to inhibit T-cell activation. Collectively, these features create an environment resulting in impaired immune recognition, that supports tumor cell growth and cancer progression. Figure created using FigureLabs, adapted from YanYan et al[11].

In their seminal paper, Hanahan and Weinberg enumerated a set of hallmarks unifying all cancers, acquired as the tumor cells undergo a state of normalcy to a state of neoplastic growth[12]. These hallmarks demonstrate the complexity of cancer and include: sustained proliferative signaling, evading growth suppressors, resisting cell death, enabling replicative immortality, inducing angiogenesis, activating invasion and metastasis, reprogramming cellular metabolism and avoiding immune destruction. An updated framework expands this model and includes four new hallmarks[12]: unlocking phenotypic plasticity, non-mutational epigenetic reprogramming, polymorphic microbiomes and cellular senescence.

Underlying these hallmark capabilities are genetic alterations that disrupt normal cellular regulatory mechanisms. Cancer susceptibility genes have been broadly divided into three categories: caretaker, gatekeeper and landscaper genes[13]. Caretaker genes maintain genomic integrity through DNA repair, and when mutated, lead to genomic instability. One such example is tumor suppressor p53, often dubbed "guardian of the genome", involved in maintaining cellular integrity by regulating the cell cycle, facilitating DNA repair and initiating apoptosis in response to genetic damage[14]. In fact, about half of all cancers result due to mutations in *p*53[15]. Gatekeeper genes, in contrast, directly regulate cell proliferation by restraining cell cycle progression, and when mutated, the cell cycle becomes disrupted, enabling cancerous cells to divide uncontrollably. An example of this is the retinoblastoma gene (*RB1*), a tumor suppressor which typically arrests the cell cycle in instances of cellular damage, but when mutated leads to development of tumors, as observed in the case of retinoblastoma, a malignant pediatric intraocular tumor[16]. Lastly, landscaper genes foster an environment conducive to the survival of tumor cells.

1.2 Oncogenic viruses

The interplay between tumor suppressors and oncogenes plays a key role in tumorigenesis, as it became discovered that cancer cells can disable their senescence or apoptosis-inducing circuitry to adapt to oncogenic signalling[17]. Since the early 20th century, it has been known that certain viruses are tumor causing agents. In 1911, Peyton Rous discovered that a virus (Rous sarcoma virus, RSV) could induce solid tumors in infected fowl, demonstrated by the transmission of sarcomas using cell-free filtrates of tumor extracts[18]. In the 1970s, studies performed by the labs of Harold Bishop and Mike Varmus demonstrated that the *src* gene of RSV (v-*src*) was a transduced allele of a cellular gene (c-*src*), acquired by recombination during the retroviral life cycle, leading to the discovery of retroviral oncogenes and their normal cellular counterparts (proto-oncogenes)[18]. By the 1980s, it became understood that several viruses are capable of causing tissue specific cancers[19]. For instance, certain types of human papillomaviruses (HPVs) were identified as the causative agents of cervical cancer as well as subsets of head and neck cancers[20]. HPV types are classified as either high-risk or low-risk based on their potential to induce malignant transformation[21]. Infections arising from high-risk types, particularly HPV 16 and HPV 18, are the main cause for cervical cancer.

HPVs are small, non-enveloped dsDNA viruses with an 8 kilobase (kb) genome encoding six early genes (E1, E2, E4, E5, E6 and E7) and two late structural genes (L1- the major capsid protein and L2- the minor capsid protein)[22]. In low-risk HPV types, the viral genome typically remains episomal. In contrast, high-risk HPV types integrate into the cellular genome of the host, and cancer formation is driven by the activity of viral oncoproteins E6 and E7. Under normal conditions, the E2 protein suppresses E6 and E7 activity by regulating the viral promoter region. However, integration of the HPV genome causes disruption of the E2 open reading frame (ORF),

resulting in loss of E2-mediated regulation[23]. Consequently, E6 and E7 become constitutively expressed in high-risk HPV-associated cancers, where they promote oncogenesis by inhibition of tumor suppressor pathways[24] (**Figure 2)**.

E6 associates with the cellular E3 ubiquitin ligase E6-associated protein (E6-AP), promoting the degradation of tumor suppressor p53. As a result, functions mediated by p53 are suppressed, including transcriptional activation of p21, a cyclin-dependent kinase inhibitor which plays a pivotal role in cell cycle control[25]. E7 sequesters Retinoblastoma (Rb), resulting in release of transcription factor E2F and promotion of cellular proliferation[24]. Loss of E6 activity would therefore be predicted to restore p53-mediated apoptosis, while inhibition of E7 has been associated with induction of senescence[26]. Further, oncogenic HPV E6 and E7 contribute not only to cervical cancer, but also to other anogenital and oropharyngeal cancers[27].

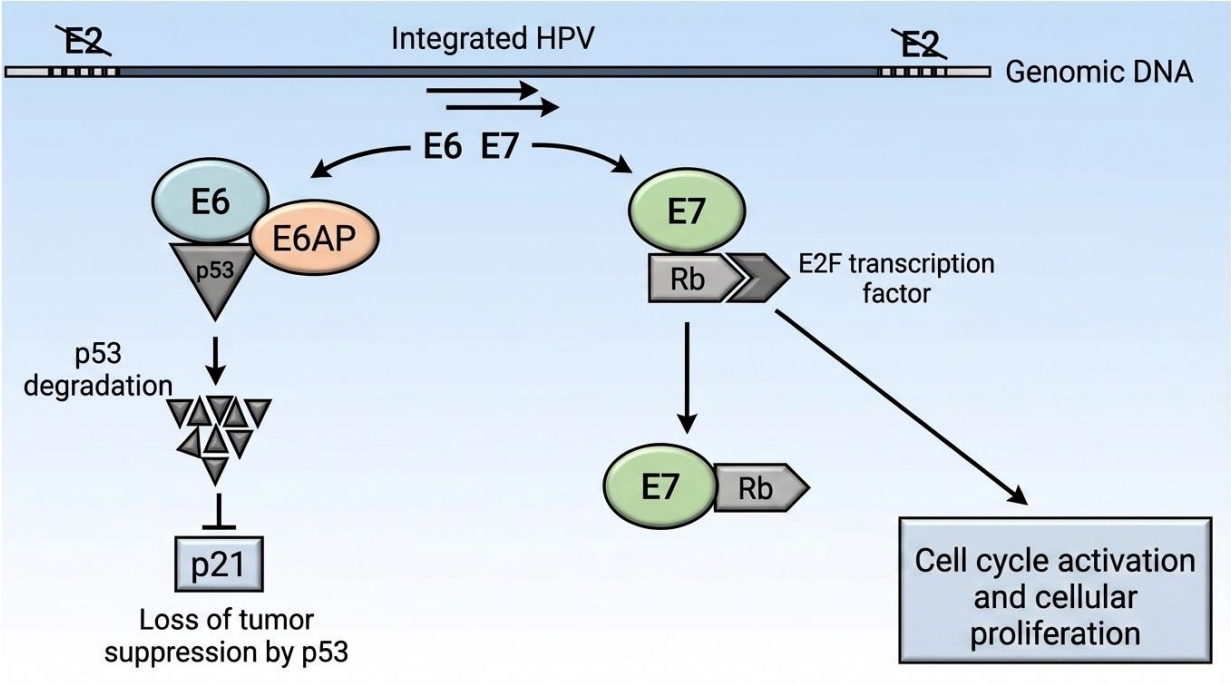

Figure 2: Mechanism of oncogenesis driven by high-risk HPV E6 and E7 oncogenes. Following integration of the HPV genome into the host genome, the E2 open reading frame is disrupted, resulting in loss of the regulation of E6 and E7. The E6 protein binds to E6-associated protein (E6-AP), an intracellular E3 ubiquitin ligase, promoting ubiquitination of p53 for proteasomal degradation. As a result, functions mediated by p53 are suppressed, including transcriptional activation of p21, a cyclin-dependent kinase inhibitor. The E7 protein sequesters tumor suppressor Rb, freeing transcription factor E2F, leading to cell cycle activation and cellular proliferation. Figure was created using FigureLabs. Adapted from Ruttkay-Nedecky et al[28].

1.3 Genome editing with CRISPR-Cas9

Genome editing enables the modification of genomic sequences at specific target sites to induce insertions, deletions or base substitutions, resulting in inactivation of target genes, acquisition of novel genetic traits or correction of pathogenic gene mutations[29]. The clustered regularly interspaced short palindromic repeat (CRISPR)-Cas9 system has emerged as a versatile and widely used genome editing technology. CRISPR-Cas9 evolved naturally in bacteria and archaea as an adaptive immune system that protects against phage infection. The system is composed of a CRISPR RNA (crRNA) which targets the specific DNA sequence, a trans-activating CRISPR RNA (tracrRNA) which serves as a scaffold for Cas9 binding, and CRISPR-associated (Cas) proteins with endonuclease activity[29]. For genome engineering applications, the crRNA and tracrRNA are fused together to create a single-guide RNA (sgRNA), which directs Cas9 to a target DNA sequence adjacent to a protospacer adjacent motif (PAM). Upon Cas9-mediated cleavage of a target DNA sequence, the target locus undergoes one of two major DNA damage repair pathways: non-homologous end joining (NHEJ) or homology directed repair (HDR) **(Figure 3).** NHEJ can be used for generating gene knock-outs, since insertions or deletions can lead to frameshift mutations or premature stop codons within the ORF of the target gene[30]. In contrast, HDR can generate precise modifications at a target locus in the presence of an exogenously introduced repair template.

The CRISPR-Cas9 system derived from *Streptococcus pyogenes* is one of the most extensively characterized and widely utilized genome editing platforms. Owing to its programmability and efficiency, CRISPR-Cas9 has therapeutic potential, including disruption of disease-causing genes, such as oncogenes[31].

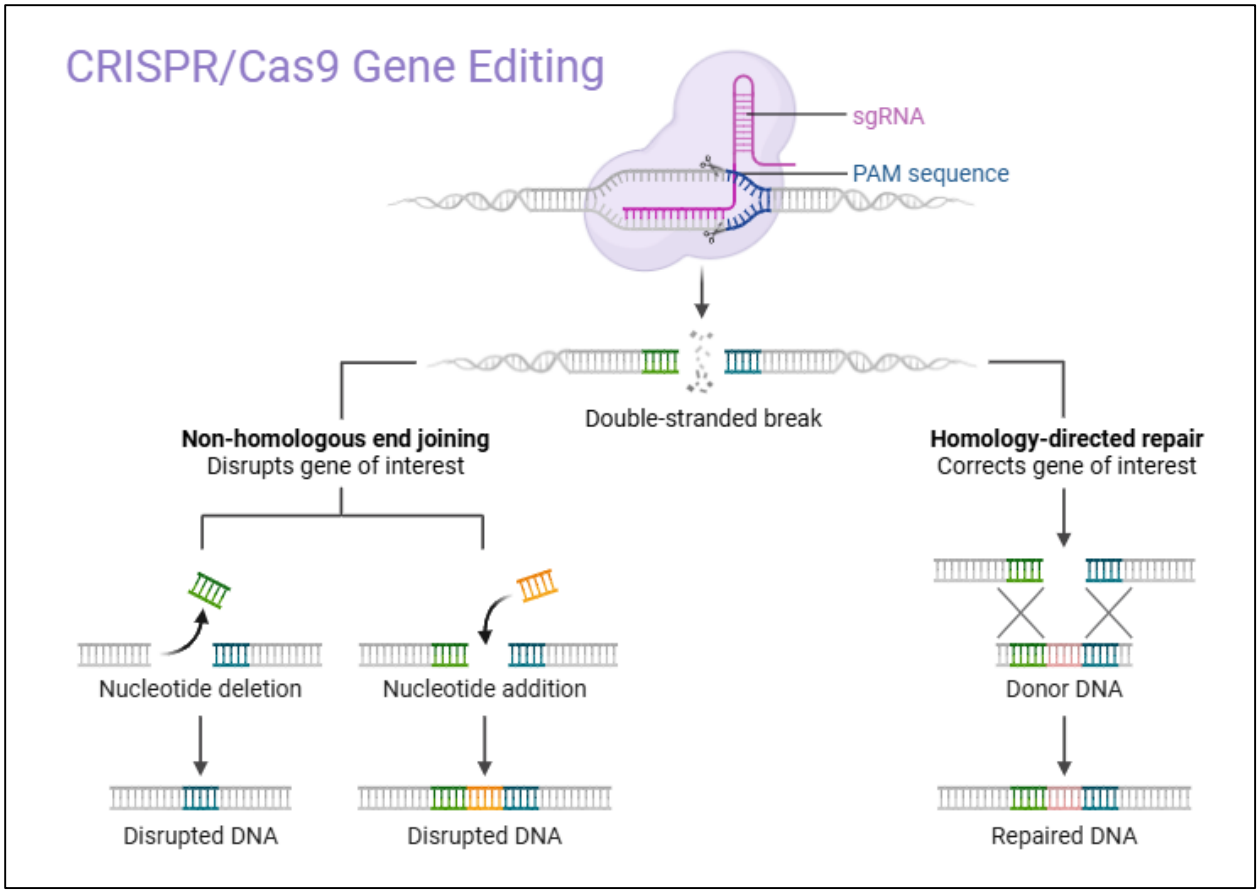

Figure 3: Repair pathways following Cas9-mediated double-stranded DNA breaks. Non-homologous end joining can be used for generating gene knock-outs, since insertions or deletions can lead to frameshift mutations or premature stop codons within the ORF of the target gene. In contrast, homology-directed repair can generate precise modifications at a target locus in the presence of an exogenously introduced repair template. Figure created in BioRender.

1.4 The rise of immunotherapy

The traditional anti-cancer treatment modalities, including surgical resection of accessible tumors, chemotherapy and radiation therapy[32], are collectively known as the three pillars of cancer therapy. The failure of immune recognition is a focal point in the development of cancers and this realization has led to the rise of cancer immunotherapy over the last two decades, leading to transformative clinical outcomes. As a result, immunotherapy is now regarded as the fourth pillar of cancer treatment[33].

The idea of unleashing the immune system of the host to eradicate malignant cells represents an enormous breakthrough in the field of oncology. One of the earliest reports of immunotherapy is traced back to 1891, when physician Dr. William Coley observed that injecting sarcoma patients with mixtures of live and inactivated bacteria resulted in tumor regression. He was able to treat multiple patients with this mixture, which soon became known as Coley's Toxins. These early scientific reports provided initial insights regarding the correlation between the immune system and cancer[34]. However, Coley's idea was met with intense skepticism and his toxins were categorized as an investigation drug that lacked safety and efficacy data[35,36]. Excitingly, the concept of cancer immunotherapy resurfaced with the advent of new technologies. The "three Es" model of cancer immune editing has provided a useful framework for guiding the development of immunotherapeutic strategies[37], and has contributed to the concept of countering cancer immunoediting through immunotherapy [38].

Since modulation of immune checkpoints allows tumors to avoid immune surveillance by promoting T-cell exhaustion and inhibition of cytotoxic T-cell activity in the TME, one immunotherapeutic strategy that has emerged is immune checkpoint blockade therapy (IBT)[39]. In

2011, ipilimumab, a CTLA-4 blocking monoclonal antibody was the first immunotherapy drug to receive FDA approval for treatment of late-stage melanoma patients[40]. Inhibition of the PD-1/PD-L1 pathway is also explored, with clinical approval of antibodies such as pembrolizumab and nivolumab for PD-1 blockade and atezolizumab and durvalumab for PD-L1 blockade[41]. Immune checkpoint inhibitors are in fact the most common class of immunotherapies, highlighted by the clinical success of IBT, especially in melanoma, colorectal and lung cancers, where PD-L1 is highly expressed[39].

Another major class of immunotherapies involves manipulation and expansion of immune cells. This approach is termed adoptive cell therapy and includes tumor-infiltrating lymphocyte (TIL) therapy and chimeric antigen receptor (CAR) T-cell therapy. TIL therapy involves isolation of lymphocytes from a patient's resected tumors, followed by expansion to high numbers using IL-2, and then re-infusion of the cells into the patient, alongside IL-2[42]. In 2024, lifileucel (Amtagvi)- the first TIL-based therapy, was granted accelerated approval for patients with advanced or unresectable melanoma, representing yet another success for immunotherapies[43].

CARs are synthetic receptors consisting of an endodomain, a transmembrane domain and an ectodomain, the latter which is a ligand-specific domain consisting of a single chain variable-fragment (scFv) and a hinge region[44]. The scFv is a fusion protein of the variable regions of the light and heavy chains of immunoglobulins. The hinge (or spacer) separates binding units from the transmembrane domain. A major advantage of CAR-engineered T-cells is their ability to recognize tumor-associated antigens (TAAs) independently of MHC presentation, thereby overcoming a common tumor immune evasion mechanism involving downregulation of MHC[45].

The first generation of CAR T-cells relied on the CD3ζ chain for TCR signalling, but this design demonstrated limited T-cell proliferation and cytokine production[45]. The second generation of CARs were then modified to include co-stimulatory domains from CD28 or 4-1BB to enhance proliferation, cytotoxicity and persistence. Third generation CARs then integrated multiple co-stimulatory signaling domains. Fourth generation CARs, known as "T-cells redirected for universal cytokine-mediated killing" or TRUCKs, were modified to release cytokines in the TME. CAR T-cell therapies have evolved through five generations, with the fifth generation currently underway (**Figure 4**). It differs from previous generations since it includes a membrane receptor, such as IL-2 receptor signaling to enable JAK/STAT activation[44]. CD19 is highly expressed on B cells, making it an ideal CAR target antigen. Another common target is B-cell maturation antigen (BCMA), which plays a role in B cell proliferation and maturation[34]. Both these antigens are restricted to the B cell lineage, rendering them suitable targets for B cell malignancies[46].

In 2010, William Ludwig, diagnosed with chronic lymphocytic leukemia, was the first adult patient to be treated with CAR-T therapy. Two years later, in April 2012, Emily Whitehead was the first pediatric patient with B cell acute lymphoblastic leukemia to receive CD19 CAR-T therapy[34]. Both achieved remission, highlighting the clinical successes of CAR-T cells. There are currently seven FDA approved CAR products targeting CD19 and BMCA antigens for treatment of hematological malignancies: Kymriah and Yescarta in 2017, followed by Tecartus and Breyanzi in 2021, and Aucatzyl in 2024 all targeting CD19, and Abecma in 2021 and Carvykti in 2022, both targeting BCMA[34]. Six of these products are also approved by Health Canada (**Table 1**).

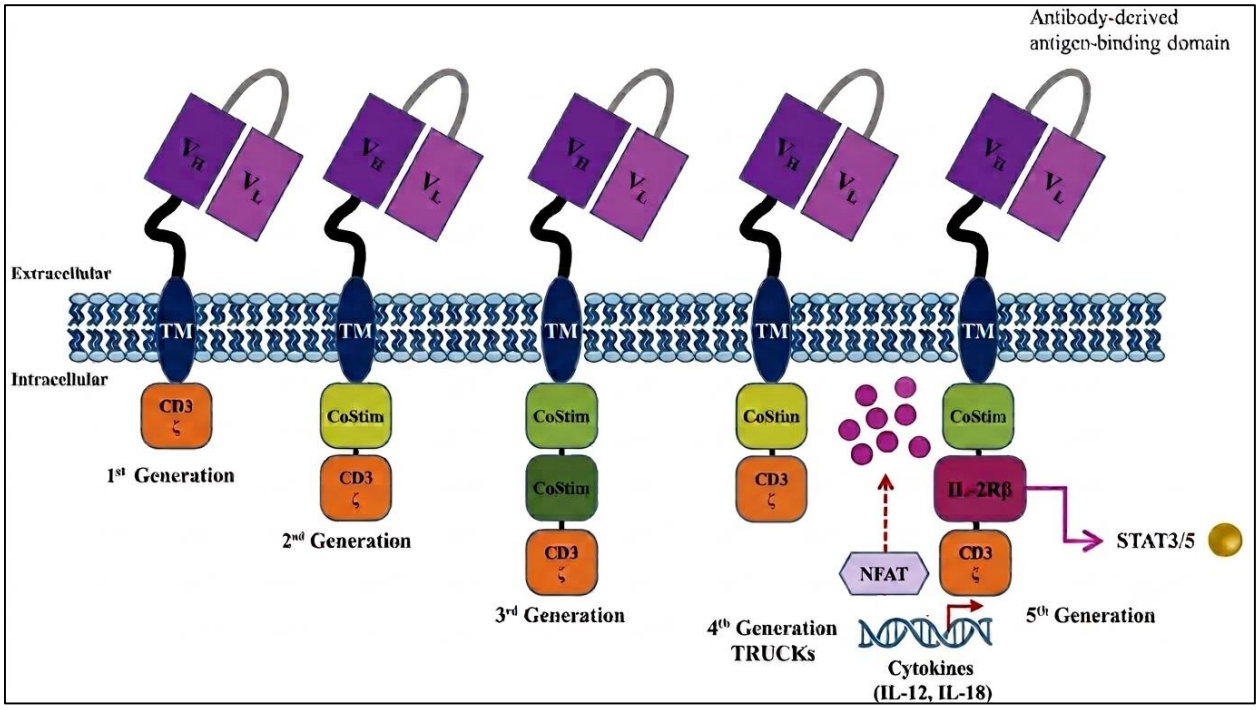

Figure 4: Evolution of the different generations of CARs. The first generation of CAR T-cells relied on the CD3ζ chain for TCR signalling, but failed to show promising clinical results. The first generation was superseded by second generation CARs, featuring co-stimulatory domains such as CD28 to enhance T-cell proliferation. The third generation was further modified to include more than one co-stimulatory domain (often CD28 and 4-1BB). Fourth generation CARs, also called TRUCKS, are engineered to release cytokines in the tumor microenvironment. Lastly, the fifth generation of CARs are currently underway, and include a membrane receptor, such as IL-2 receptor signaling to enable JAK/STAT activation. VH and VL= variable heavy and light region of immunoglobulins. TM= transmembrane domain. CoStim= co-stimulatory domain. Figure was generated using FigureLabs. Adapted from Zugasti et al[44].

Product (Brand / Generic)	Target Antigen	Cancer Indications
Kymriah (tisagenlecleucel)	CD19	B-cell acute lymphoblastic leukemia (ALL); diffuse large B-cell lymphoma (DLBCL); follicular lymphoma
Yescarta (axicabtagene ciloleucel)	CD19	Large B-cell lymphoma (including DLBCL); follicular lymphoma
Tecartus (brexucabtagene autoleucel)	CD19	Mantle cell lymphoma (MCL); B-cell ALL
Breyanzi (lisocabtagene maraleucel)	CD19	Large B-cell lymphoma; follicular lymphoma; mantle cell lymphoma
Abecma (idecabtagene vicleucel)	BCMA	Multiple myeloma
Carvykti (ciltacabtagene autoleucel)	BCMA	Multiple myeloma
Aucatzyl (obecabtagene autoleucel)	CD19	B-cell acute lymphoblastic leukemia (ALL)

Table 1: Clinically approved CAR-T cell products in North America. There are 7 FDA approved products all targeting hematological malignancies, with 6 of these approved by Health Canada (shown in blue).

1.5 The development of tumor-targeting viruses for cancer therapy

Although certain viruses have been recognized as a cause for cancer, viruses have also become promising biotechnological tools for cancer therapy. The concept of using viruses to treat cancers arose from clinical observations of tumor shrinkage following natural viral infections, dating back to the 1900s, most notably, where a patient displayed remission of leukemia during a flu-like illness[47]. This important observation laid the groundwork for future investigation using viruses for cancer therapy. Oncolytic viruses (OVs), which have an inherent or engineered specificity for tumor cells, while exerting little to no pathogenicity against the host, have emerged as an innovative immunotherapeutic approach in clinical development. It is now understood that many of the hallmarks of cancer that enable tumor cell growth, such as immune evasion, resistance to apoptosis, increased proliferative capacity, metabolic reprogramming and enhanced migration, also allow for successful viral infection. In addition, one of the reasons for the ability of tumor cells to respond to viral infection is owed to cell-intrinsic impairments in innate anti-viral signaling pathways (i.e. type I interferon (IFN) pathway) as well as local suppression of adaptive immunity[47], equally important for immune-evasion of the tumor.

OVs confer several advantages given their multi-mechanistic nature (**Figure 5**), which includes inducing direct oncolysis, leading to the release of TAAs (including neoantigens) followed by subsequent stimulation of the host anti-tumor immune response and recruitment of immune cells to the TME[48]. In this process, OVs induce both innate and adaptive immunity. Lysed tumor cells release viral pathogen associated molecular patterns (PAMPs) and danger associated molecular patterns (DAMPs), thus stimulating immunogenic cell death[49]. Through Toll-like receptor (TLR) signalling, PAMP and DAMP release promotes dendritic cell maturation and antigen presentation to cytotoxic CD8+ T-cells, and triggers the production of pro-inflammatory cytokines such as type

I IFN, TNF-α and IL-2[50]. This in turn leads to recruitment of neutrophils and NK cells to the site of infection[51].

Further research has demonstrated that in addition to these mechanistic approaches, OVs can also indirectly contribute to anti-tumor immunity, by inducing vascular collapse[52]. Viral infection initiates an inflammatory reaction involving neutrophil-dependent formation of microclots within tumor blood vessels, leading to disruption of the tumor vasculature.

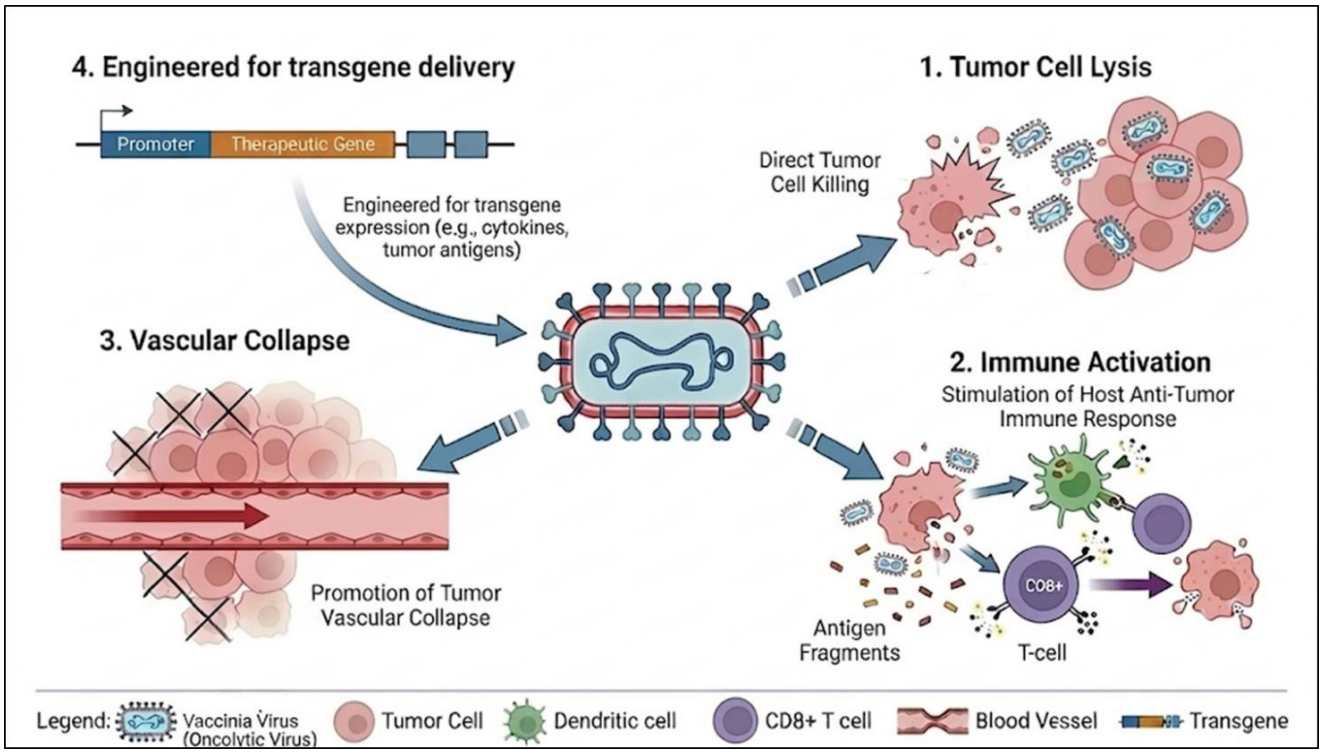

Figure 5: Oncolytic viruses are multi-mechanistic tumor-targeting agents. The center depicts an OV (using vaccinia virus as an example). Infection of tumor cells leads to (1) direct lysis which then leads to release of tumor antigens, then (2) stimulating the anti-tumor immune response of the host, with increased antigen presentation and recruitment of immune cells such as dendritic cells and CD8+ T-cells to the tumor. OVs can also promote (3) vascular collapse. Lastly, (4) the ability to engineer OVs for transgene delivery contributes to therapeutic benefits. Figure was generated using FigureLabs.

There are currently four clinically approved OV products highlighting advances in the field[53]: (1) Rigvir, a non-pathogenic type 7 human enteric cytopathic orphan virus (ECHO-7), approved in Latvia for treatment of melanoma, (2) Oncorine, an adenovirus approved in China for nasopharyngeal carcinoma (3) Imlygic (T-vec), an oncolytic HSV-1 encoding granulocyte macrophage colony stimulating factor (GM-CSF) for treatment of melanoma, FDA approved in 2015, and more recently, (4) Teserpaturev (Delytact), an oncolytic HSV-1 approved in Japan in 2021 for treatment of malignant gliomas[54].

The advent of genetic engineering facilitated the precise manipulation of viral genomes, thus contributing to the creation of safer and more therapeutically robust OV platforms. The first generation of OVs was based on increasing tumor selectivity by deletion of viral genes which would restrict replication to tumor cells. For example, Herpes Simplex virus (HSV) deficient in thymidine kinase (TK) demonstrated increased tumor selectivity in preclinical models. TK is an enzyme essential for viral DNA synthesis which is not expressed at high levels in healthy cells, while increased intracellular TK levels in cancer cells facilitate viral replication[55]. Deletion of TK then became a common staple in building many OV platforms. The second generation of OVs involved introduction of therapeutic transgenes in the viral backbone. One of the most prominent examples of this is inclusion of GM-CSF, to induce proliferation and differentiation of myeloid precursors and improve dendritic cell recruitment to the site of the tumor[56]. Combining tumor selectivity with improving immunogenicity was a significant advance in the OV field. To further improve viral vectors, third generation OVs featured strategies to avoid immune clearance and synergize with other therapeutics, including other forms of immunotherapy, thus providing potential to improve clinical outcomes. For example, Park et al. engineered VV encoding a truncated CD19 antigen for delivery to solid tumors for recognition by CD19 CAR-T cells,

alleviating the challenge of antigen availability in solid tumors[57]. Exploring a similar concept, Taha et al. employed a complementary dual-virus strategy wherein oncolytic VSV encoding truncated HER2 was combined with VV encoding a HER2- targeted T-cell engager, thus tailoring the TME with OVs[58].

1.6 Vaccinia virus: a historical medical mainstay repurposed as a cancer therapeutic

1.6.1 Key biological properties of VV

Vaccinia virus is the prototypic member of the poxvirus family, a group of large DNA viruses whose replication is confined to the cytoplasm of the cell. The cytoplasmic replication profile is made possible since the large genome encodes for complete DNA and RNA replication machinery, thus lowering dependency on host factors[55]. Historically, VV has played a crucial role as the vaccine used for global eradication of smallpox. VV particles are brick-shaped, ~300 nm in diameter, and possess a linear double-stranded DNA genome of ~200 kb, encoding ~250 genes, including those involved in DNA replication, recombination and repair[59], and exhibits a rapid and lytic replication cycle of ~12 hours[48,60]. The viral genome and numerous virus-encoded enzymes, including a DNA-dependent RNA polymerase, transcription factors, capping and methylating enzymes and a poly(A) polymerase, are packaged within the core to enable synthesis of mRNA after entry into the cell[61].

The replication cycle of VV is temporal- with early, intermediate or late gene expression occurring in sites known as viral factories, and the transition from one state to another is accompanied by hallmark events, providing a programmed cascade mechanism of gene regulation[61] (**Figure 6**). VV entry into the cell involves either direct fusion of the viral and cellular membranes, or macropinocytosis, where membrane fusion is triggered by low pH and occurs within endosomal vesicles[62]. Virus entry is then followed by loss of the wrapping membrane (uncoating)[63]. Rapidly following entry, the components found in the viral core initiate transcription of the viral genome, producing a set of early mRNAs, which encode proteins involved in DNA replication, which starts ~2 h after infection. The onset of DNA replication then triggers expression of intermediate genes, followed by late genes, encoding products involved in assembly of mature particles[62].

Virion morphogenesis undergoes a complex pathway- the first visible structure is crescent-shaped, which then maintains the curvature and grows to form a spherical structure called immature virion (IV) **(Figure 7A**), finally culminating in the formation of two distinct virion forms that are produced from infected cells. Firstly, the intracellular mature virus (IMV), surrounded by a single membrane, remains within the cell until lysis and is the most abundant form. Structurally, IMVs have a dumbbell shaped core containing the viral dsDNA genome, two proteinaceous structures called lateral bodies that flank the core, and a single lipid membrane (**Figure 7B**)[64]. Secondly, the IMV acquires a second host-derived membrane (from the Golgi apparatus) and is termed intracellular enveloped virus (IEV), which is exported from the cell where it then remains on the cell surface, known as cell-associated enveloped virus (CEV) (**Figure 7C**) or extracellular enveloped virus (EEV) if released from the cell surface. CEVs induce the formation of actin tails from the cell surface, thereby propelling virus particles towards uninfected cells, facilitating cell-to-cell spread, while EEVs mediate long-range dissemination[65]. Further, since CEVs and EEVs are wrapped by a host-cell derived membrane, they also exert a role in evading the host antibody and complement-mediated responses.

The physical autonomy of VV particles from the host nucleus can pose a challenge, since the virus will need to evade detection by cytoplasmic sensors[60]. As such, a large portion of the genome consists of a sophisticated set of genes involved in counteracting the host anti-viral defense mechanisms.

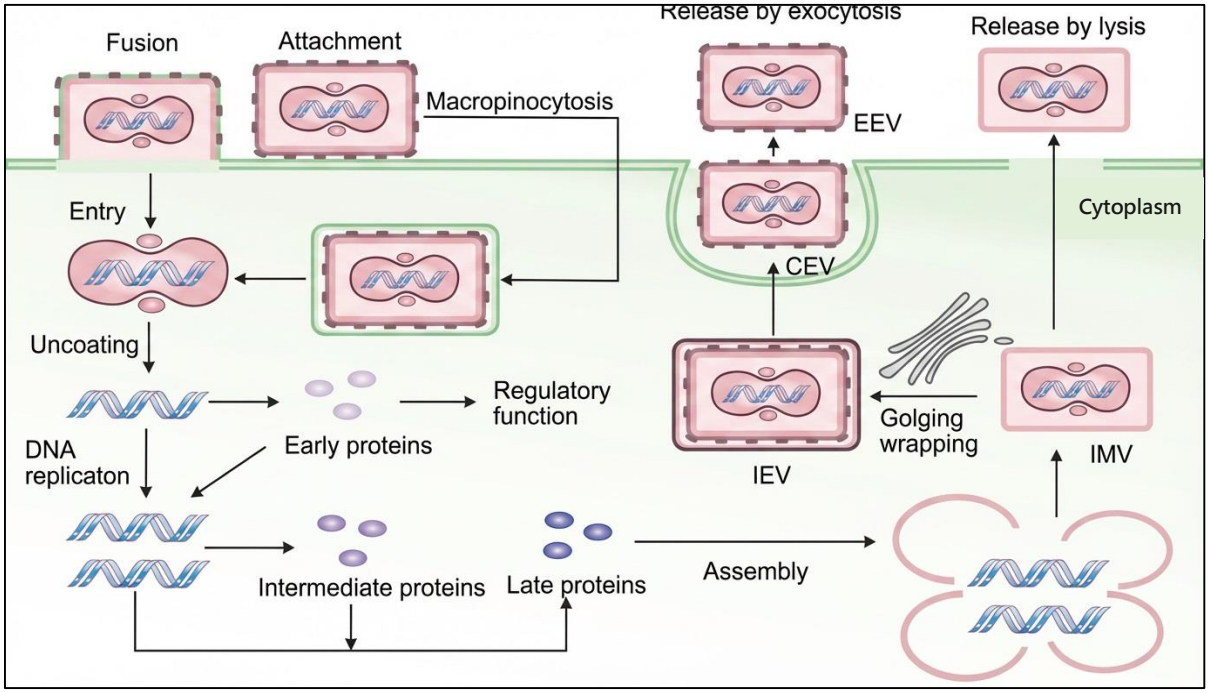

Figure 6: The cytoplasmic life cycle of vaccinia virus. VV enters the cells either by fusion with the cell membrane or by macropinocytosis. Following entry into the cell, the particle is uncoated. The viral core contains proteins involved in initiating transcription of early genes, which promote viral DNA replication and suppress host antiviral responses. Transcription of intermediate genes is triggered by DNA replication. The latter then triggers transcription of late genes, involved in virion assembly. VV has four main virion forms: intracellular mature virus (IMV), surrounded by a single membrane, remains within the cell until lysis and is the most abundant form. Secondly, the IMV acquires a second host-derived membrane (from the Golgi apparatus) and is known as intracellular enveloped virus (IEV), which is exported from the cell where it then remains on the cell surface, known as cell-associated enveloped virus (CEV) or extracellular enveloped virus (EEV) if released from the cell surface. Figure generated using FigureLabs, adapted from Stawowczyk et al[62].

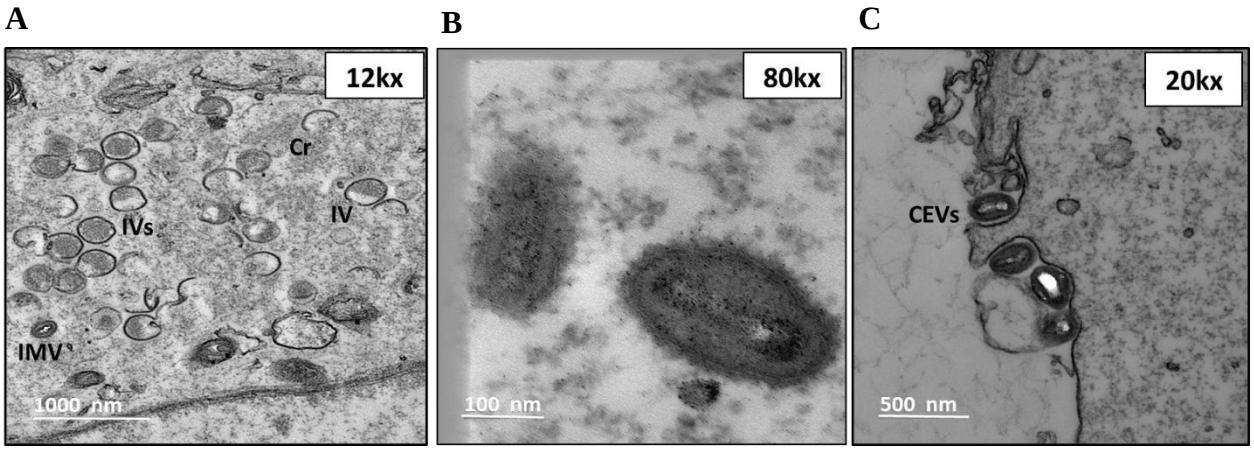

Figure 7: Electron micrographs of vaccinia virus infected cells. A. Viral crescents, immature virions and intracellular mature virions observed in VV infected U20S cells 24 h post-infection. Abbreviations: Cr: crescents, IV: immature virions, IMVs: intracellular mature virions. **B.** Structurally, VV particles have a dumbbell shaped core containing the viral dsDNA genome, two proteinaceous structures called lateral bodies that flank the core, and a single lipid membrane. **C**. Mature VV particles released from the cell are located on the periphery as cell associated enveloped virions (CEVs). See materials and methods section 5.24 for preparation of samples and generation of electron micrographs.

1.6.2 VV as an oncolytic platform for transgene expression

Although the World Health Organization (WHO) declared that smallpox was eradicated in 1980, and routine smallpox vaccination has ceased, VV is still a widely studied viral vector, given that it is a model system to gain an understanding of poxvirus biology, remains an expression vector for vaccination, and can be harnessed as a cancer therapeutic[66]. The development of recombinant poxviruses was first demonstrated in the early 1980s, using a process known as marker rescue, wherein transfected DNA containing the desired gene fragment shares regions of homology with the viral genome[67]. The construct typically contains a desired transgene and a selection marker, each driven by separate VV promoters[68]. Recombination occurs between the homologous sequences on the plasmid and the viral genome, enabling the virus to incorporate the desired

sequences. These discoveries opened the doors for construction of recombinant poxviruses containing essentially any gene-of-interest (GOI).

One of the focuses in the oncolytic virotherapy field is the bio-engineering of oncolytic VV by incorporating therapeutic molecules in the viral backbone to generate robust and improved vectors for cancer therapy. Key findings from the Bell lab showcased that (1) a single intravenous infusion of VV can productively infect metastatic tumors in a phase 1 clinical trial[69] (2) VV has potent anti-angiogenic activity, and (3) VV can deliver multiple therapeutic payloads to the tumor. Building on the latter idea, various approaches have been under investigation, including the incorporation of immune-stimulating molecules such as cytokines or bispecific T cell engagers (BiTEs) into VV for tumor-localized delivery[70,71], thus contributing to reversing the "cold" immunosuppressive TME into a "hot" TME conducive to an anti-tumor immune response.

To improve the generation of therapeutic VVs, various methods reliant on recombination-based genetic engineering, known as 'recombineering', have been employed. To enhance the recovery of transgene-containing viruses, certain groups have employed CRISPR-Cas9 cleavage of the viral genome along with a homology template to streamline the VV rescue process[72,73]. Alternatively, use of antibiotic- resistance genes incorporated in the virus backbone followed by culturing the virus in the presence of the cognate antibiotic allows rapid isolation of recombinant VV[74].

In a clinical setting, VV has been explored as an oncolytic agent in numerous Phase I, II or III clinical trials alone or in combination with chemotherapeutic drugs, with modifications to the viral backbone, including gene deletions to render the virus more cancer selective and/or insertions of

immune stimulating molecules[75]. A well-known example and one of the most clinically advanced candidates is JX-594 (Pexa-Vec), an engineered VV harboring a TK deletion along with incorporation of GM-CSF, which demonstrated promising results in phase I and II trials for advanced hepatocellular carcinoma[76]. Although Pexa-Vec progressed to a phase III trial but failed to show survival benefit, the use of engineered VV in a clinical setting was still a crucial step in the development of OV-based therapies, and Pexa-Vec is still explored in other Phase I and II trials for patients with metastatic cancers[56].

The center of the VV genome is highly conserved among poxviruses and encodes genes required for virion morphogenesis and transcription, but the extremities are variable and encode virulence factors that determine host range. Disruption of non-essential genes for generating an oncolytic backbone combined with the large genome size allows for incorporation of multiple therapeutic transgenes[48]. In fact, Smith and Moss first demonstrated that VV could harbor an insertion of 25 kb of foreign DNA into the TK locus while maintaining replication[77]. TK is mapped near the center of VV DNA and provides a stable site for transgene insertion[78]. In addition to deletion of TK from the virus backbone as described above (section 1.5), other genes involved in DNA synthesis have also been targeted to generate a tumor selective platform. Deletion of ribonucleotide reductase subunits (encoded by genes F4L and I4L) attenuates growth in healthy cells while increasing cancer tropism[55,79]. The multifunctional A56 protein (encoded by the A56R gene) binds two other viral proteins, a serine protease inhibitor (K2) and the vaccinia complement control protein (VCP), leading to their expression at the cell surface[80]. The A56-K2 complex reduces superinfection, while the A56R-VCP complex protects infected cells from complement-mediated attack. However, since the A56R gene is non-essential for VV replication, it has been used for insertion and expression

of foreign genes. For example, in the oncolytic VV GLV-1h68, the A56R gene is inactivated by insertion of β-glucuronidase, a reporter enzyme[81].

An example of another gene deletion is B8R, which encodes for a secreted protein with sequence similarity to the IFN-γ receptor, as part of the VV immune evasion strategies[82]. Deletion of this gene attenuates the virus *in vivo*. Collectively, these gene deletions facilitate insertions of multiple therapeutic transgenes within one virus, generating armed VVs capable of unleashing various therapeutic molecules to counteract tumors.

Aside from strategic deletion of VV genes, directed evolution provides an alternative method for creation of tumor selective viruses[55]. For example, VV Ankara was passaged 570 times in chicken embryonic fibroblasts to produce replication-deficient modified VV Ankara (MVA), containing large genomic deletions which span genes mainly involved in host range and immune evasion. MVA is used as the backbone in several recombinant VV-based cancer vaccines.

1.7 Retroviral vectors for protein or gene delivery

1.7.1 Engineered retrovirus-derived virus-like-particles (VLPs) as platforms for transient protein delivery

VLPs are assemblies of viral proteins which lack viral genetic material, and are thus considered as non-replicating and non-infectious particles, but they retain the ability to transduce mammalian cells and release cargo[83]. Classically, VLPs have been used as vaccine agents, but interest has shifted towards their use as protein delivery vehicles.

Retroviruses are RNA viruses whose genomes are reverse-transcribed into DNA, with murine leukemia viruses (MLV) being one of the simplest types. MLVs encode only 3 polyproteins involved in virus particle assembly. Firstly, group-specific antigen (Gag) provides the structural proteins. Gag is composed of a matrix domain, which targets the protein to the plasma membrane, a capsid domain, involved in assembly of virions, and a nucleocapsid, which plays a role in interaction of Gag with the RNA genome[84]. Secondly, the Pol protein comprises the retroviral enzymes (1) protease (PR), which catalyzes particle maturation, (2) reverse transcriptase, known for copying the viral RNA into DNA, and (3) integrase, which inserts the viral DNA into the genomic DNA of the host cell. Lastly, the Env protein induces fusion of the viral membrane with that of the host cell for particle entry. The Gag and Pol coding sequences are found in the same reading frame, and are separated by a stop codon (UAG). This stop codon is finely tuned for translation suppression- in 5% of the translation products, a 57 base cis-acting signal downstream of the stop codon induces insertion of glutamine (encoded by CAG). As a result, the Gag product is extended into Pol, by “mis-translation” of the stop codon as a sense codon[84].

The concept of using engineered retroviral VLPs has been explored by various research groups- all which follow the same principle; the retroviral structural protein Gag is fused to the protein of interest, separated by a proteolytic site which is cleaved by the Gag-Pol encoded protease during particle maturation[85]. VLP production is achieved by co-transfecting plasmids encoding the Gag-fusion construct, Gag-Pol and the desired envelope glycoprotein (typically VSV-G) into Human Embryonic Kidney (HEK) 293T producer cells. Gag proteins polymerize at the cell membrane and VLPs carrying the protein cargo of interest then bud out into the supernatant **(Figure 8**). After the particle is released from the cell, it undergoes maturation, whereby PR cleaves the Pol moiety of Gag-Pol as well as Gag[84]. Approximately 2000-5000 Gag molecules are delivered by a single VLP in the transduced cell[86]**.**

Kaczmarczyk et al. developed a VLP system based on an avian retrovirus, composed of Gag fusion proteins to deliver GFP, Cre recombinase, cytotoxic enzymes (cytosine deaminase) and human caspase 8 to induce cell death[86]. Similarly exploring the concept of cytotoxic payload delivery, Wu et al. employed MLV VLPs for delivery of bacterial toxins to induce cell death[87]. These examples collectively demonstrate the versatility of retroviral VLPs for protein delivery, and their potential in inducing tumor cell death.

In recent years, one of the applications of VLPs has been for delivery of gene editing agents such as ribonucleoprotein complexes (RNPs), since engineering DNA-free VLPs to package Cas9 RNPs has potential to enable therapeutic gene editing. Mangeot et al. coined the term 'Nanoblades' to describe Cas9 and single guide (sgRNA) loaded VLPs, and demonstrated genome editing in a variety of cell types, including primary fibroblasts and human and murine CD34+ bone marrow

cells[88]. Another advantage of VLPs includes the ability to modulate retrovirus tropisms by pseudotyping particles with different envelope glycoproteins, enabling the targeting of VLPs to various tissues[83].

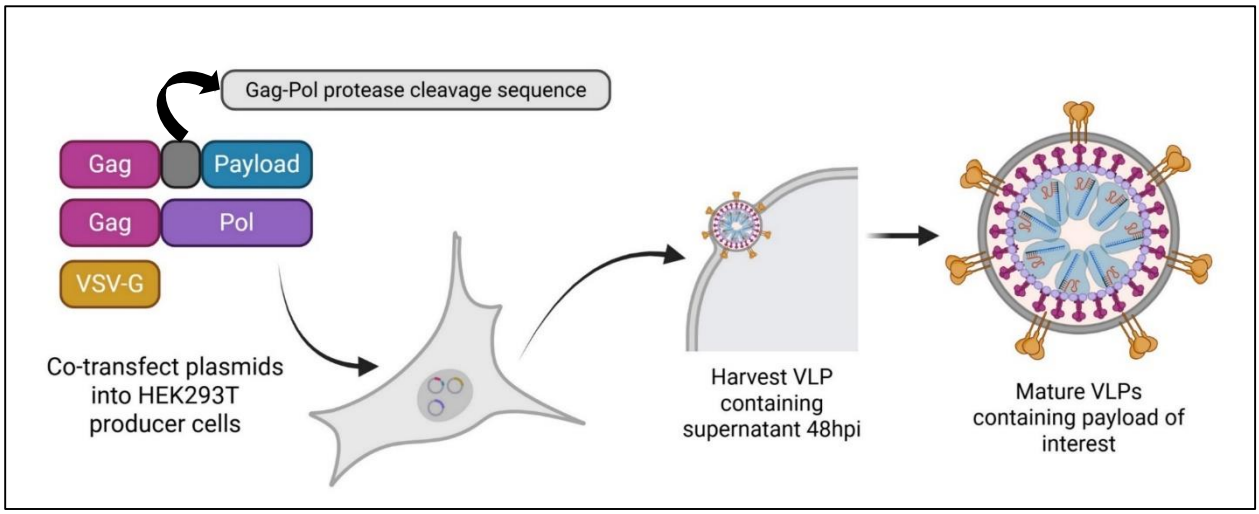

Figure 8: Overview of the production process for retroviral VLPs. Structural protein Gag is fused to the payload of interest, separated by a protease cleavage sequence which is recognized by Gag-Pol encoded protease. Transfection of plasmids encoding the Gag-fusion construct, Gag-Pol and the desired envelope glycoprotein (classically VSV-G) into HEK 293T producer cells results in the production of cargo carrying VLPs which are released into the supernatant. Example depicted in schematic shows Cas9 and sgRNA loaded VLPs. Figure created using BioRender.

1.7.2 Lentivirus biology as a foundation for cell and gene therapies

Roughly 50 years ago, Howard Temin and David Baltimore rewrote the central dogma of biology, by documenting that virions from two-tumor causing viruses, RSV and MLV, carried a virally encoded enzyme that converted single-stranded RNA into DNA, eventually leading to molecular details regarding the production of DNA from RNA templates[89]. Retroviral vectors, which rely on reverse transcription and genomic integration, have long been considered as attractive tools for gene therapy. They are well-known for stable integration of their genome into the host cell chromosome, and provide a relatively large cloning capacity, sufficient for delivering a GOI in most clinical settings. Lentiviral vectors (LVs), derived from human immunodeficiency virus-1 (HIV-1), offer yet another advantage over their retroviral counterparts- they transduce not only dividing, but also non-dividing cells, crucial for targeting tissues such as the brain, muscle, liver, lungs and the hematopoietic system.

Gene therapy relies on two components: the packaging elements, which provide the structural proteins and enzymes required to generate a mature particle, and the vector genome itself, which contains the GOI to be transferred to target cells. These elements have gone through generations of engineering to generate safe and robust lentivirus-based gene delivery vehicles **(Figure 9**). The first-generation of lentiviral vectors that were developed comprised all HIV-1 proteins except for the envelope[90]. However, risk of replication-competent recombinants was a major concern, leading to the demonstration that deletion of four additional viral accessory genes involved in pathogenesis and virulence (*Vpr, Vif, Vpu* and *Nef*) still enabled production of transduction-competent lentivirus particles, giving rise to the second generation. The third generation of lentiviral vectors conserve only three of the nine HIV-1 genes: *gag,* which encodes the structural proteins which form the

viral core, *pol*, encoding the enzymes involved in particle maturation and *rev*, involved in nuclear export of the viral genomic RNA.

The vector genome is characterized by 5' and 3' long terminal repeats (LTRs) at the left and right ends, which are divided into U3, R and U5 regions. The U3 regions of the 5'LTR serves as the viral promoter. The lentiviral system underwent further improvements with the finding that transcriptional elements could be removed from the vector, ultimately giving rise to self-inactivating (SIN) vectors, whereby a 400-nucleotide deletion in the U3 region of the 3'LTR was introduced (ΔU3), while maintaining vector titers and transgene expression[91]. During reverse transcription, this deletion is transferred to the 5' LTR of the proviral DNA, whereby the truncated LTR no longer acts as a promoter. This region was replaced with a strong constitutive promoter for transcription of full-length RNA, such as the human cytomegalovirus (CMV) or Rous sarcoma virus (RSV) promoters[92], and an internal promoter for transgene expression in recipient cells. Viral tropism can be modified through pseudotyping, wherein the native surface protein is replaced with a viral envelope glycoprotein of interest, enabling particles to enter based on interactions between the pseudotyping glycoprotein and corresponding cellular receptors for vector entry[93]. The most commonly used pseudotyped envelope protein is VSV-G, which displays broad tropism through interaction with the ubiquitously expressed low-density lipoprotein receptor (LDL-R)[92].

In 1990, the first gene therapy trial employed an MLV-derived retroviral vector for treatment of Adenosine deaminase (ADA) deficiency, one of the causes of severe combined immunodeficiency (SCID). The human ADA enzyme was delivered in autologous T-cells of a four-year old patient, and 10 years after treatment, lymphocytes carrying and expressing the gene were still detected,

demonstrating the remarkable long-lasting effects of retroviral gene transfer[94]. Two early trials in the gene therapy field then focused on treatment of SCID in 20 children, using an MLV-derived vector and *ex vivo* infection of CD34+ cells to correct the defective cytokine receptor subunit responsible for SCID[95]. However, follow-up revealed that five of the children developed leukemia due to insertional mutagenesis- vector integration occurred in proximity to the LMO2 proto-oncogene promoter[92]. MLV-derived vectors demonstrate different integration profiles than HIV-based lentiviral vectors. HIV integration preferentially targets active genes, while MLV integrates near start sites of gene transcription[96]. In the realm of oncology, one of the biggest applications of lentiviral vectors has been the generation of CAR-T cells, whose clinical success is described in section 1.4.

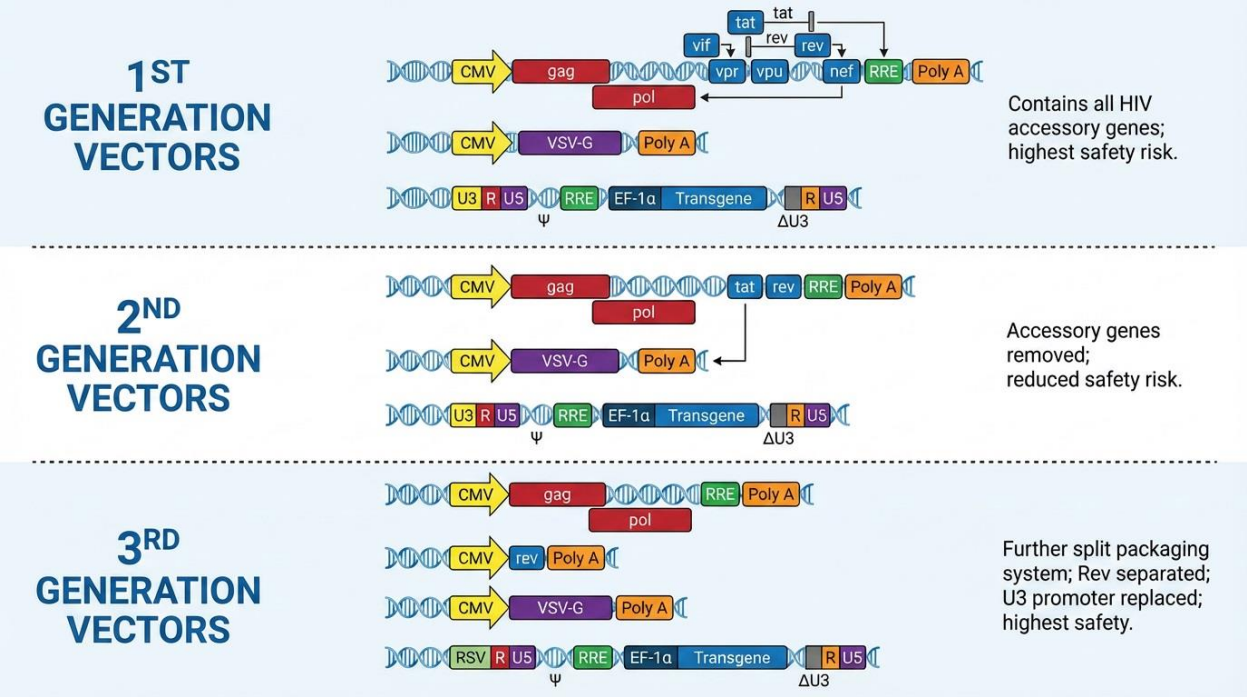

Figure 9: Evolution of lentiviral vector designs across generations. First generation lentiviral vectors retained all 9 HIV genes except for the envelope gene. However, risk of replication-competent lentivirus formation led to vector modifications. Second generation vectors were developed when it was discovered that deletion of accessory genes *Vpr*, *Vpu*, *Vif* and *Nef* could still generate functional lentivirus particles. Third generation vectors conserve only three of the nine HIV genes (*gag*, *pol* and *rev*). Figure was made using FigureLabs, adapted from Duverge et al[97].

1.8 The viral Trojan Horse: conceptualizing "a virus within a virus"

For roughly two decades now, poxviruses have been under exploration for the delivery of retroviral vector components. In fact, Holzer et al. first constructed VV to express the (MLV) retroviral genome containing GFP as a transgene in the TK locus, and found that infecting retroviral packaging cells (which provided Gag-Pol and VSV-G) with the recombinant VV gave rise to transduction competent retroviral particles[98]. Shortly afterwards, Konetschny et al. cleverly inserted an intron containing retroviral cassette into the VV TK locus[99], given that standard retroviruses do not allow for inclusion of introns due to splicing. As a follow up, nearly two decades ago, Konetschny et al. then generated an engineered VV which encodes the complete MLV retroviral system (genes encoding for *Gag, Pol,* and *Env*), thus producing defective retroviral particles[100].

The concept of one virus carrying another has also been observed in evolution. Fowlpox virus (FPV), an avian poxvirus, has been used to vaccinate poultry to prevent disease. Interestingly, multiple reports have indicated that in naturally occurring evolutionary events, multiple FPV vaccine strains were found to contain integrated sequences from reticuloendotheliosis virus (REV), an avian retrovirus[101,102]. In these reports, it was demonstrated that integration of nearly intact REV provirus occurred, with 3'LTR rearrangements such that part of the U3 and U5, and all of the R region was lacking. Despite this, REV maintained infectivity since FPV gave rise to REV particles upon infection of chicken embryo fibroblasts[101]. Remnants of REV LTRs have been retained in the genomes of multiple FPV vaccine strains. These examples demonstrate the potential for VV to serve as a delivery vehicle for retroviral particles.

1.9 Current OV limitations, project rationale and hypothesis

Despite the advantages conferred by use of multi-mechanistic OVs for cancer therapy, as our understanding of OV infection within tumor cells has grown, it has become apparent that OV infection of tumor cells alone is not sufficient for complete tumor eradication. For this to be the case, the OV would have to infect every cancer cell- this is difficult considering barriers such as tumor heterogeneity, eventual immune-mediated virus clearance and the metastatic nature of tumors.

These observations have given rise to the concept of arming OVs with genes or therapeutic payloads to enhance efficacy. Given that virally infected tumor cells will eventually be destroyed by viral-mediated lysis or immune targeting, the use of transgenes that induce a bystander effect, leading to manipulation of surrounding uninfected cells in the tumor microenvironment, may provide a superior therapeutic benefit. As such, my thesis focuses on the development of retrovirus-derived therapeutic delivery platforms that could be integrated with oncolytic VV to enable localized transient or stable manipulation within tumors.

The aforementioned examples involving poxviruses containing retroviral systems were not explored in a therapeutic context, thus, the rationale for my thesis work was to develop retrovirus-derived therapeutic delivery platforms for cancer therapy, including a VLP-based system for transient CRISPR-Cas9-mediated oncogene targeting and a VV-based platform engineered to encode the components of a self-inactivating lentivirus for stable gene delivery to bystander cells **(Figure 10**).

Based on this rationale, *I hypothesized that retrovirus-derived particles could be engineered for complementary therapeutic applications in cancer, including (1) transient CRISPR-Cas9-mediated oncogene targeting using VLPs or (2) stable gene delivery using VV-encoded lentiviral vectors.*

1.9.1 Specific project aims:

1. Develop and evaluate an MLV-derived VLP platform for transient genome editing.
2. Characterize a triple engineered VV encoding lentivirus vector components (envelope glycoprotein VSV-G, packaging component Gag-Pol, and lentivirus genome).

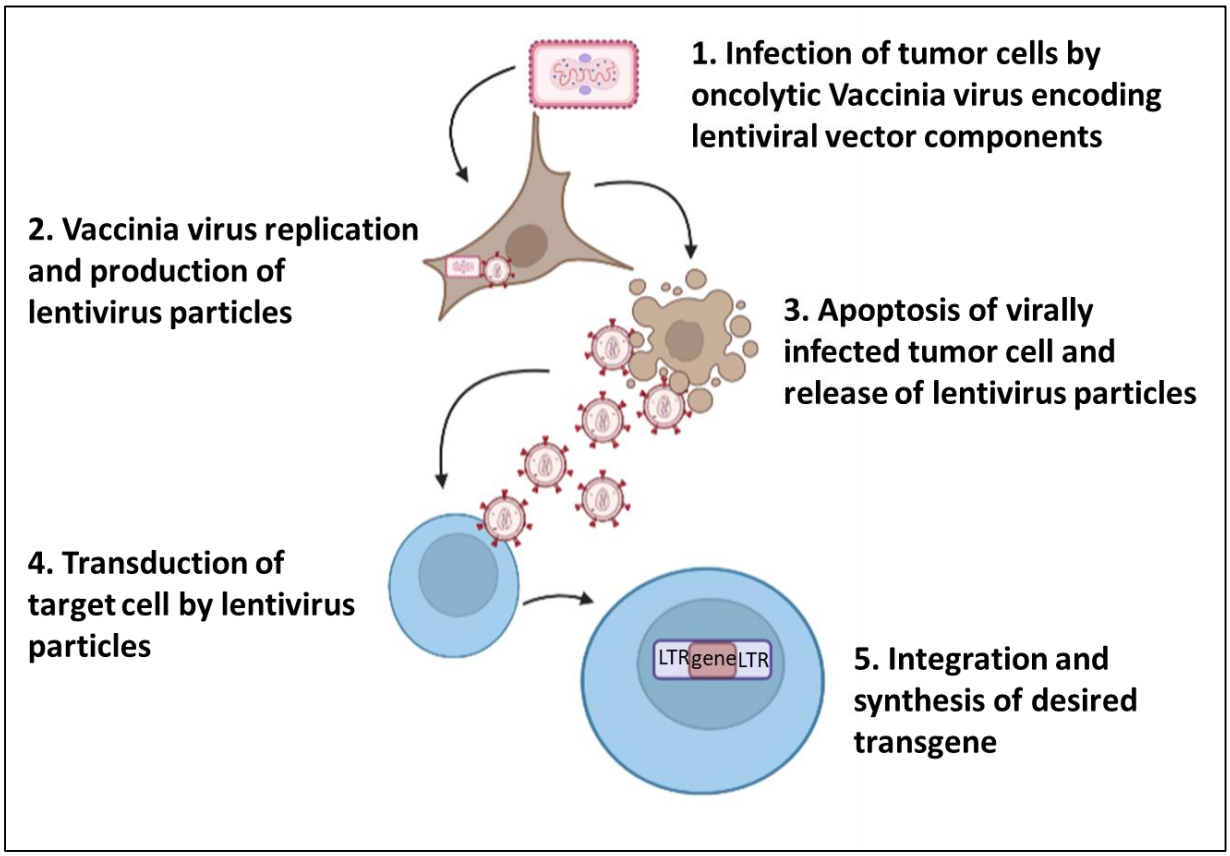

Figure 10: Oncolytic vaccinia virus engineered to contain the components of a SIN lentivirus vector. In theory, infection of tumor cells with VV encoding the lentivirus vector components would result in budding of lentivirus particles from the VV-infected cells, which will eventually by lysed to release tumor antigens for immune stimulation. The lentivirus particles would transduce neighboring cells in the TME for stable gene delivery. Figure created using BioRender.

Chapter 2: Establishing a retroviral VLP platform for transient intracellular protein delivery

2.1 Engineered VLPs enable the delivery of functional protein cargo to recipient cells

2.1.1 MLV-derived VLPs mediate efficient delivery of biologically active protein cargo

I performed preliminary studies to establish an MLV-based VLP platform for delivery of various protein cargo to target cells. I first cloned the *egfp* coding sequence (gene encoding enhanced green fluorescent protein) in frame with MLV Gag, separated by the Gag-Pol protease cleavage sequence. I selected eGFP due to increased fluorescence emission compared to GFP[103]. VLPs were produced by co-transfecting plasmids encoding Gag-eGFP, Gag-Pol and VSV-G into HEK 293T producer cells. I then collected and concentrated VLPs, and transduced freshly plated HEK 293T recipient cells, given that these cells have an excellent transduction efficiency[104]. Fluorescence microscopy analysis readily detected a substantial number of eGFP expressing HEK 293T cells, while no background fluorescence was observed in the untransduced cells (**Figure 11A**). I then tested transduction in HeLa cells, with HEK 293T cells included as a transduction control, and observed eGFP in the transduced cells, indicating that VLPs can be used for protein delivery **(Figure 11B**).

To then demonstrate the functionality of this technology, I produced VLPs loaded with NanoLuciferase (NLuc), a small and bright luciferase reporter[105]. HEK 293T cells were transduced with concentrated VLPs at incremental volume increases (25, 50, 75 and 100 µL), and the luminescent signal was detected from lysed cells 24 h later. I observed a dose dependent effect, with higher signal amplification at increasing volumes, which plateaued at 75 µL and 100 µL (**Figure 11C).**

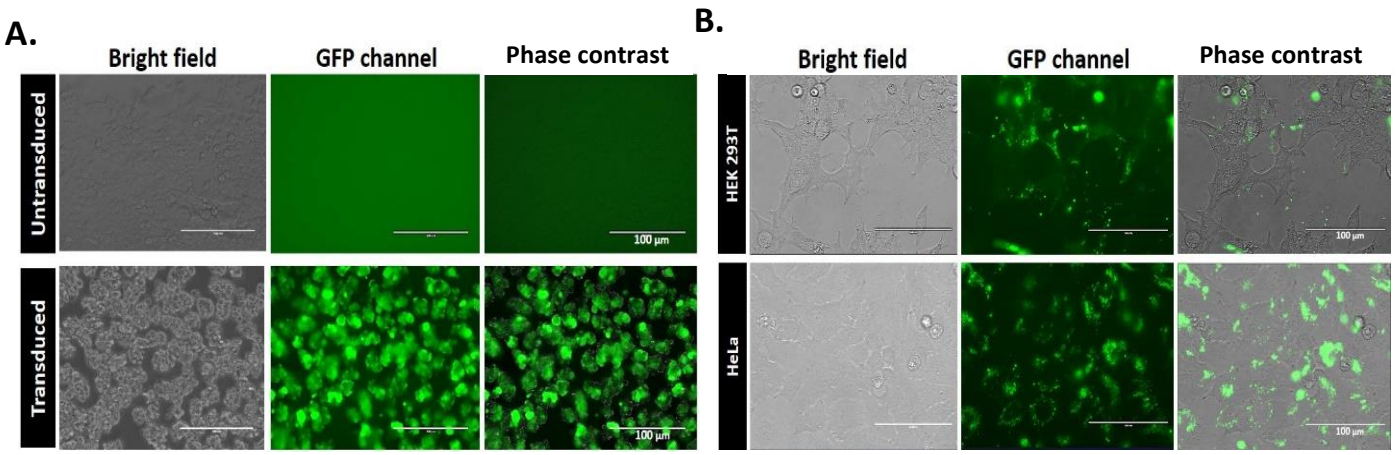
A.
Bright field
GFP channel
Phase contrast
Untransduced
Transduced
100 µm
B.
Bright field
GFP channel
Phase contrast
HEK 293T
HeLa
100 µm

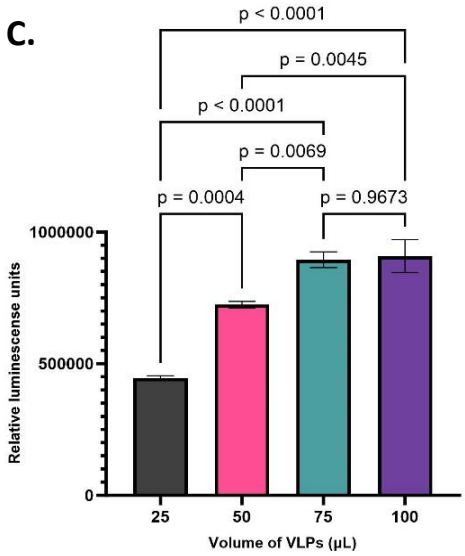
C.
p < 0.0001
p = 0.0045
p < 0.0001
p = 0.0069
p = 0.0004
p = 0.9673
1000000
500000
0
Relative luminescense units
25
50
75
100
Volume of VLPs (µL)

Figure 11: Proof-of-concept demonstrating VLP-mediated delivery of reporter payloads eGFP and NanoLuciferase. A. VLPs were produced by co-transfecting producer cells with plasmids encoding Gag-eGFP, Gag-Pol and VSV-G. 48 h post-transfection, VLPs were harvested from the supernatant of producer cells, concentrated and used to transduce HEK 293T recipient cells. Fluorescence microscopy performed 24 h post-transduction demonstrates eGFP delivery in transduced cells compared to untransduced cells**.** Images were taken at 10X magnification by EVOS M5000 microscope. Scale bar =100 µm. **B.** Transduction of eGFP in HEK 293T cells (top panel) or HeLa cells (bottom panel), imaged at 10X magnification by EVOS M5000 microscope. Scale bar =100 µm **C.** VLPs were produced as described in panel A, except that Gag-eGFP was replaced with a plasmid encoding a Gag-NLuc fusion construct. HEK 293T cells were transduced with increasing volumes of concentrated VLPs. Data shown is normalized to untransduced cells (n=3). Shown is the mean ± standard deviation (SD), p-value computed using One-way ANOVA with Tukey's correction test.

While most research groups have focused on generating Gag fusion constructs at the C-terminal end of Gag, it has also been reported that N-terminal fusions result in functional protein delivery[106]. Protease cleavage of the C-terminal Gag fusion does not result in a clean-cut; a short sequence of amino acid residues from the protease cleavage site remains at the N-terminus of the protein of interest, and while many proteins can support this, certain proteins require a free N-terminus for functionality. For example, Granzyme B, a serine protease found in the granules of cytotoxic CD8+ lymphocytes and NK cells occurs as an inactive zymogen containing an N-terminal pre-pro leader sequence in its native form[107]. The signal peptide is then cleaved to generate an inactive pro-enzyme containing an N-terminal pro-peptide, which is then cleaved by Cathepsin C to generate an active Granzyme. Since one of the potential downstream project applications was delivery of a cytotoxic molecule such as Granzyme B to induce tumor cell death, I also wanted to validate VLP-mediated delivery of an N-terminal Gag-fusion construct. To this end, I generated VLPs containing mCherry at the N terminus of Gag, separated by the Gag-Pol encoded protease cleavage sequence. VLP transduction in VERO African green monkey kidney cells resulted in protein delivery, as seen by expression of eGFP and mCherry (**Appendix Figure 1**). I then wanted to determine if dual payload delivery within the same particle was possible so I generated a fusion construct whereby mCherry was fused to the N terminus of Gag and eGFP was fused at the C terminus (**Figure 12A**). I validated the construct by transfecting HEK 293T cells with either single payload containing VLPs (mCherry-Gag or Gag-eGFP) as controls, or dual payload engineered VLPs, containing mcherry-Gag-eGFP. Overlapping yellow fluorescence was observed as a result of both mCherry and eGFP (merged image, **Figure 12B**). Flow cytometric analysis in transduced cells revealed a drop in eGFP mean fluorescence intensity (MFI) from the single payload to the dual payload (MFI of 307 to 89.6), while a modest drop in mCherry fluorescence was observed (MFI of 352 to 316)

(**Figure 12C**). The decreased fluorescence intensity was also observed by microscopic assessment of transduced HEK 293T cells (**Figure 12D**). These data suggest that engineered VLPs can package and deliver functional protein cargo to recipient cells.

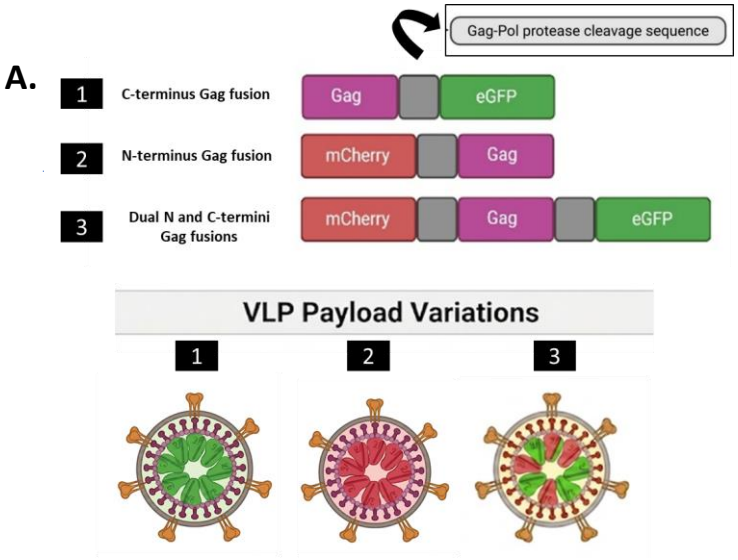

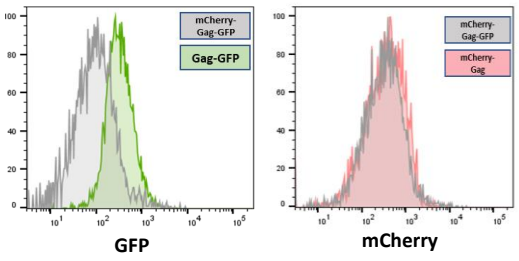

Sample name	MFI GFP	MFI mCherry
Gag-GFP VLP	307	-
mCherry-Gag VLP	-	352
mCherry-Gag-GFP VLP	89.6	316

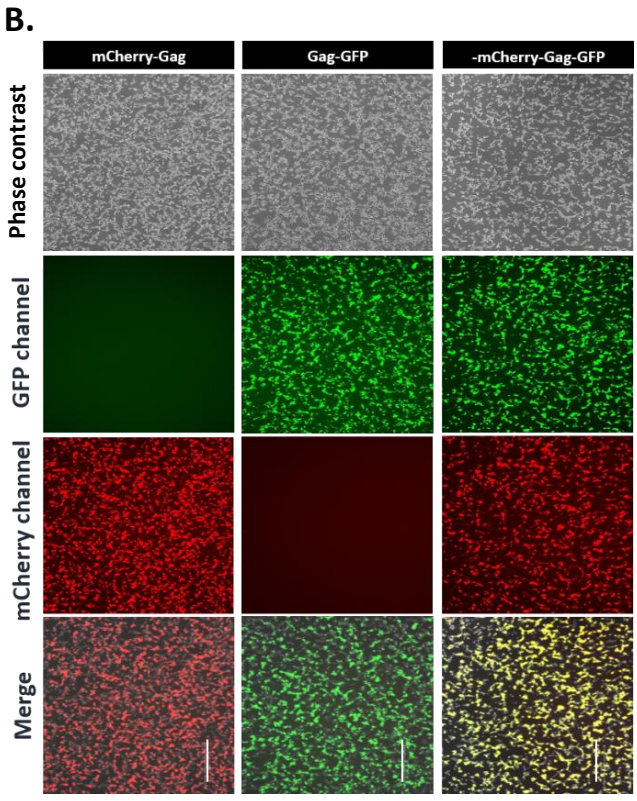

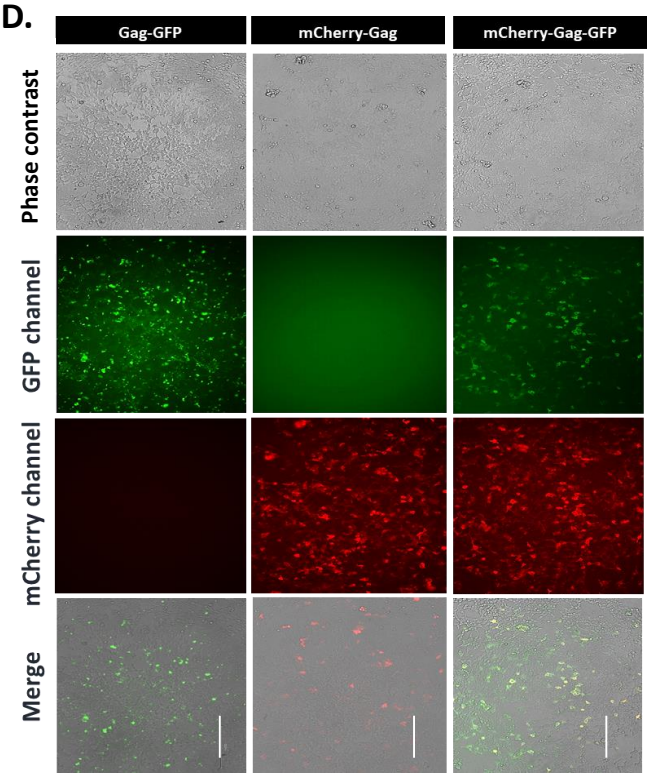

Figure 12: Evaluating VLP-mediated delivery of dual N and C-termini Gag fusion constructs. A. Schematic representation of Gag fusion designs, including single reporter constructs or dual-reporter constructs incorporating both N- and C- terminal Gag fusions. Proteins are separated from Gag by Gag-Pol protease cleavage site (shown in gray). **B.** HEK 293T VLP producer cells were imaged by fluorescence microscopy. Images were acquired at 4X magnification 24 h post-transfection. Scale bar= 600 µm. **C**. Flow cytometric analysis of single or dual reporter containing VLP-mediated protein transduction in HEK 293T cells 24 h post-transduction. Table summarizes MFI values of eGFP and mCherry. **D.** VLP transduction in HEK 293T cells shows eGFP alone, mCherry alone or delivery of both proteins within the cell. Images were taken at 4X magnification 24 h post-transduction by EVOS M5000, scale bar= 600 µm.

2.1.2 CRISPR-Cas9 loaded VLPs mediate efficient genome editing in recipient cells

As one of the project applications was to develop an efficient and modular VLP platform with potential to target cancers of several tissues, I wanted to employ VLPs for the delivery of genome editing Cas9-sgRNA complex for site-specific editing of DNA. The sgRNA directs endonuclease Cas9 to a specific DNA target site, introducing a site-specific double-stranded break[108]. Preliminary optimization studies were conducted to determine the optimal conditions for efficient VLP production and subsequent transduction of recipient cells. This was assessed based on analysis of *egfp* editing in eGFP-expressing HEK 293T cells, and evaluating the impact of varying plasmid DNA amounts and types of envelope glycoproteins.

Immunoblotting using lysates from HEK 293T producer cells confirmed the expression of the Gag-Cas9 fusion protein, detected at a molecular weight of about 220 kDa, corresponding to the combined molecular weights of the individual proteins (MLV Gag is reported to be 65 kDa while Cas9 is 160 kDa) **(Figure 13A)**. Next, I examined if the amount of plasmid DNA encoding VSV-G influenced VLP production efficiency. VLPs loaded with an *egfp* targeting sgRNA and Cas9 were produced in the presence of different amounts of VSV-G plasmid DNA (0.3 µg, 0.5 µg, 1 µg, 2 µg). A direct correlation was observed between the amount of VSV-G used for pseudotyping VLPs and the efficiency of VLP-induced loss of eGFP expression. VLPs produced by transfecting 2 µg of VSV-G showed the highest proportion of cells which lost eGFP expression (72%), followed by 1 µg (61%) (**Figure 13B, C**). However, since VSV-G toxicity in mammalian cells has been reported in the literature[109], I opted to transfect 0.5 µg of VSV-G plasmid for all subsequent studies, which showed ~55% of cells lost eGFP expression, which was comparable to the efficiency observed with 0.3 µg of VSV-G plasmid (53% loss of eGFP).

I next investigated whether the transfer of non-concentrated supernatant containing VLPs would result in comparable editing efficiencies to those achieved with particles concentrated using the commercially available reagent Lenti-X concentrator. I tested various volumes of non-concentrated VLP-containing supernatant (100, 250, 500, 1000, 2500 and 4000 µL), and observed a dose-dependent effect on eGFP editing, as determined by the MFIs of eGFP negative (eGFP-) cells at 120 h post-transduction. The transfer of 4 mL of supernatant resulted in the most pronounced reduction in eGFP signal **(Figure 13D**). In contrast, concentration of VLPs using the commercially available reagent Lenti-X concentrator followed by transduction of eGFP-expressing HEK 293T cells resulted in overall higher editing efficiencies compared to non-concentrated particles. Editing efficiency reached a plateau when 100 µL, 250 µL or 400 µL of concentrated particles was added to cells (**Figure 13E**). For both concentrated and non-concentrated VLPs, control VLPs (containing Cas9 and sgNTC) showed no changes in MFIs of eGFP. Based on these observations, I opted to use 100 µL of concentrated VLPs in subsequent experiments.

Next, I sought to determine if VLP production and transduction efficiency were affected by the type of envelope glycoprotein used for pseudotyping the particles. The VLPs produced for the delivery of eGFP, mCherry, Nanoluciferase and Cas9 in the data described thus far were pseudotyped with VSV-G, a well-known fusogenic glycoprotein which confers broad cellular tropism. However, I wanted to determine if use of an alternative envelope protein could further improve VLP transduction or enhance target cell specificity.

It has been reported that VLPs equipped with both the baboon endogenous virus Rless envelope protein (Brl) and VSV-G can improve Cas9 delivery in various cell lines[88]. To this end, I tested VSV-G and Brl for pseudotyping VLPs individually, or as a combination. Flow cytometric analysis of eGFP expression showed that at 72 h post-transduction, cells transduced with VLPs pseudotyped with VSV-G only displayed reduced eGFP expression, and by 120 hours, approximately 85% of cells lost eGFP expression in this condition, compared to 44% in cells which received Brl-pseudotyped VLPs and 61% in cells which received VLPs pseudotyped with the combination of VSV-G and Brl (**Figure 13F, G).** Together, these preliminary data suggest that in HEK 293T cells, VLPs pseudotyped with VSV-G provide superior Cas9/sgRNA delivery for genome editing compared to those pseudotyped with Brl alone or with a combination of VSV-G and Brl envelope proteins. Thus, I opted to use VSV-G alone for pseudotyping VLPs in all subsequent studies.

To visualize loss of eGFP expression in edited cells, I performed a colony formation assay and observed a comparable number of colonies in both control and experimental conditions. Importantly, colonies lacking eGFP expression were detected in the *egfp* targeting condition (**Figure 13H**). Among the cells which were transduced with Cas9 and *egfp* targeting VLPs, 40% of colonies were eGFP+ while 60% of colonies were eGFP- **(Figure 13I).** These results are consistent with the data obtained by flow cytometry, which showed 43.8% eGFP+ compared to 55.2% eGFP- cells following transduction (**Figure 13B)**. Together, these data suggest that VLPs can be used for efficient delivery of proteins with varying sizes and enable genome editing.

A.

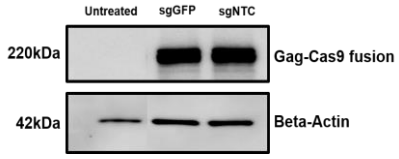

B.

VSV-G plasmid DNA (µg)	Edited cells (% GFP-)	Non-edited cells (% GFP+)
0.3	53.5	46.3
0.5	55.2	43.8
1	61.3	37.8
2	72	27

C.

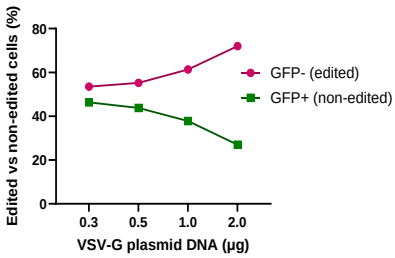

D.

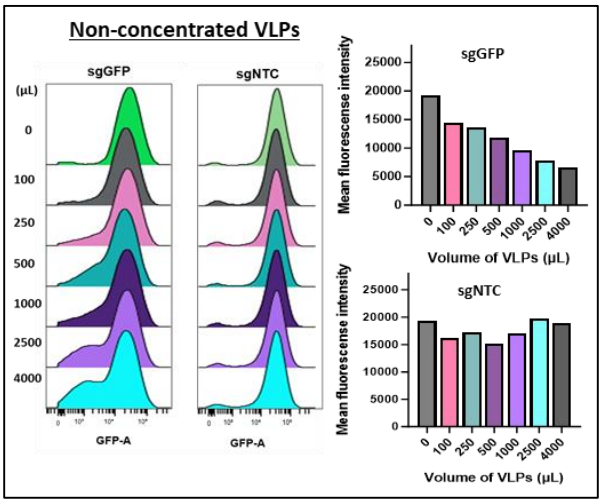

E.

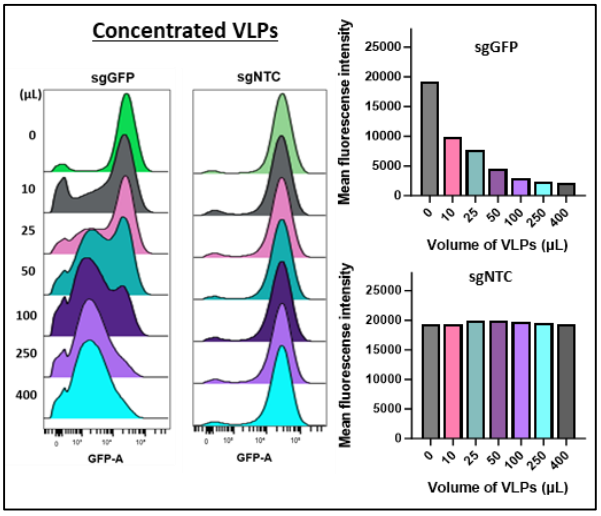

F.

Condition	Edited cells (% GFP-)	Non-edited cells (% GFP+)
VSV-G+ Brl	61.6	36.5
Brl	44.2	54.4
VSV-G	85.5	12.2

G.

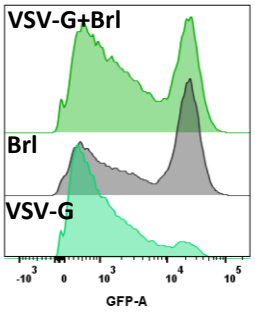

I

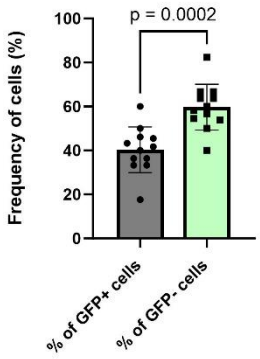

H.

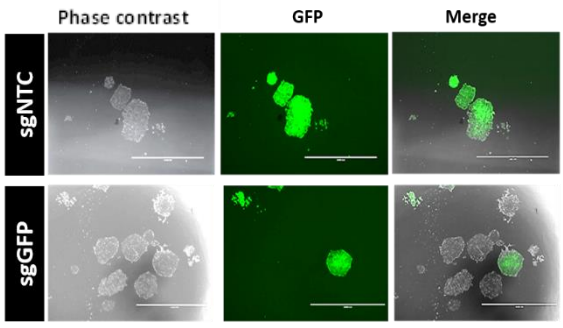

Figure 13: Optimizing MLV derived VLP production conditions. A. Immunoblot analysis of Gag-Cas9 fusion protein expression in HEK 293T transfected VLP producer cells. Blot was probed with anti-Cas9 antibody. Beta-actin loading control is shown in the bottom panel. **B, C.** Frequencies of eGFP edited cells following delivery of VLPs produced with varying amounts of VSV-G plasmid DNA (0.3 µg, 0.5 µg, 1 µg, 2 µg) at 120 h post-transduction (n=1). **D.** Flow cytometric assessment of mean fluorescent intensities of eGFP following delivery of various volumes of non-concentrated VLPs in eGFP expressing HEK 293T cells 120 h post-transduction. Overlapping histograms are shown in the left panel and quantification of MFIs is shown in the right panel. **E.** Similar to D, except comparison of MFIs following delivery of different volumes of VLPs concentrated with Lenti-X concentrator. **F.** VLPs were pseudotyped with different viral envelope glycoproteins; individually with VSV-G, Brl or a combination thereof**.** Table shows frequencies of edited cells at 120 h post-transduction as measured by flow cytometry. **G.** Overlapping histograms corresponding to cellular frequencies from F. **H.** Colony formation assay using HEK 293T cells which received control VLPs (top panel) or *egfp* targeting VLPs (bottom panel)**,** scale bar= 100 µm. **I.** Quantification of edited and non-edited colonies following delivery of VLPs loaded with Cas9 and *egfp* targeting sgRNA. (n=12 technical replicates). Shown is the mean ± standard error of the mean (SEM), p-value computed using unpaired Student's t-test.

2.1.3 Oncogenic inactivation of HPV18 E6 in cervical carcinoma cells results in cell death

HPVs are the causative agent of most cervical carcinomas as well as other tumor types, including head and neck cancers. Tumorigenesis is the result of deregulated expression of the viral onco-proteins E6 and E7, which induce degradation of tumor suppressors p53 and retinoblastoma (Rb) respectively. As a proof-of-principle to demonstrate the potential of VLP-mediated genome editing in a tumor context, I engineered MLV derived VLPs to deliver RNA-guided Cas9 and a sgRNA targeting the E6 or E7 coding sequences in human cervical carcinoma HeLa cells, which contain copies of the integrated HPV 18 genome.

As a means to rapidly identify and quantify insertions and deletions (indels) that arise after the introduction of double stranded breaks (DSBs), I employed Tracking of Insertions and Deletions by DEcomposition (TIDE) to predict the editing efficiencies of various sgRNAs targeting either E6 or E7 (**Figure 14A**). Among these, candidate sgRNA E6 0 was predicted to exhibit the highest gene editing efficiency. Consistent with this prediction, microscopic assessment revealed a substantial reduction in the number of HeLa cells 120 h post-VLP delivery, compared to untreated cells (mock) or cells which received Cas9 and a non-targeting control sgRNA (sgRNA NTC) (**Figure 14B**). TIDE analysis also predicted a 61% probability of adenine (A) insertion at the indel site, which was confirmed by sanger sequencing **(Appendix Figure 2A, B**). The remaining sgRNAs targeting E6 (E6 1, E6 2 and E6 3) produced a more modest impact on cell viability compared to sgRNA E6 0, in line with their lower editing efficiencies predicted by TIDE (43.1% for sgRNA E6 1 and 23% for both sgRNAs E6 2 and E6 3). In contrast, the sgRNAs targeting E7 had minimal impact on cell viability, and displayed relatively low predicted editing efficiencies (9.9% for sgRNA E7 1 and 35.1% for sgRNA E7 2). Based on these data, I selected sgE6 0 as the top candidate for subsequent assays.

Functional assays further supported the cytotoxic effect of E6 editing. A ~50% reduction in metabolic activity of edited cells was observed, as assessed by alamar blue assay (**Figure 14C**). Similarly, a colony formation assay demonstrated a significant decrease in clonogenic survival in E6 targeted HeLa cells compared to cells which received control VLPs (**Figure 14D**). To further assess cell death post-editing, flow cytometric assessment of Annexin-V staining comparing E6-targeted cells to controls, which consisted of empty vector VLPs (containing Cas9 but no sgRNA) and VLPs loaded with Cas9 and sgNTC showed higher MFIs at 72, 96 and 120 h post-VLP delivery (**Figure 14E**). Consistently in line with the MFIs, the % of Annexin-V+ cells following E6 editing was also elevated at 72, 96 and 120 h (**Appendix Figure 2C**).

As mentioned, loss of E6 protein expression is predicted to not only result in activation of p53, but also downstream effectors of p53 such as the cyclin-dependent kinase inhibitor p21. Indeed, I found a robust upregulation of both p53 and p21 protein levels in cells which received Cas9 and E6 targeting sgRNA loaded VLPs (**Figure 14F-J**). Taken together, these data suggest that Cas9 loaded VLPs can efficiently target and edit viral oncogenes in cancer cells, leading to induction of cell death.

A.

sgRNA	% efficiency predicted by TIDE
E6 0	78.5
E6 1	43.1
E6 2	23
E6 3	23
E7 1	9.9
E7 2	35.1

B.

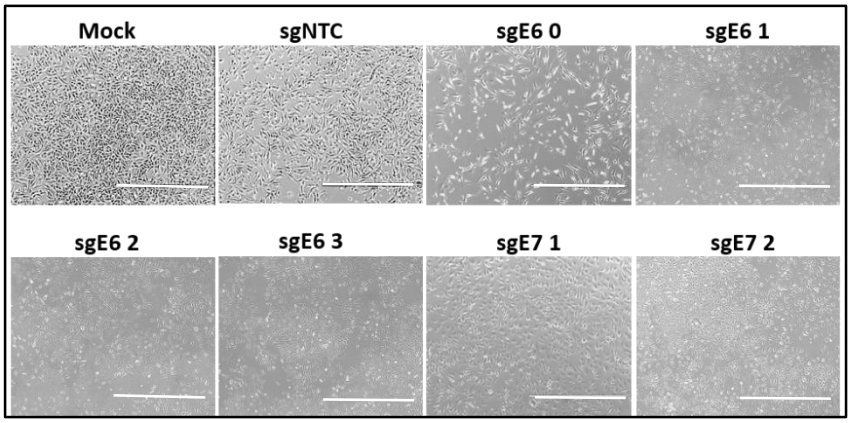

C.

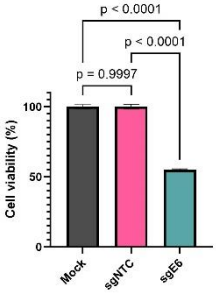

D.

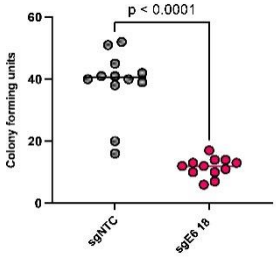

E.

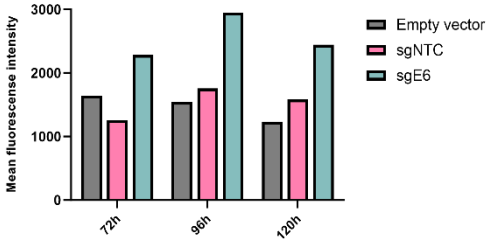

F.

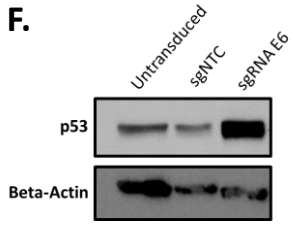

G.

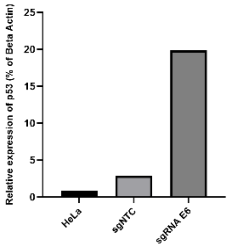

H.

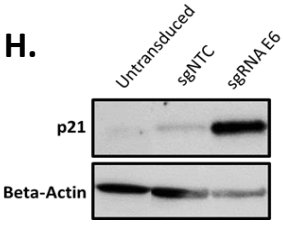

I.

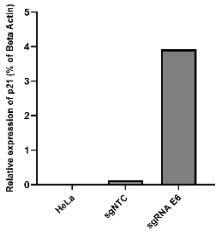

J.

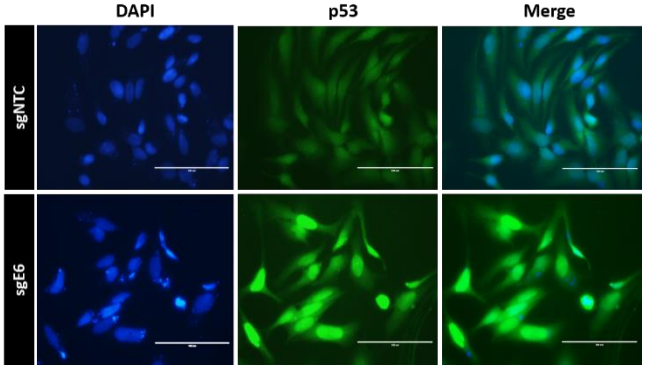

Figure 14: Targeting high-risk HPV 18 E6 and E7 oncogenes in HeLa cells using CRISPR-Cas9 loaded MLV VLPs. A. Table depicting the % of editing efficiencies for various E6 or E7 sgRNA candidates, as determined by TIDE analysis. **B.** Bright field microscopy images taken 120 h post-transduction demonstrate a reduction in HeLa cell number and changes in cell morphology following delivery of E6 or E7 specific sgRNAs. Images were acquired at 4X magnification using EVOS M5000. Scale bar =1000 μm. **C.** Metabolic activity of transduced cells was determined by alamar blue assay relative to sgNTC (n=3). Shown is the mean ± standard deviation (SD), p-value computed using one-way ANOVA. **D.** Colony forming assay following treatment of HeLa cells with Cas9/sgE6 or Cas9/sgNTC loaded VLPs (n=12 technical replicates). Shown is the mean ± SEM, p-value computed using unpaired Student's t-test. **E.** Mean fluorescence intensities of Annexin-V as determined by flow cytometric analysis. (n=1) **F-I.** Immunoblot of p53 and p21 expression in E6 edited HeLa cells. Beta-Actin was used as a loading control. (n=1) **J.** Immunofluorescence analysis of p53 upregulation in E6 edited HeLa cells compared to cells which received Cas9 and a control sgRNA, scale bar =100 μm.

Chapter 3: Bioengineering an oncolytic vaccinia virus for tumor localized lentivirus production

3.1 Characterizing a triple engineered virus

3.1.1 Generating a triple VV designed to encode SIN lentivirus vector components

Cytoplasmic replication is a unique feature for poxviruses, as DNA viruses typically replicate inside the host nucleus. As such, VV encodes factors required for cytoplasmic transcription and DNA replication[110]. Traditional recombinant VV rescue involves infection of cells with the virus followed by delivery of a homologous recombination template which includes a transgene, a selection marker and flanking homology arms that target the locus of insertion[73]. However, from the progeny virus, recombination rates have been reported to be quite low— ranging from 0.1-5%[73]. For efficient rescue of a triple engineered VV containing the lentivirus components, I employed CRISPR-Cas9 technology, which has been used to increase homologous recombination rates. I infected cells stably expressing Cas9, followed by transfection of a synthetic sgRNA targeting the locus of interest **(see Table 5 for sgRNA sequences)**. Recombinant clones are then enriched through marker selection by multiple rounds of plaque purification[66]. The virus rescue strategy was based on first inserting the lentivirus packaging component encoded by the *Gag* and *Pol* ORFs (referred to as Gag-Pol), followed by insertion of VSV-G, and then the lentivirus genome containing the desired transgene to generate a virus designated VV-lenti (**Figure 15A**). The rationale for insertion of Gag-Pol and VSV-G prior to the LV genome was to generate a modular platform, since the packaging and envelope remain constant irrespective of the desired lentivirus transgene. For transcription of each lentivirus element from the genome of VV, I employed a synthetic and compact VV promoter which was optimized with overlapping early and

late regulatory sequences for transgene expression (VV pE/L)[111]. I employed VV strain Western Reserve (WR), which was murine adapted[112], to facilitate downstream *in vivo* studies.

Gag-Pol was inserted into the A56R locus of VV WR and viral plaques were purified based on blue fluorescent protein (BFP) expression (**Appendix Figure 3A**). The resulting gene products were detected by Immunoblotting of cell lysate from infected cells; protein expression of both full-length capsid (p55) as well as the precursor proteins (p41 and p24)[113] was detected (**Appendix Figure 3B).** Following confirmation of Gag-Pol protein expression, I then inserted VSV-G into the B8R locus. Double recombinant plaques were selected based on expression of both BFP and eGFP by plaque purifying the virus for five passages. VSV-G protein was detected via Immunoblotting, and I confirmed that Gag-Pol expression remained stable in the double insertion containing virus (**Appendix Figure 3E-G**). Additionally, the viruses containing both single and double insertions showed no differences in growth kinetics or plaque diameters (measured 48 h post-infection), when compared to control viruses expressing only fluorophores from the same loci **(Appendix Figure 3 C, D, H, I).** Lastly, I inserted the lentivirus genome (containing eGFP as a transgene) in the TK locus of VV to construct a triple insertion containing VV. Here, I employed mCherry as a marker for selecting desired insertion-bearing plaques and purified VV expressing triple colored plaques (BFP+ GFP+ and mCherry+) (**Figure 15B**). Once again, immunoblotting of infected cells revealed the presence of Gag-Pol and VSV-G protein in the triple engineered virus (**Figure 15C, D**). To assess for the presence of the LV genome, I isolated viral genomic DNA and subjected the complete virus genome to Nanopore sequencing. Interestingly, despite the presence of mCherry indicative of homologous recombination of the insert on the VV genome, I observed loss of the entire lentivirus genome from VV, with only the presence of a solo LTR (**Figure 15E).**

I then postulated that periodic plaque purifications may have caused a population bottleneck resulting in selection of the LV-genome deleted virus, and that screening multiple clones may enhance the probability of selecting a stable virus. To this end, I subjected infected cells to multiple rounds of single cell sorting, with each infected cell representing a virus clone (**Figure 16A**). For a simple and rapid assessment of the lentivirus genome from VV, I devised a multiplexed PCR screening strategy which would inform me of three possible scenarios: (1) the presence of parental virus containing an intact TK locus, (2) VV containing the intact LV genome in the TK locus and (3) VV which has lost the LV genome.

Six overlapping PCR primers pairs were designed to screen for the presence and integrity of the LV genome within VV (**Figure 16B**). Forward primer 1 (1F) was designed to bind in the VV genome upstream of the left TK locus homology arm, while reverse primer 6 (6R) binds downstream of the right TK locus homology arm. VV WR with an intact TK locus and uninfected cells were included as controls, along with the lentiviral genome plasmid containing TK homology arms used in the virus rescue process. Amplification of WR (without a TK disruption, indicative of the parental virus) with primer 1F+6R should yield a ~1.1kb amplicon. In contrast, amplification of a ~2.2kb fragment using the same primer pair would strongly suggest that the lentiviral genome underwent rearrangement, resulting in retention of only a solo LTR and mCherry sequence. In theory, if the complete LV genome is present, amplification with primer pair 1F+6R should yield a ~7.2kb fragment.

After each round of sorting, initial screening of viral clones was performed in a multiplexed PCR reaction containing primer 1F+6R along with primer pair 3, the latter which targets sequences

located in the center of the lentiviral genome, and yields an expected band of ~1.4kb; detection of this band would indicate the presence of a likely intact lentiviral genome in VV (**Figure 16B, C**). Clones were categorized based on the observed banding patterns: those containing only the desired band (1401bp), mixed populations consisting of both the desired band and LV-genome deleted virus (1401bp and 2265bp) or clones demonstrating complete loss of the LV genome (2265bp band). Fifty clones were screened per round. After the first round of screening, none of the clones exhibited the desired band alone; the majority consisted of a mixed population, while the remainder contained only the LV-genome deleted virus. To continue selection of the triple virus, a clone in which amplification of 1401bp band with primer set 3 was observed was selected and further analyzed using all six PCR primer pairs before moving to the next round of virus passaging (**Figure 16E, F**). To confirm that amplicons were the expected products, upper (2265 bp) and lower (1401 bp) bands were subjected to sequencing (**Appendix Figure 4**), confirming PCR results. By the third round, the majority of clones exhibited loss of the LV genome, and after a total of five rounds of single cell sorting, all clones demonstrated loss of the LV genome **(Figure 16D).** Thus, both plaque purification and single cell sorting approaches failed to permit stable selection of the desired triple virus.

To facilitate rapid antibiotic selection of lentivirus-transduced target cells, the lentiviral genome construct was designed to express a puromycin resistance gene under the control of a mammalian phosphoglycerate kinase (PGK) promoter (**Figure 15A**). Despite the observation that serial passaging resulted in LV genomic loss from VV, LV particles could still be recovered from the supernatant of cells infected with the mixed VV populations. HEK 293T cells were transduced with the supernatant, and following puromycin-based selection of transduced cells (with 1 µg/

mL), a complete eGFP+ population was obtained and expanded in culture for up to one month (**Appendix Figure 5**).

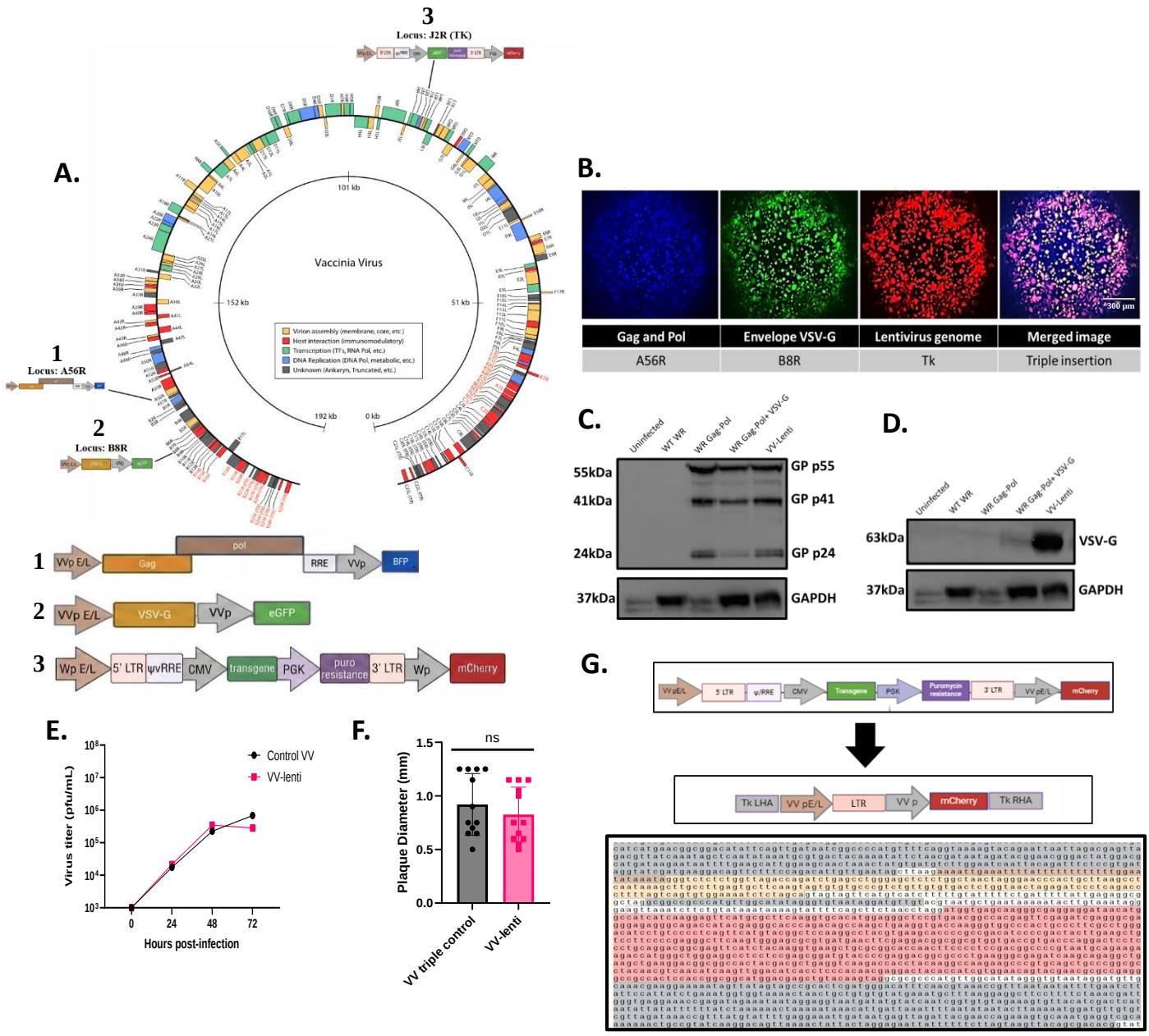
A.
3
Locus: J2R (TK)
1
Locus: A56R
2
Locus: B8R
Vaccinia Virus
101 kb
152 kb
51 kb
192 kb
0 kb
Virion assembly (membrane, core, etc.)
Host interaction (immunomodulatory)
Transcription (TFs, RNA Pol, etc.)
DNA Replication (DNA Pol, metabolic, etc.)
Unknown (Ankaryn, Truncated, etc.)
1 VVp E/L Gag pol RRE VVp BFP
2 VVp E/L VSV-G VVp eGFP
3 Wp E/L 5' LTR ψvRRE CMV transgene PGK puro resistance 3' LTR Wp mCherry
B.
300 µm
Gag and Pol
Envelope VSV-G
Lentivirus genome
Merged image
A56R
B8R
Tk
Triple insertion
C.
Uninfected
WT WR
WR Gag-Pol
WR Gag-Pol+ VSV-G
VV-Lenti
55kDa
41kDa
24kDa
37kDa
GP p55
GP p41
GP p24
GAPDH
D.
Uninfected
WT WR
WR Gag-Pol
WR Gag-Pol+ VSV-G
VV-Lenti
63kDa
37kDa
VSV-G
GAPDH
E.
Control VV
VV-lenti
Virus titer (pfu/mL)
Hours post-infection
F.
ns
Plaque Diameter (mm)
VV triple control
VV-lenti
G.
VV pE/L 5' LTR ψ/RRE CMV Transgene PGK Puromycin resistance 3' LTR VV pE/L mCherry
Tk LHA VV pE/L LTR VV p mCherry Tk RHA

Figure 15: Characterizing a triple insertion containing VV engineered to encode the components of a self-inactivating lentivirus vector. A. Construct design for sequential insertion of LV components: (1) *Gag* and *Pol* genes into the A56R locus (referred to as Gag-Pol), (2) VSV-G in the B8R locus and (3) lentivirus genome in TK (encoded by the J2R gene). Circular map of VV genome generated by Dr. Adrian Pelin. **B**. Representative fluorescence microscopy images of triple engineered VV plaques in U2OS cells were captured 48 h post-infection following plaque purification, at 10X magnification using EVOS M5000 microscope. Merged image shows overlapping fluorescence for BFP, eGFP and mCherry. Respective transgene and locus of insertion is shown below each color. Scale bar= 300 µm. **C.** Immunoblotting of lentivirus capsid (HIV-1 p24) expression from whole cell lysates of U2OS cells infected with triple engineered VV. Single and double engineered VV encoding Gag-Pol were used as positive controls (lanes 3, 4). GAPDH was used as a loading control. GP denotes Gag-Pol. **D**. Immunoblotting of VSV-G expression, performed to confirm the presence of VSV-G in triple engineered VV using whole cell lysates of infected U2OS cells. GAPDH was used as a loading control. **E.** Multistep growth curves comparing triple engineered VV with only fluorophores as a control to VV encoding the lentivirus components (n=1). **F**. Plaque diameters comparing triple engineered control virus to VV-lenti, as measured using EVOS M5000. (n=12), shown is the mean ± SD, p-value computed using unpaired Student's t-test. **G.** Viral genomic DNA was isolated from purified virus, and the complete genome was sequenced with Nanopore technology. Sequences highlighted in grey represent left and right homology arms for the TK locus, VV early-late promoter transcribing the lentiviral insert is shown in brown, the sole remaining sequence from the lentiviral genome (solo LTR) is shown in beige and selection marker mCherry is in red.

A.

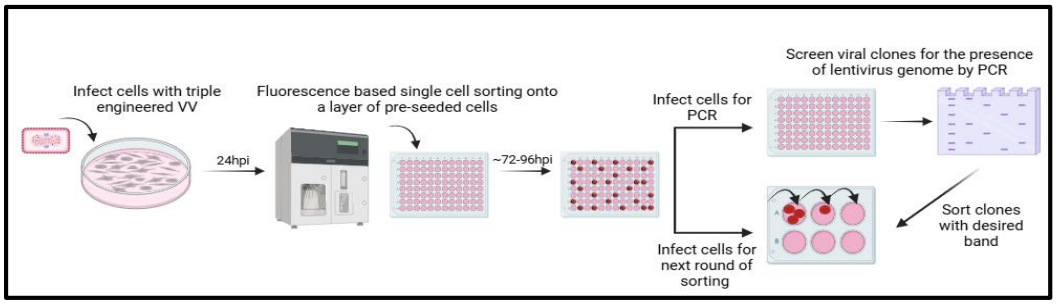

B.

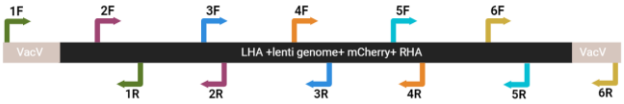

C.

Sample name	Complete lentiviral genome						WT WR	Complete lentiviral genome	Solo LTR recombinant lentiviral genome
Primer pair	1	2	3	4	5	6	1F+6R		
Expected band (bp)	1109	1191	1401	1412	1335	1283	1153	7228	2265

D.

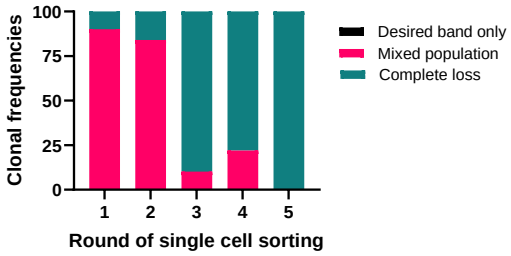

E.

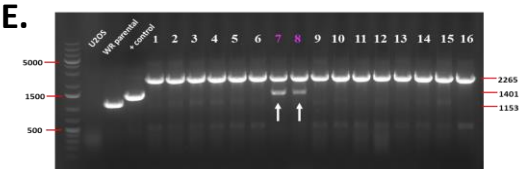

F.

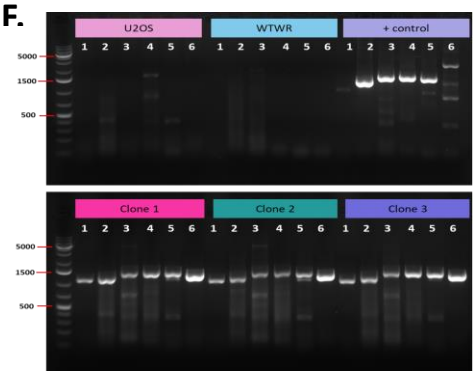

Figure 16: High-throughput rescue strategy does not enable stable VV rescue as revealed by a PCR screening strategy. A. Schematic representation of single cell sorting procedure for the generation and selection of engineered VV clones. **B.** Schematics of overlapping PCR primer design for detecting the complete lentiviral genome from VV. Center region shows left and right TK homology arms (denoted LHA, RHA) while extremities represent the VV genome excluding TK homology arms. **C.** Expected band lengths (in bp) of primer pairs used to screen for the presence of lentiviral genome from VV. **D.** Frequency of virus clones based on banding patterns, as determined by PCR with primer set 3 and 1F+6R. 50 clones were screened/round. **E.** Agarose gel electrophoresis of PCR amplified products using primers 1F+6R along with primer pair 3 (top panel) and primer pairs 1-6 (middle and bottom panel) described in B. Uninfected U2OS cells and VV encoding Gag-pol+VSV-G infected U2OS cells were used as negative controls (referred to as parental virus), while the plasmid used for homologous recombination (lentivirus genome flanked by TK homology arms) was used as a positive control. White arrows indicate 1401bp band in clones 7 and 8. **F.** Clones in which amplification of 1401bp band with primer set 3 was observed were then subjected to PCR with primer sets 1-6 to detect complete lentivirus genome from the TK locus.

3.1.2 Deletion of an LTR abrogates recombination of the lentiviral genome from VV

Since I observed persistent expression of mCherry despite the loss of the LV genome from VV, and the mCherry sequence is situated downstream of the 3'LTR, I wanted to investigate if genetic instability of the lentivirus genome in VV was due to active transcription or was due to sequence homology between the LTRs at the genomic level. To address this, I generated constructs in which either the VV early-late promoter transcribing the lentiviral genome or either the 5'LTR or the 3'LTR was removed (VV-lenti$^{-/-}$5'LTR or VV-lenti$^{-/-}$3'LTR) **(Figure 17A, C, E).**

I hypothesized that if transcription-dependent recombination, potentially mediated by RNA-DNA hybrid structures was occurring, then implementing an inducible system would reduce recombination events. However, after only three rounds of single cell sorting, I found that the promoter deleted lentiviral genome was unstable, as by the third round all viral clones showed complete loss of the LV genome from VV by PCR. These findings suggest that transcription-driven recombination of the LV genome from VV is unlikely (**Figure 17B**).

The continual presence of a solo LTR in the triple engineered VV suggests that LTR sequences themselves contribute to genomic instability, which could be due to homologous recombination events occurring between the identical 5' and 3' LTR sequences flanking the lentiviral genome. When screening both VV-lenti$^{-/-}$5'LTR and VV-lenti$^{-/-}$3'LTR by multiplexed PCR with primer pairs 1F+ 6R and 3F+ 3R, I observed that by 4 rounds of sorting, every clone screened remained stable, and no amplicon suggestive of a LV-deleted genome was detected (**Figure 17D, F**). These results suggest that LTR mediated-recombination explains the loss of the lentiviral genome when expressed from VV (**Figure 17G**).

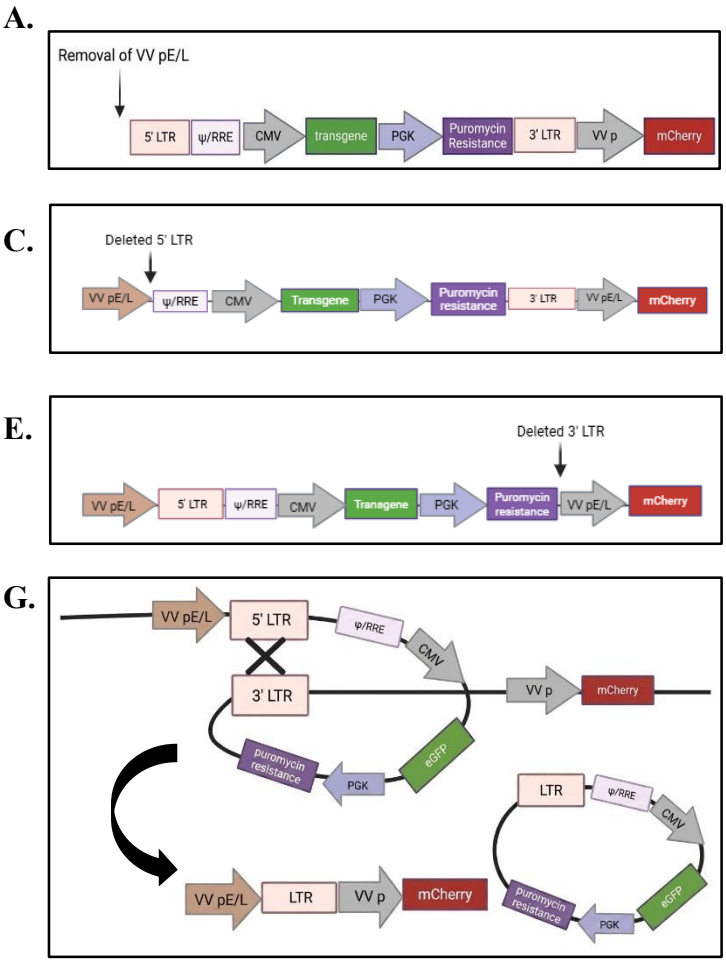
A.
Removal of VV pE/L
5' LTR
ψ/RRE
CMV
transgene
PGK
Puromycin Resistance
3' LTR
VV p
mCherry
C.
Deleted 5' LTR
VV pE/L
ψ/RRE
CMV
Transgene
PGK
Puromycin resistance
3' LTR
VV pE/L
mCherry
E.
Deleted 3' LTR
VV pE/L
5' LTR
ψ/RRE
CMV
Transgene
PGK
Puromycin resistance
VV pE/L
mCherry
G.
VV pE/L
5' LTR
ψ/RRE
CMV
3' LTR
VV p
mCherry
puromycin resistance
PGK
eGFP
LTR
ψ/RRE
CMV
VV pE/L
LTR
VV p
mCherry
puromycin resistance
PGK
eGFP

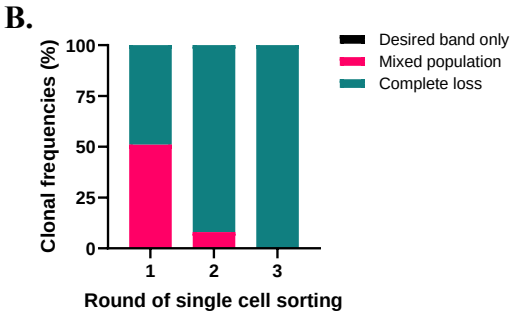
B.
Clonal frequencies (%)
100
75
50
25
0
1
2
3
Round of single cell sorting
Desired band only
Mixed population
Complete loss

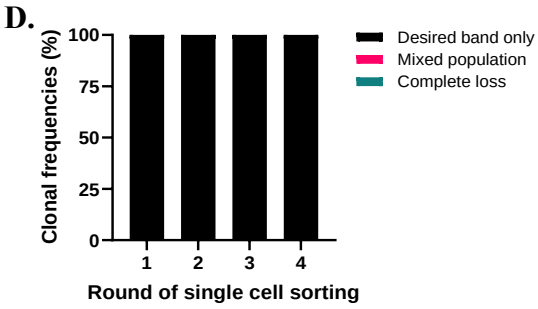
D.
Clonal frequencies (%)
100
75
50
25
0
1
2
3
4
Round of single cell sorting
Desired band only
Mixed population
Complete loss

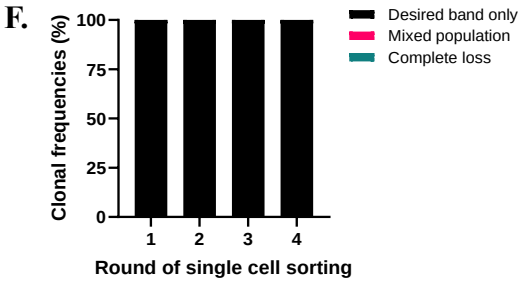
F.
Clonal frequencies (%)
100
75
50
25
0
1
2
3
4
Round of single cell sorting
Desired band only
Mixed population
Complete loss

Figure 17: Determining the mechanism of LV genome recombination from VV. **A**. Lentiviral genome construct lacking the synthetic VV promoter, preventing transcription from engineered VV. **B.** After three rounds of single cell sorting, PCR amplification with primer 1F+6R and primer pair 3 showed a decrease in clones containing the desired insert. 50 clones were screened per round. **C**. Construct design for deletion of the 5'LTR from the lentiviral genome. **D**. After four rounds of single cell sorting, PCR amplification with primer 1F+6R and primer pair 3 shows that deletion of 5' LTR results in stable insertion of the LV genome from VV. 50 clones were screened per round. **E**. Construct design for deletion of the 3'LTR. **F.** Similar to results obtained in D, PCR amplification with primer 1F+6R and primer pair 3 shows that deletion of 3' LTR results in a stability of the LV genome from VV, following four rounds of single cell sorting. 50 clones were screened per round. **G.** Proposed mechanism of LTR-mediated recombination. Association of the two LTRs leads to excision of the intervening sequence and deletion of the LV genome from VV. The resulting recombination products are shown. Schematics were made using BioRender and FigureLabs.

3.1.3 Introduction of a puromycin resistance gene under transcriptional control of a VV promoter permits stability of the lentiviral vector genome from VV

Viruses are considered obligate intracellular parasites- strictly dependent on host cell translation machinery, while the host cell in turn has mechanisms to dampen translation to inhibit virus replication within the cell. Our research group previously built on this concept by using antibiotics at minimal concentrations, such that virus replication is limited without impacting cell viability for rapidly generating transgene containing viruses[74]. This strategy involved incorporating an antibiotic resistance gene within the viral backbone, resulting in survival of only viral copies which successfully incorporated the antibiotic resistance when passaged in the presence of the cognate antibiotic. My initial construct design featured a puromycin resistance gene under transcriptional control of a PGK promoter, typically used for rapid selection of lentivirus transduced cells in the presence of puromycin (**as shown in Appendix Figure 5**). Due to the instability of the lentiviral genome expressed from VV during attempts to rescue the recombinant virus by plaque purification or single cell sorting, combined with the observation that the presence of two LTRs was causing recombination of the intervening sequence, I modified initial design of the construct such that the puromycin resistance gene was now controlled by a VV transcription unit, driven by VV H5R promoter, a naturally occurring early-late promoter, to generate VV-lenti-puro-eGFP (**Figure 18A**).

The modified VV-lenti-puro-eGFP virus was passaged in the presence of puromycin at a concentration of 1µg/mL. After continuous passages in the presence of puromycin, multiplexed PCR screening detected the amplicon of interest (1401 bp), and importantly, the presence of undesired recombination was undetected (**Figure 18B**). Interestingly, I observed that amplification

of WR without a disruption of the TK locus, representative of the parental virus, was detected even with puromycin supplementation (1153 bp band), despite this virus lacking the puromycin resistance gene. However, this population was cleared by passage 5 with the presence of puromycin, suggesting that continuous passaging under puromycin selection enables the generation of a stable VV.

After only one passage in the absence of puromycin followed by plaque purification of 4 different clones, three of them showed a mix banding pattern consisting of the desired band at 1401bp but also LV-genome deleted VV, detected by the presence of a 2265 bp band (clones 1-3, denoted as C1-C3) and one VV clone showed complete loss of the LV genome, as evidenced by detection of only an amplicon of 2265 bp (clone 4, denoted as C4) (**Figure 18C**). To characterize the newly generated VV-lenti-puro-eGFP, I performed multi-step growth kinetics and measured viral plaque diameters by microscopy, compared to a triple deleted control virus containing only fluorophores in A56R, Tk and B8R loci, and observed no changes (**Figure 18D, E**).

To evaluate the ability of the modified VV to generate the components for production of functional, transduction-competent LV particles, I infected CV-1 cells in the presence of puromycin for 48 h, after which I collected the supernatants. To avoid risk of VV-based contamination, I filtered the supernatant through a 0.1 μm filter, concentrated particles and transduced a monolayer of CV-1 cells (**Figure 18F**). By day one post-transduction, a few eGFP+ cells were seen, with expansion of these cells by day five. Since VV was triple colored, the BFP and mCherry channels were also imaged, and no fluorescence was detected, suggesting that VV was cleared and the eGFP+ cells were a product of lentivirus transduction.

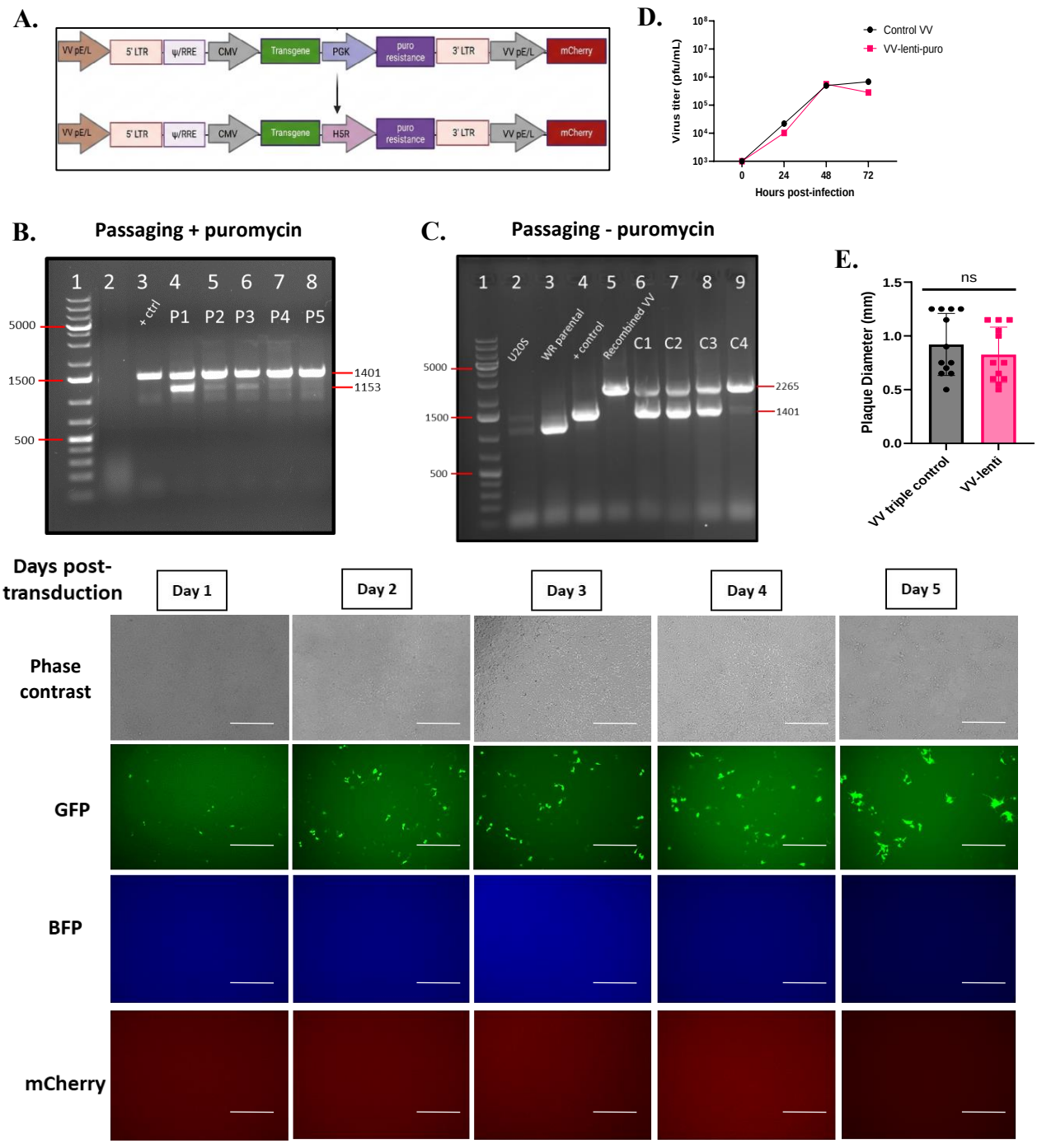
A.
VV pE/L
5' LTR
ψ/RRE
CMV
Transgene
PGK
puro resistance
3' LTR
VV pE/L
mCherry
H5R
D.
Control VV
VV-lenti-puro
Virus titer (pfu/mL)
Hours post-infection
B.
Passaging + puromycin
+ ctrl
P1
P2
P3
P4
P5
1401
1153
C.
Passaging - puromycin
U20S
WR parental
+ control
Recombined VV
C1
C2
C3
C4
2265
1401
E.
ns
Plaque Diameter (mm)
VV triple control
VV-lenti
F.
Days post-transduction
Day 1
Day 2
Day 3
Day 4
Day 5
Phase contrast
GFP
BFP
mCherry

Figure 18: Puromycin selection facilitates the generation of a stable triple engineered VV platform that is capable of producing lentivirus particles. A. Schematics show the swapping of PGK promoter driving the puromycin resistance gene in the original LV genome construct to VV early/late H5R promoter. **B.** PCR analysis with primer pairs 1F+6R and 3F+3R, after five passages of triple recombinant VV in the presence of 1 µg/mL of puromycin. **C.** Virus described in C was grown in the absence of puromycin, after which plaques from four individual clones were picked and analysed by PCR with primer pairs 1F+6R and 3F+3R. C1-C4 represent 4 different plaque purified clones. **D.** Multistep growth curves comparing VV with triple insertion of fluorophores as a control, to VV-lenti encoding the LV components, with the LV genome containing a VV driven puromycin resistance gene (n=1). Viruses were grown in the absence of puromycin. **E.** Plaque diameters measured at 10X magnification using EVOS M500 microscope (n=12). Shown is the mean ± SD, p-value computed using unpaired Student's t-test. **F.** Transduction of CV-1 cells with lentivirus encoding *egfp* produced from cells infected with triple engineered VV that was maintained under puromycin selection (1 µg/mL). Images taken at 10X magnification using EVOS M5000, scale bar= 300 µm.

3.1.4 Lentivirus particles produced from VV infected cells can deliver functional transgenes

Since lentivirus-mediated delivery of *egfp* was based on assessment of reporter expression, I then wanted to test a functional readout of the developed platform. I employed the Cre-LoxP system by engineering VV-lenti to deliver Cre recombinase. This assay was based on observing a color switch in reporter expressing cells. Briefly, cells which have not been transduced with Cre encoding lentivirus express dsRED, but upon delivery of Cre, cells are converted to GFP expression (**Figure 19A).** Lentivirus was produced from VV-lenti-puro-Cre in a similar manner to that described for production of LV from VV-lenti-puro-eGFP. Concentrated lentivirus was added to HEK 293T reporter cells or murine MC38 colorectal cancer reporter cells. In the HEK 293T cells, red-to-green conversion, indicative of lentivirus transduction, was imaged at 72 h (**Figure 19B**). Similarly, in the MC38 cells, GFP+ cells were imaged at 72 h **(Figure 19C).** Untransduced cells did not demonstrate any signs of GFP expression, indicating that GFP conversion was a result of Cre transduction and not background fluorescence. Based on fluorescence conversion, this data demonstrated the production of LV particles from VV-infected cells.

A.

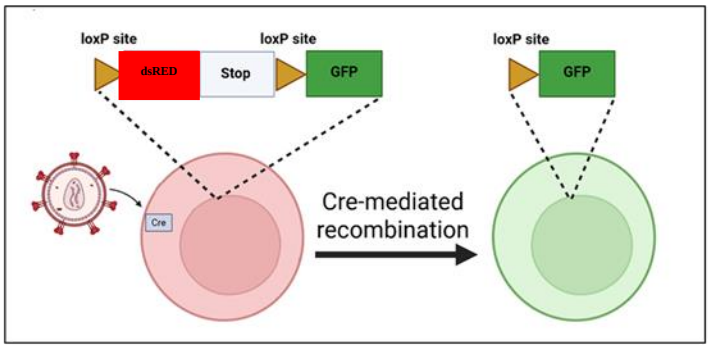
loxP site
dsRED
Stop
loxP site
GFP
loxP site
GFP
Cre
Cre-mediated
recombination

B.

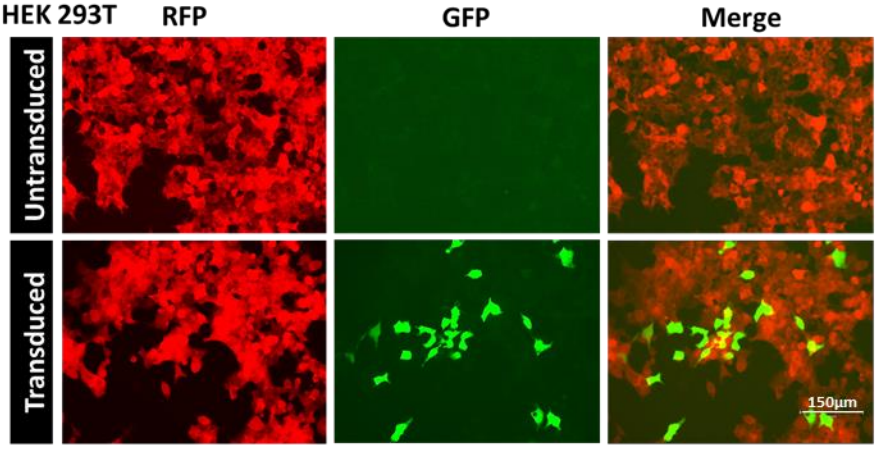
HEK 293T
RFP
GFP
Merge
Untransduced
Transduced
150µm

C. MC38

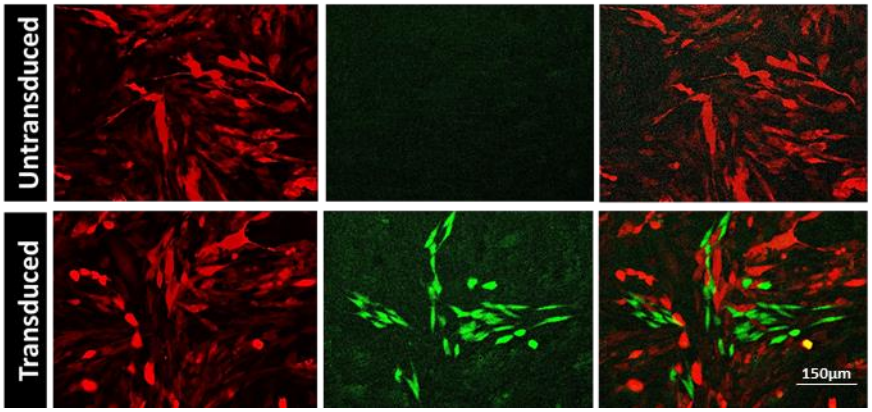
Untransduced
Transduced
150µm

Figure 19: Assessing the functionality of Cre recombinase containing lentivirus particles produced from engineered VV infected cells. A. Color switch based on Cre-mediated recombination of LoxP sites. Cells constitutively expressing dsRed convert to GFP upon Cre-mediated recombination. CV-1 cells were infected with engineered VV at an MOI of 0.02 and lentivirus was harvested from the supernatant 48 h post-infection. **B.** Transduction of Cre in HEK 293T Cre reporter cells 72 h post-transduction with concentrated lentivirus particles. Images taken at 20X magnification, on EVOS M5000 microscope. **C.** Similar to B, except transduction of Cre in MC38 Cre reporter cells 72 h post-transduction. Scale bar in B and C= 150µm.

3.1.5 Detection of intracellular VV and LV particles released into the supernatant of engineered VV infected cells

Transmission electron microscopy (TEM) was performed to assess the presence of VV particles within infected cells and lentivirus particles in the culture supernatant from VV-lenti infected cells. Based on virus biology, LV particles were expected to be released by budding from the host cells, and thus detected primarily in the supernatant, while VV is predominantly an intracellular virus (most of the particles remain within the infected cell as IMVs)[114].

Consistent with these expectations, TEM analysis of U2OS cells infected with control wild type (WT) VV at an MOI of 0.5, imaged 24 h post-infection, revealed the presence of VV particles at various stages of the viral morphogenic pathway. The earliest formed structures in the VV replication cycle- viral lipid crescents- were observed within the cytoplasm. In addition, multiple characteristic brick-shaped IMVs were detected (**Figure 20A, left image**). Most notably, imaging of cells infected with VV-lenti revealed the presence of CEV (a double membrane enclosed particle) on the periphery of the infected cell, in close association with released LV particles, spherical in shape and surrounded by a membrane (**Figure 20A, right image**).

As a control for LV particle detection in the supernatant, U2OS cells were transfected with LV producer plasmids encoding the packaging, envelope glycoprotein VSV-G and the genome, the typical laboratory method for LV production. Concentrated supernatant collected from the control condition clearly depicted a spherical LV particle surrounded by a membrane (**Figure 20B left image**). Since Gag assembly culminates in the formation of LV particles devoid of a viral genome, I also infected cells with VV engineered to encode for Gag-Pol and VSV-G in the absence of the LV genome (double engineered virus described in **Appendix Figure 3**). Concentrated supernatant from VV-Gag-Pol+VSV-G also revealed the presence of LV particles (**Figure 20B, middle**

image). In addition to detecting LV particles on the periphery of cells infected with VV-lenti, LV was also detected from the supernatant of VV infected cells (**Figure 20B, right image**). Importantly, the detection of both VV and LV particles by TEM shows that integrity of the viral particles arising from the engineered vector is maintained when compared to respective controls.

A.

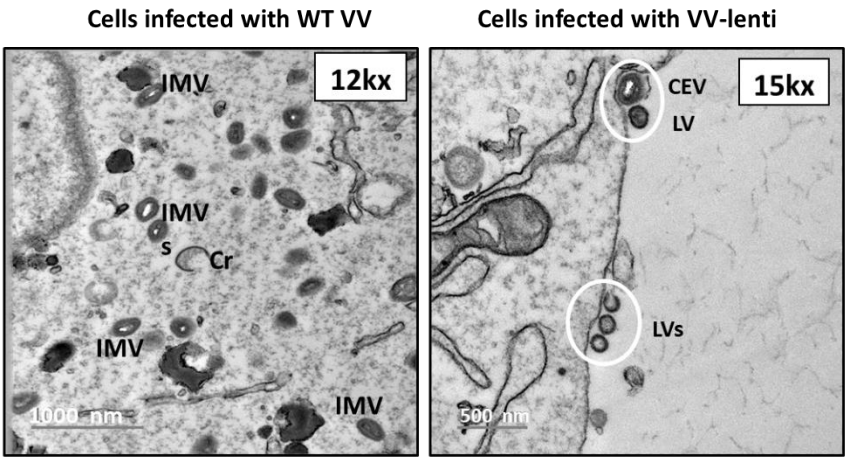
Cells infected with WT VV
Cells infected with VV-lenti
12kx
IMV
IMV
s
Cr
IMV
IMV
1000 nm
15kx
CEV
LV
LVs
500 nm

B.

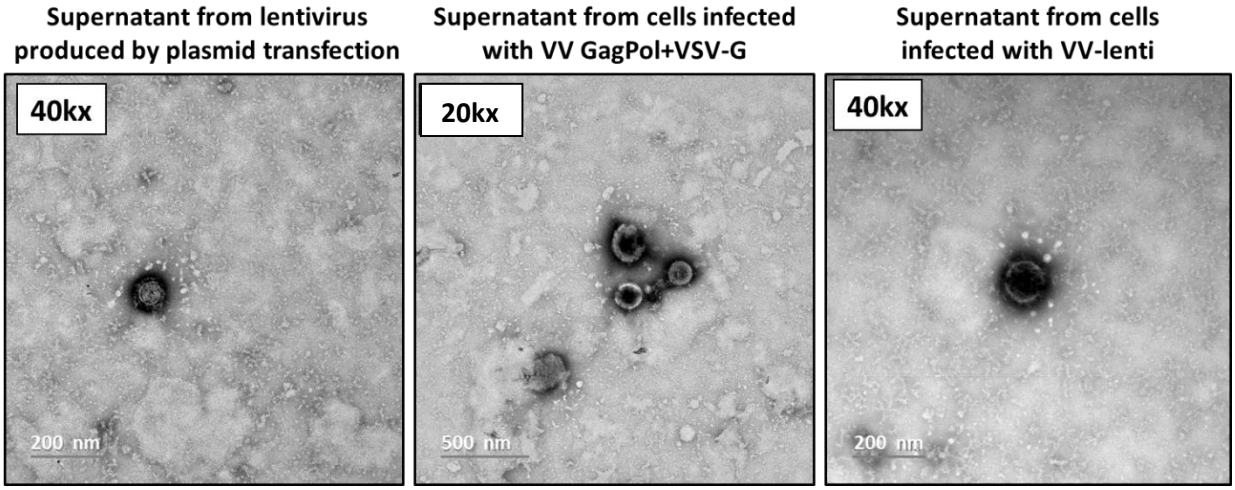
Supernatant from lentivirus produced by plasmid transfection
Supernatant from cells infected with VV GagPol+VSV-G
Supernatant from cells infected with VV-lenti
40kx
200 nm
20kx
500 nm
40kx
200 nm

Figure 20: Electron microscopic assessment of VV and LV particles from infected cells and their supernatants. A. Representative TEM images of U2OS cells infected with WT VV (left image) or with VV-lenti (right image) at an MOI of 0.5, imaged 24 h post-infection. In VV-lenti infected cells, the periphery of the cell shows an EEV particle with surrounding LV particles (circled in white). **B**. EM images of LV particles detected from the concentrated supernatants of (1) control LV produced by transfection of plasmids encoding the packaging, envelope glycoprotein and genome; (2) cells infected with double insertion containing VV encoding Gag-Pol and VSV-G; and (3) cells infected with VV-lenti. Image magnifications are shown in the top corners. Cells and supernatant were harvested 24 h post-infection. Abbreviations: Crescents (Cr), intracellular mature virus (IMV), extracellular enveloped virus (EEV), lentivirus (LV). Scale bar shown in bottom left corner of each image.

3.1.6 Abortive VV infection in Chinese Hamster ovary (CHO) cells enables detection of eGFP+ cells, consistent with lentivirus-mediated transduction

VV has a broad host-range, however, productive infection depends on viral host-range factors[115]. VV lacks a functional CP77 host-range gene, required for productive infection of CHO cells. Although VV can enter CHO cells and initiate early stages of infection, productive VV infection is restricted due to impaired intermediate and late stage viral gene expression[116,117]. As such, this cell line was a suitable model to bypass the requirement of physical removal of VV from the culture supernatant (as previously conducted by filtration), a process which could result in loss of some lentivirus. Of note, puromycin was not added to the cell culture medium in this experiment to avoid any selection-associated toxicity.

A monolayer of CHO cells was infected with VV-lenti-eGFP at an MOI of 0.5 and within the first 48 h post-infection, VV infection was observed based on the presence of triple fluorescence (eGFP+, BFP+, mCherry+) in infected cells. By one-week post-infection, minimal VV-associated triple fluorescence was observed, suggesting that many of the VV infected cells were cleared and the monolayer of cells recovered. Further, a population of cells which were only eGFP+ was observed, consistent with lentivirus-mediated transduction (**Figure 21**).

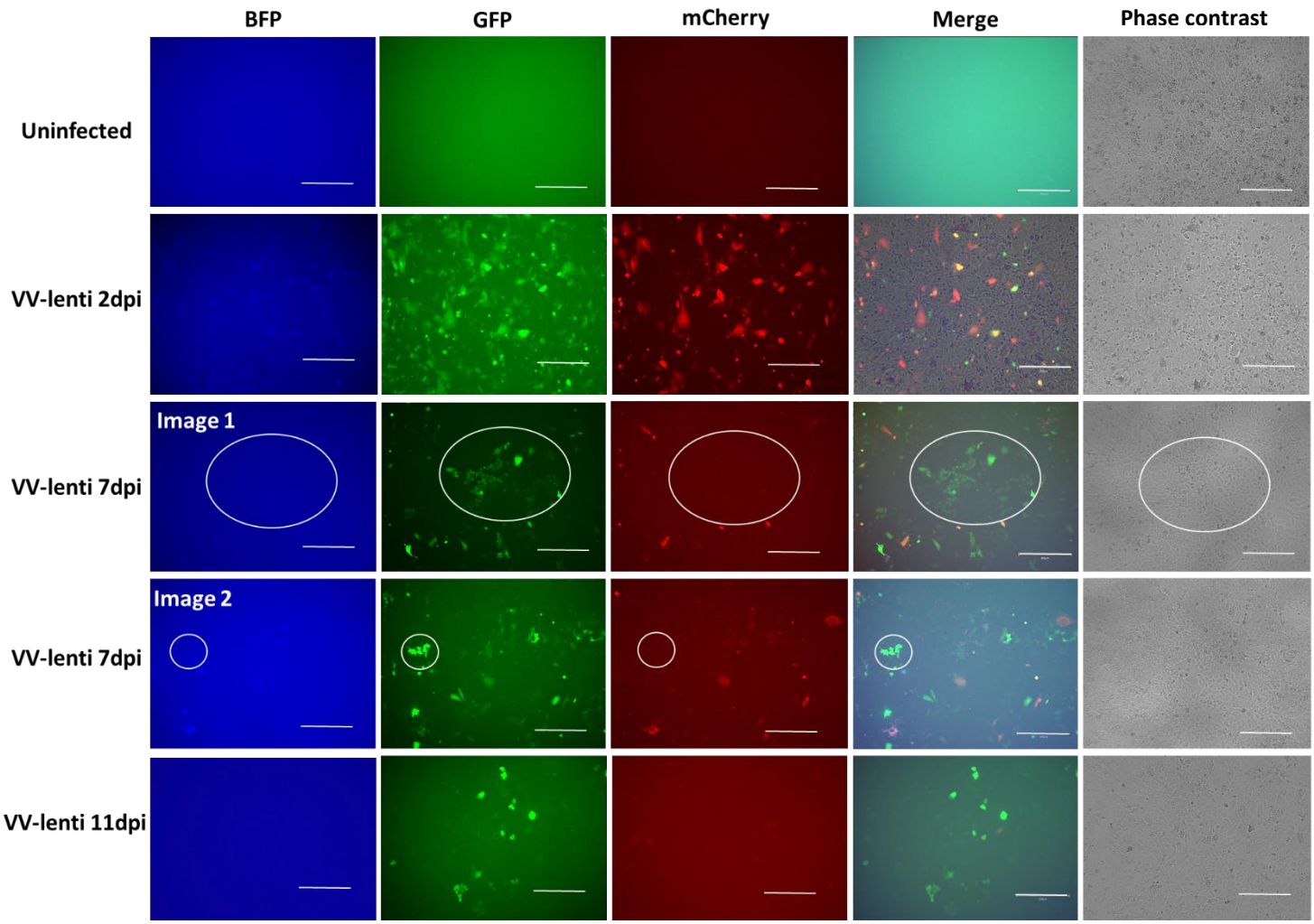
BFP
GFP
mCherry
Merge
Phase contrast
Uninfected
VV-lenti 2dpi
Image 1
VV-lenti 7dpi
Image 2
VV-lenti 7dpi
VV-lenti 11dpi

Figure 21: Abortive VV infection in CHO cells enables detection of eGFP+ cells, consistent with lentivirus-mediated transduction. CHO cells were infected with engineered VV at an MOI of 0.5. By 48 h post-infection, VV infection was detected based on triple positive fluorescence (BFP, GFP, mCherry). One-week post-infection, most VV-infected cells were cleared and a population of only eGFP+ cells were observed (circled in image 1 and image 2), consistent with lentivirus-mediate delivery of eGFP. Cells were also imaged on day 11. Scale bar= 300 µm.

Chapter 4: Discussion

4.1 Summary of research findings and general discussion

Viral vectors have emerged as powerful platforms in the development of cancer immunotherapies. In this study, I first developed a retroviral VLP platform for transient delivery of proteins. In a proof-of-concept, preliminary data demonstrated that engineered VLPs containing Gag fusion constructs at either the N-terminus, the C-terminus, or both, delivered reporter payloads to recipient cells (**Figures 11, 12**). Since VLPs are not constrained by strict cargo size limitations, and can package RNP complexes, they are well-suited for transient delivery of genome editing agents. This transient exposure reduces the risk of off-target editing by limiting the duration of exposure of the genome editing agent[85]. Using this platform, I first conducted optimization studies (**Figure 13**), and then delivered CRISPR-Cas9 for targeting the HPV 18 oncogene E6 in HeLa cervical carcinoma cells, where I observed a reduction in cell viability **(Figure 14**).

It is now well-established that OVs contribute to combination therapy regimens which fall into three categories[118]. First, OVs can be combined with current standard of care options. Second, combination strategies can be designed to overcome barriers to OV efficacy by pairing OVs with therapeutics that target these barriers. Third, OVs have been explored with combinations of other forms of immunotherapies. However, rather than a "cocktail" of combinations which rely on administration of multiple therapeutic agents, OVs provide tremendous advantage owed to the construction of rationally designed and engineered vectors that engage the immune system through multiple mechanisms, thereby representing an innovative strategy in cancer immunotherapy.

Building on this concept, I then designed a hybrid viral platform combining the oncolytic capacity of VV with the gene delivery properties of LV vectors, thereby generating a single vector encompassing the properties of both tumor-targeting viruses and stable gene delivery. The application of sequencing has provided molecular insights into how recombination affects poxvirus biology[67]. As such, based on whole-genome sequencing of the initially designed virus, I identified a key limitation: LTR-mediated recombination resulting in excision of the LV genome from VV (**Figures 15-17**). Additionally, the high resolving power of EM enables nanometer scale studies, providing direct images of virion structure, localization and measurement of particles[119]. VV virions were first visualized by EM as large, brick-shaped particles measuring 360 x 270 x 250 nm[120,121], while EM-based detection of lentivirus particles demonstrated spherical structures between 80 and 120 nm in diameter[122]. Thus, I employed EM to detect both VV and LV particles in the cellular and supernatant fractions of VV-lenti infected cells (**Figure 20**).

My observation of LTR-mediated recombination is consistent with prior reports of retroviral sequence instability within large DNA viruses. As outlined in the introduction, FPV was found to harbor integrated sequences of REV in both field isolates (wild-type strains) and commercial vaccine strains. Characterization of various FPV strains revealed REV LTRs of various lengths found within the FPV genomes, including LTR truncations or deletions[102]. These observations are consistent with our findings, supporting the notion that LTR-mediated recombination can drive deletion events from large DNA virus genomes, such as VV.

More broadly, LTR-mediated recombination is perhaps not unexpected, as recombination plays a critical role in evolution, contributing to creating genetic diversity. Human endogenous

retroviruses (HERVs), which are sequences derived from ancient retroviruses, comprise ~8% of the human genome[123]. Over time, their LTRs have accumulated mutations and have undergone homologous recombination, reducing them to the so-called 'solo' LTRs, which account for about 90% of HERV insertions[124].

4.2 Exploring alternative strategies for generation of a stable VV containing LV vector components

I observed that successive passaging of engineered VV in the absence of any selective pressure ultimately resulted in a virus which lacked the lentivirus genome, leaving only a single-LTR in the VV genome. I then demonstrated that providing a puromycin-based pressure enabled selection of a stable VV, containing the components for generation of functional, transduction competent lentivirus particles **(Figure 18).** While I evaluated the feasibility of this platform *in vitro*, there are foreseeable challenges with translation to the clinic since the virus is ultimately unstable without puromycin addition. While puromycin-based selection of engineered VV provided a rapid means of generating a stable virus, the potential for this strategy is limited for *in vivo* use, given that puromycin is a general inhibitor of translation and would lead to undesired cellular toxicity. Thus, devising alternative selection strategies that can be incorporated into the viral vector to facilitate genomic stability is of interest.

4.2.1 Repurposing approved drugs

One alternative approach to achieving a stable VV which may facilitate downstream translational applications of this platform involves leveraging clinically approved drugs as selection agents. In fact, a well-established example of a compound which has previously been used in VV engineering is mycophenolic acid (MPA)- an FDA approved immune-suppressant used for preventing rejection

in organ transplant patients. Mechanistically, in the presence of xanthine and hypoxanthine, MPA enables replication of VV expressing the *E.coli* xanthine-guanine phosphoribosyltransferase gene (*gpt)* gene, favoring rapid selection of the engineered virus[125].

4.2.2 Embedding a VV essential gene in the LTR flanked sequence

VV encodes nearly 200 genes, many of which are characterized as non-essential for virus growth if viable deletion mutants can be isolated. These so-called non-essential genes are typically situated at the ends of the genome and provide immune protection to the virus. One of the major advantages conferred by VV is the ability to interrupt these non-essential viral genes for insertion of therapeutic transgenes in the virus backbone, as I conducted in this study by inserting the LV components into TK, A56R and B8R loci. Conversely, essential genes are clustered within the center of the genome, and are conserved across poxviruses[126]. While disruption of an essential viral gene would be lethal to the virus, this strategy can actually be advantageous for mediating stable expression of the lentivirus genome from VV, mitigating the need for drug-based selection. As an example, the VV E9L gene encodes for the viral DNA polymerase, which also catalyzes recombination, and is essential for viability of VV[127]. As such, embedding this gene within the sequences flanked by LTRs would strongly favor retention of an intact lentiviral genome sequence from VV, by creating a direct selective pressure at the viral level. This strategy would involve first deleting the endogenous gene from VV, and growing the E9L deleted virus in a cell line stably expressing E9L or in the presence of an E9L encoding plasmid, followed by engineering VV to encode the LV genome with E9L embedded in the sequence between the LTRs (**Figure 22**). After rescue of the engineered virus, E9L complementation would no longer be required.

4.2.3 The potential of solo LTR containing lentiviral vectors

Ma et al. demonstrated that a single LTR containing lentivirus vector was capable of transducing target cells[128]. To explore an alternative to puromycin-mediated stable VV selection, I engineered VV to encode either a 3' or a 5' LTR deleted LV vector genome construct in the TK locus, using mCherry as a recombinant plaque selection marker. To determine the functionality of this construct, U2OS cells were infected with either VV-lenti$^{-/-}$5'LTR or VV-lenti$^{-/-}$3'LTR while Gag-pol and VSV-G were provided by transient transfection. 48 h post-infection, the supernatant was harvested and HEK 293T cells were transduced. Preliminary data shows eGFP transduction in the HEK 293T recipient cells, as seen by eGFP+ cells that are not mCherry+ (**Appendix Figure 6),** providing proof of principle for this alternative strategy. As a follow-up, constructing a triple VV with either a 5' LTR or 3'LTR deleted genome also containing Gag-Pol and VSV-G insertions and investigating whether the production of lentivirus particles from these viruses is feasible is the next step.

4.3 Current experimental limitations and proposed future experiments

4.3.1 Alternative uses for CRISPR-Cas9 loaded VLPs

4.3.1.1 CRISPR-based transcriptional activation

As demonstrated in chapter 2, I conducted preliminary studies for delivery of retroviral VLPs to recipient cells. I built on published work of other research groups, many of which explored VLP-mediated delivery of genome editing agent CRISPR-Cas9. The rationale was to focus on oncogenic targeting in cervical carcinoma cells, since expression of E6 and E7 oncogenes is exclusive to the cancer cells. Although I observed that knock-out of E6 in HeLa cells results in cell death, from a clinical perspective, this approach poses limitations. The effectiveness of

oncogene targeting would be beneficial if every cell can be edited. Alternative uses of CRISPR-based approaches include transcriptional activation (CRISPRa) or inactivation (CRISPRi) of target genes, and this is perhaps a more suited approach from a therapeutic standpoint. Cas9 contains two distinct nuclease domains responsible for double-stranded DNA cleavage: the HNH domain cleaves the target DNA strand while the RuvC domain cleaves the non-target strand[108]. To achieve CRISPRa, the two nuclease domains of Cas9 are mutated into a deactivated, catalytically inactive form of the enzyme (dCas9), which no longer possesses endonuclease activity, but remains an RNA-guided DNA-binding protein. CRISPR/dCas9-mediated gene activation systems can target a promoter or enhancer region of the gene of interest by fusion of the C-terminal end of the dCas9 to one or several activation domains, such as VP64 (consisting of four copies of HSV virus protein 16), a viral trans-activator[108]. Additionally, with this approach, it has been shown that the use of multiple sgRNAs was able to achieve synergistic activation of broad range of endogenous genes, leading to greater protein expression levels (as observed in the case of VEGFA and NTF3)[129]. In the context of cancer, CRISPRa can be used to reactivate silenced tumor suppressor genes[130].

4.3.1.2 CRISPR base and prime editors

Since cancers can be caused by single nucleotide point mutations, reversing those mutations for therapeutic applications is of interest[131]. Hence, the development of CRISPR base editors represents a potential solution to correct these mutations. Base editors are chimeric proteins consisting of dCas9 fused with a deaminase enzyme, such as APOBEC3A[132]. There are two main base editors developed to date: cytosine base editors (CBEs), which introduce C to T mutations and adenine base editors (ABEs) for A to G editing, resulting in precise editing at the target nucleotide[131]. Remarkably, a modified version called prime editor enables precise small insertions, deletions and base changes, without the introduction of dsDNA breaks or requirement for donor

DNA templates. Prime editors are engineered proteins consisting of a Cas9 nickase fused to a reverse transcriptase domain[85]. A prime editing guide RNA specifies the target sequence, and encodes the desired edits in the reverse transcription template.

4.3.1.3 Genome editing to improve *in vivo* immune cell engineering

Further, and as an alternative to oncogene targeting, the genome editing potential of VLPs for use in immunotherapy has been highlighted in a recent study conducted by Nyberg et al., wherein the authors employed a two-vector system, combining Adeno-associated virus (AAV) in combination with modified VLPs (termed enveloped delivery vehicles in their study) for site-specific transgene integration in primary human T-cells *in vivo*[133]. CD3-targeted Cas9 and sgRNA loaded particles targeted the TCRα constant region (TRAC locus) in T-cells, while AAV-hT7, a serum-resistant serotype, delivered a homology-directed repair template containing the CD19 CAR. This *in vivo* CAR-T cell approach was validated in multiple tumor models; B cell acute lymphoblastic leukemia, myeloma and sarcoma, demonstrating the potential of VLPs to contribute to advancing cellular immunotherapies.

4.3.2 Delivery of dual payloads in a single VLP

To further explore protein delivery and as a rather novel approach, I generated dual payload containing VLPs, consisting of both N and C-terminal Gag fusions within the same particle, to enable simultaneous delivery of two proteins. Preliminary data suggested that the fluorescence intensity of eGFP in recipient cells was decreased compared to the single construct. As a more immediate next step, immunoblotting the VLPs to evaluate the cleavage patterns will aid in understanding if Gag-Pol mediated cleavage of both payloads was efficient. Further, swapping the orientation of the fluorophores by placing eGFP at the N–terminus and mCherry at the C-terminus

to then assess respective fluorescence intensities in transduced cells would be of interest. Additionally, comparing the protein loading and subsequent transduction efficiencies of dual payload containing VLPs or VLPs generated by co-transfecting equal amounts of single Gag fusion constructs (mCherry-Gag and Gag-eGFP) would provide insight regarding which approach is more effective in dual protein delivery. This approach could be useful as a tool for preclinical studies, wherein a therapeutic is incorporated along with a reporter to visualize protein delivery within the target cell. For example, co-delivery of Granzyme B and a fluorophore in recipient cells would enable the visualization of transduced cells by fluorescence, and their subsequent eradication by Granzyme B.

4.3.3 Refining experimental design to evaluate the VV-lenti platform

One of the experiments conducted in this thesis involved infection of a VV-restrictive cell line; infection of CHO cells with VV-lenti showed clearance of VV one-week post infection, with evidence of eGFP+ only cells, with cells monitored up to 11 days post-infection. Although this was highly in line with lentivirus transduction, to truly confirm that the presence of eGFP was in fact due to lentivirus-mediated delivery and not residual VV, a refined experimental design includes a condition whereby anti-VSV-G neutralizing antibodies block VSV-G mediated lentivirus transduction. Here, one would expect that only cells infected with VV-lenti in the absence of anti-VSV-G antibodies would result in eGFP+ cells. Further, isolation and subsequent expansion of the eGFP+ cells combined with PCR analysis to assess the presence of VV DNA will solidify the findings.

In a proof-of-concept, I demonstrated the production of LV particles from engineered VV infected cells and subsequent transduction of commonly used cell lines, including HEK 293T, CV-1 and

MC38 colon adenocarcinoma cells. C57BL/6 mice bearing MC38 tumors, characterized as a highly immunogenic tumor model with high T-cell infiltration[134], are used as a common preclinical model in oncolytic virotherapy[70,135]. Following *in vitro* validation of the platform in MC38-Cre responsive cells **(Figure 19)**, *in vivo* infection of this tumor model in the future may provide a sensitive method to screen LV-transduced cells, which can be assessed by fluorescence microscopy combined with flow cytometry.

4.4 Potential project applications

4.4.1 Reshaping the immunosuppressive tumor microenvironment by armed VV

Cancer is a highly complex ecosystem, with the TME consisting of not only malignant cells, but also a rich diversity of non-cancerous cells, such as cancer-associated fibroblasts, endothelial cells, pericytes and several immune components[136], the latter which includes immune cells and secreted molecules such as cytokines and chemokines.

The cells in the TME along with the secreted molecules are collectively involved in driving pathogenesis, and consequentially, each of these components represent attractive therapeutic targets. The platform developed in this project has potential for direct targeting of tumor cells, but also for targeting other cell types in the TME, which involves immune cell recruitment and their reprogramming, and improving immune recognition of the tumor (**Figure 23)**.

4.4.1.1 In vivo immune cell engineering

Mechanistically, OVs are known to stimulate host anti-tumor immunity, and can promote the recruitment of TILs, thus reprogramming and reshaping an immunosuppressive TME. The

recruitment of TILs marks the potential for *in vivo* immune cell engineering, a topic of immense interest to further improve the immunotherapy field.

The currently approved CAR products are based on *ex vivo* engineering of autologous T-cells. Direct *in vivo* modifications of tumor-specific T-cells by gene delivery vehicles such as lentiviral vectors have the potential to mitigate the challenges of *ex vivo* TIL manufacturing, including a reduction in costs associated with the process. The current classical approach for manufacturing CAR T-cells requires patients to undergo leukapheresis, have their T-cells modified to express the CAR construct by lentivirus transduction, expand the engineered T-cells, and then return the cells back to the patient (**Figure 24**). Prior to CAR-T cell infusion, patients undergo lymphodepletion[137]. The turnaround times for CAR-T cell production (from cell collection to patient infusion) range from three to six weeks, which can potentially cause delays for patients, affecting not only access to the treatment but also treatment effectiveness, since some patients succumb to the disease before getting treated and because some patients get treated later in their disease course[138-140].

A recent clinical trial (KNL-1010) by Kelonia Therapeutics demonstrated the remarkable potential of direct *in vivo* T-cell engineering by delivery of BCMA-targeting CAR encoding lentivirus modified to surface display an anti-CD3 antibody in patients with multiple myeloma[141]. Of course, larger studies are required to understand how off-the-shelf *in vivo* approaches are comparable to existing autologous therapies, but the advent of *in vivo* immune cell engineering represents an exciting time in the world of immunotherapies. CAR-T cell therapy has transformed the treatment of hematological malignancies, as evidenced by clinical approval of multiple CAR-T products particularly for treatment of acute lymphoblastic leukaemia, B cell lymphomas and multiple myelomas[142] (**Table 1).** However, CAR application in the treatment of solid tumors has encountered obstacles, including poor trafficking and infiltration into the TME[34]. To further

advance the concept of *in vivo* CAR, a VV-LV hybrid vector may be advantageous compared to delivery of LV particles on their own, given that administration of VV directly to the site of the tumor may enable tumor-localized LV production, circumventing the potential of immune-mediated clearance from intravenous LV delivery. This platform may be particularly suited for CAR generation in solid tumors, whereby VV can first infect the tumor, followed by release of lentivirus particles from infected cells and their subsequent transduction of TILs in the TME. Further, this strategy may potentially mitigate the need for a lymphodepleting regimen.

The developed VV-lenti platform represents a versatile and modular technology, with potential to generate not only CAR-T, but other CAR products as well. More recent data has shed light on the emergence of CAR-NK or CAR-macrophages (CAR-M). One company (Interius BioTherapeutics) developed a platform to generate autologous CAR-T and CAR-NK cells *in vivo*. Their product (INT2104) is an intravenously administered lentiviral vector encoding an anti-CD20 CAR transgene, designed to display an engineered fusogen and binder for targeted transduction of CD7+ cells[143], a molecule involved in T-cell and NK cell activation[144]. CAR-Ms are beginning to receive attention for two main reasons. First, the innate phagocytic nature of macrophages renders them effective at internalizing nanoparticles, which enhances their susceptibility for *in vivo* transduction[142]. Second, macrophages naturally infiltrate and persist in the TME, rendering them well-suited for solid tumor targeting. CAR-M therapies are now advancing in early stage clinical trials, aiming to assess safety, efficacy and therapeutic potential. For example, in a phase 1 study, Carisma Therapeutics CT-0508 (NCT04660929) is assessing the safety profile of CAR-M in patients with HER2+ tumors[145]. CAR-M therapies have potential to shift the pro-tumor M2 polarization into an anti-tumor M1 polarization. Generating therapy relevant cells directly *in vivo*

by transduction of target cells with lentivirus carrying a payload of interest would enable the generation of '***living drugs'*** for cancer therapy.

4.4.1.2 Exploring modulation of tumor antigen presentation

As part of immune evasion strategies, many tumors reduce their immunogenicity by downregulating expression of tumor antigens or through mutations in the antigen processing and presentations machinery[146]. MHC class I molecules form a tri-molecular complex consisting of the heavy chain, peptide antigen and β2-microglobulin (β2M) light chain[147]. Given the importance of MHC class I molecules for presentation and recognition of tumor antigens by cytotoxic CD8+ T cells, a well-known mechanism which impairs cytotoxic CD8+ T-cell recognition of cancer cells is suppression of MHC class I expression, which is associated with poor patient outcomes. This is achieved either by downregulation of the genes encoding the MHC class I chain itself, or the associated β2-microglobulin required for the complex to be presented at the cell surface[147]. This escape strategy enables the tumor to behave as a "stealth" target, and has been reported in a variety of tumor models. Flow cytometric and immunohistological analyses have demonstrated a near 100% loss of MHC I molecules in some tumor types, such as 96% loss in cervical and breast carcinomas and 87% in colorectal carcinomas[147]. Restoration of the normal MHC class I phenotype may provide an avenue to restore efficient immune responses in cancer. NLRC5 (also known as MHC class I transactivator (CITA)) is a key regulator. One study demonstrated that expression of NLRC5 in B16 melanoma cells restored MHC-1 expression and improved antigen presentation[148], an avenue which could be explored with the VV-lenti platform.

Some tumors impair the transfer and/or processing of antigens in the endoplasmic reticulum. As previously described, one group engineered VV to encode a truncated CD19 antigen for OV-

mediated antigen delivery to tumor cells, which then became susceptible to CD19 CAR-T cell-mediated tumor destruction[57]. However, in this approach, the VV-infected cell will ultimately undergo lysis. Thus, a strategy to target bystander tumor cells may increase the therapeutic potential of antigen delivery, particularly in the case of solid tumors, where identification of a tumor-confined target antigen is difficult. As such, this platform can be harnessed for antigenic delivery in a tumor-localized manner.

4.4.1.3 Direct tumor cell targeting with cytotoxic payloads

Lastly, the proposed platform can be harnessed for direct targeting and eradication of tumor cells as a suicide gene therapy. A widely used example for cytotoxic payload delivery is a prodrug activator gene, and subsequent prodrug treatment, which results in synchronized killing of cancer cells. For example, the cytosine deaminase gene (CD) converts the prodrug 5-fluorocytosine (5-FC) into the active chemotherapeutic drug 5-fluorouracil (5-FU), and the CD/5-FC based enzyme/prodrug therapy has been explored in combination with VV[149].

TOCA-511, a replicating retrovirus containing the intact MLV genome has been explored for tumor-specific delivery of the prodrug-converting enzyme 5-FC, supporting retroviral-based delivery of a cytotoxic payload to the tumor[47]. Since prodrug conversion only occurs in infected cells, the adverse side effects associated with this systemic chemotherapy can be minimized. TOCA-511 demonstrated highly promising early clinical results, and even progressed to a Phase III trial in patients with high grade gliomas, which unfortunately failed to meet its primary endpoint of overall survival. Despite this outcome, the use of a retroviral vector for cytotoxic payload delivery in a tumor context demonstrates the potential to engineer the VV-LV platform for a similar therapeutic application.

4.5 Strategies to improve platform specificity

4.5.1 Retargeting lentivirus entry and the use of tumor-specific promoters

Enhancing the specificity of the platform can be achieved at multiple-layers, including control of viral tropism, and transcriptional activity[148]. Modifications to the envelope glycoprotein is one strategy for targeted entry of viral particles. The lentivirus used in this thesis work was pseudotyped in the simplest form- with glycoprotein VSV-G, which binds the LDL-R, whose ubiquitous expression favors lentivirus transduction in a variety of cell types, but may also lead to transduction of undesired cell populations. Since conventional VSV-G pseudotyped LV vectors are not T-cell selective, nor do they modify resting or minimally stimulated cells, introducing targeted vector delivery can further improve the use of LVs for CAR-T generation[150]. Redirecting LV tropism by targeting T-cell lineage markers, such as CD3, CD4, CD8 and CD5 has been a widely explored concept[151]. Further, in a recent pre-clinical study, peptide-MHC targeted retroviruses were able to reprogram anti-tumor T-cells *in vivo* by mediating antigen specific gene delivery to CD8+ T-cells, which resulted in tumor-controlling long-lived memory T-cells[152]. These examples illustrate the ability to modify retroviral systems for the therapeutic manipulation of T-cells, which can enable the development of powerful anti-cancer medicines[153].

An alternative strategy to achieve platform specificity is the incorporation of tumor-specific promoters to regulate transgene expression. This strategy can restrict therapeutic gene expression to cancer cells while minimizing expression in normal tissues. The combination of "tumor on" and "normal tissue off" can result in improved safety profiles[154]. Numerous promoters have been evaluated for transcriptional targeting in cancer gene therapy, with examples including the α-fetoprotein promoter for hepatocellular carcinoma and the erbB2 (HER2) promoter for breast cancer[155]. Another example is the human telomerase reverse transcriptase (*hTERT*) promoter[156].

4.5.2 Exploring inducible systems within VV for transgene regulation

Incorporating inducible systems into OV backbones provides a means of regulating the timing and magnitude of gene expression[71,157]. The therapeutic rationale of the VV-lenti platform is that VV serves as a tumor-targeting vehicle for localized lentivirus production. This platform may benefit from inducible regulation to further enhance specificity, by ensuring that lentivirus is generated after VV has established infection within the tumor. If systemic administration of VV is desired, spatial and temporal control of lentivirus production could potentially reduce off-target transduction, and restrict lentivirus generation to sites of tumor-localized VV replication. This form of regulation may improve the safety profile of this platform, by minimizing unintended transduction of healthy tissues. One system that has been characterized for transgene inducibility from VV is the Split T7 RNA Polymerase in combination with FDA-approved and anti-cancer rapamycin-analogs as inducers[71].

4.6 Exploring alternative virus platforms for lentivirus delivery

In a similar concept to the work presented in this thesis, biotechnology company Vyriad is working towards engineering an oncolytic CMV as a delivery vehicle for generating CAR-T cells within tumors. Preclinical data presented at the 16th International Oncolytic Virus Conference demonstrated that an engineered CMV encoding the components of a CD3-targeted lentivirus resulted in the production of particles which successfully transduced T-cells to express the CAR molecule *in situ* within the TME[158]. Since the majority of the population is infected with CMV, this approach was designed to leverage pre-existing anti-CMV immunity, a strategy which does not require characterization of tumor-associated antigens, and can mobilize cytotoxic T-cell responses in the TME[159].

4.7 Significance

Immunotherapy has emerged as a transformative area for the treatment of cancer, with viral vectors emerging as valuable platforms for engineering next-generation therapeutics. The findings from this thesis establish retrovirus-derived therapeutic delivery platforms, including CRISPR-Cas9 loaded VLPs for transient genome editing and a VV-lentiviral hybrid system for localized stable gene delivery. These platforms demonstrate how programmable viral systems can be engineered for therapeutic purposes which may include oncogene disruption or oncolysis combined with stable genetic modifications of target cells.

Conventional lentiviral vector bioprocessing can be a challenge, since vector generation is reliant on transient transfection-based manufacturing methods. In contrast, the VV-lentivirus platform introduces the possibility of localized vector production in the tumor, and can also provide economic advantages by reducing the costs associated with immune cell engineering, such as for CAR-T cell generation. The field is progressively shifting towards strategies for direct *in vivo* immune cell engineering, which could mark the beginning of a new era of rapid, streamlined and accessible immunotherapies[160].

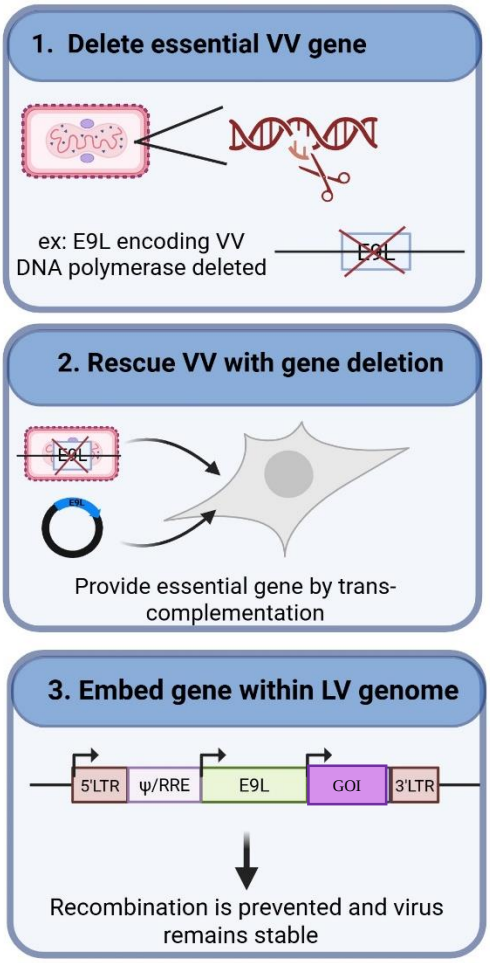

Figure 22: Embedding an essential VV gene within LTR-flanked sequences to maintain a selective pressure for lentiviral genome retention. Schematic depicting (1) deletion of the native essential VV gene (such as viral DNA polymerase E9L) from the virus backbone, (2) rescue of the deletion containing virus by trans-complementation (3) followed by reinsertion of the gene within the lentiviral genome. Recombination-mediated loss of the sequence between LTRs would result in loss of essential gene function, resulting in lethality to the engineered VV.

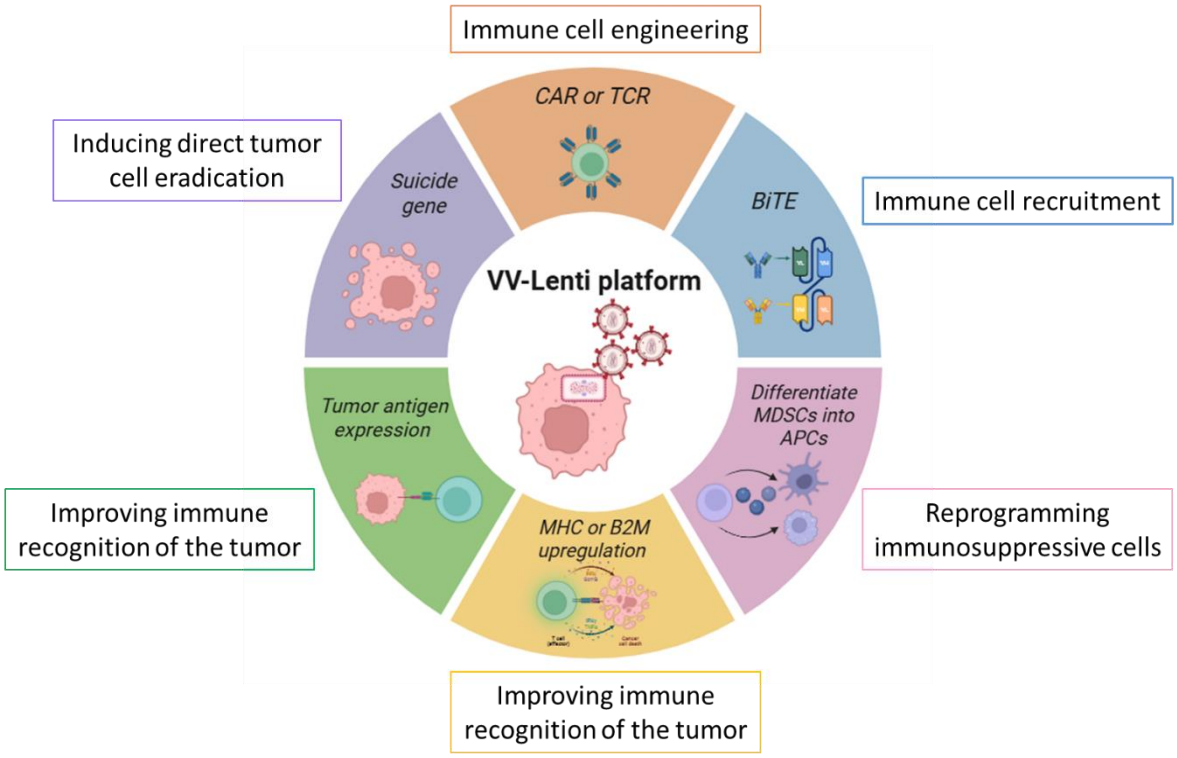

Figure 23: Harnessing the potential of a VV-lentivirus platform for cancer therapy. Schematic wheel depicting the diverse therapeutic applications enabled by the proposed VV-lenti platform. Representative transgene strategies incorporated into the lentivirus backbone are shown, including approaches targeting tumor cells directly as well as modulation of the tumor microenvironment. These include immune cell engineering and recruitment, reprogramming of immunosuppressive cells, improving immune recognition of the tumor, and direct-tumor cell targeting.

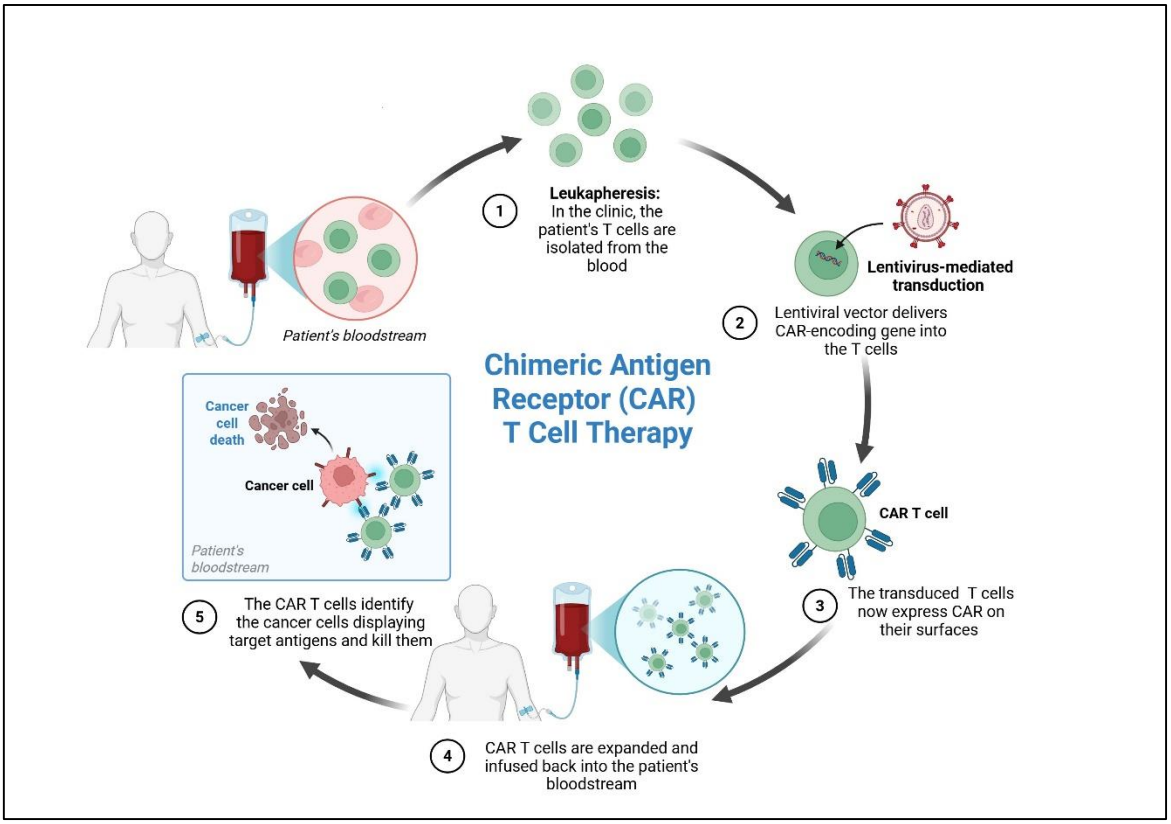

Figure 24: CAR-T cell manufacturing process. Patients undergo leukapheresis to collect T-cells from the blood. The isolated T-cells are modified to express the CAR construct by lentivirus transduction. The engineered T-cells are then expanded in culture. Prior to CAR-T cell infusion, the patient is lymphodepleted. The expanded T-cells are then infused back into the patient.

Chapter 5: Materials and methods

5.1 Cell lines, tissue culture and viruses

African green monkey kidney cell line CV-1 was a gift from the Biotherapeutics Manufacturing Center (BMC) at the OHRI. U2OS cells, HEK 293T cells and CHO cells were purchased from ATCC. All cells were cultured in Dulbecco's Modified Eagle's Medium (DMEM) supplemented with heat-inactivated 10% fetal bovine serum (FBS) and newborn calf serum (NCS) (50% FBS/50% NCS), with the exception of HEK 293T cells, which were cultured in DMEM with 10% FBS. Serum containing media is here onwards referred to as complete media. Cells were tested for mycoplasma contamination prior to experiments. U2OS cells stably expressing Cas9 were a gift from Jack Timothy Whelan[73]. Western Reserve strain of VV was purchased from ATCC (VR-1354).

5.2 Generating eGFP expressing HEK 293T cells by lentivirus transduction

Lentivirus was produced by transfecting 6 µg pSPAX2 (a gift from Didier Trono, Addgene plasmid # 12260), 3 µg pMD2.G (a gift from Didier Trono, Addgene plasmid # 12259) and 6 µg pLenti CMV GFP Puro (a gift from Eric Campeau & Paul Kaufman, Addgene plasmid # 17448) using Jetprime (Polyplus, catalog #: 101000046) following manufacturer's protocol, into a 10 cm dish of HEK 293T cells seeded at 6E6 the day prior to transfection. 48 h post-transfection, supernatant was harvested and centrifuged at 1500 rotations per minute (rpm) for 5 min to remove cellular debris. 250 µl of non-concentrated lentivirus was added to 1E6 HEK 293T cells in 1 mL complete media supplemented with 0.8 µg/mL polybrene (Millipore Sigma, catalog # TR-1003-G). After 48 h, transduced cells were selected with puromycin at a concentration of 1 µg/mL to establish a stable cell line expressing eGFP.

5.3 VLP production

VLPs were produced as per nanoblade production protocol (Nanoblade production protocol, from Ricci lab[88]). Briefly, 10 cm plates of HEK 293T cells were seeded at 6E6 cells/ plate the day prior to transfection, in 10 mL complete media. The day of transfection, media was replaced with 10 mL complete media. For production of eGFP and Nanoluciferase loaded VLPs, 1.7 µg Gag-eGFP or Gag-Nanoluciferase plasmids **(see section 5.12, cloning and construction of plasmids**), 2.7 µg Gag-Pol plasmid (a gift from Patrick Salmon, Addgene plasmid # 35614) and 0.5 µg VSV-G plasmid (a gift from Bob Weinberg, Addgene plasmid #8454) were transfected using JetPrime (Polyplus, catalog #: 101000046), following manufacturers protocol. For Cas9 loaded particles, cells were transfected with 1.7 µg Gag-Cas9 plasmid (a gift from Philippe Mangeot & Théophile Ohlmann & Emiliano Ricci, Addgene plasmid # 119942), 2.7 µg Gag-Pol, 0.5 µg VSV-G in addition to 4.4 µg sgRNA (**see section 5.7, generation of sgRNAs**). 48 h post-transfection, VLP containing supernatants were harvested and centrifuged for 10 min at 250 x g to remove cellular debris. Supernatants were transferred to new 15mL conical centrifuge falcon tubes (Falcon, catalog #: 0552790), and were incubated with LentiX concentrator at 4^{o}C (Takara Biosciences, catalog #: 631231) as per manufacturers instructions. 1 h post-incubation, supernatants were centrifuged at 1500 x g, at 4^{o}C for 45 min. Pellets were re-suspended in phosphate buffer saline (PBS) in 1/10th of the original volume, for a total of 1mL.

5.4 VLP transduction

For experiments involving eGFP and Nanoluciferase loaded particles, HEK 293T cells were seeded at 1.25E5 per well in 12-well plates containing 1 mL complete media. For experiments involving analysis of CRISPR-mediated E6 knock-out, cells were plated at 3E5 per well in 6-well plates containing 2 mL of complete media (**see genome editing HPV18+ HeLa cells, section 5.9**).

All cells were treated with polybrene (Millipore Sigma, catalog # TR-1003-G) at a concentration of 0.8 µg/mL. Spinfection was performed at 800 x g for 50 min at room temperature.

5.5 Nanoluciferase assay

HEK 293T cells were lysed in passive lysis buffer (Promega). Luciferase assay was performed using native coelenterazine (CTZ; 3.33 mM final concentration; Nanolight Technologies – Prolume Ltd., Pinetop, AZ, USA). Synergy Microplate Reader (BioTek, Winooski, VT, USA) was used to measure luminescence.

5.6 Alamar blue assay

Metabolic activity of VLP-treated HeLa cells was measured by alamar blue assay (Thermo Fisher, catalog #: DAL1025). Reagent was added to cells in a 1:10 dilution in complete media, which were incubated for ~2 h before fluorescence was measured using the Synergy Microplate Reader (BioTek, Winooski, VT, USA) with an excitation of 530nm and an emission of 590nm.

5.7 Generation of single guide RNAs

Plasmid encoding sgRNA targeting *egfp* was a gift from Philippe Mangeot & Théophile Ohlmann & Emiliano Ricci, Blade 182, Addgene plasmid # 134914. sgRNAs for targeting HPV 18 E6 or E7 oncogenes (**Table 3)** were either designed using benchling software or acquired from the literature and oligonucleotides were ordered from Integrated DNA Technologies (IDT). sgRNAs were cloned into Superblade 5 (a gift from Philippe Mangeot & Théophile Ohlmann & Emiliano Ricci, Addgene plasmid # 134913) using BsmBI restriction enzyme (following LentiCrispr v2 protocol).

Synthetic sgRNAs for rescue of engineered VV were ordered from Synthego (sequences are given in Table 5).

5.8 Flow cytometry

For analysis of eGFP expression in HEK 293T cells post-VLP mediated genome editing, 5E5 cells from each culture condition were collected, washed 2 times in PBS, and resuspended in 2% FBS-PBS for staining. Dead cells were excluded using Fixable viability stain 510 (1:1000 dilution, BD Biosciences, catalog #: 564406). Samples were run on BD LSRFortessa, and analyzed with FlowJo software v10.

For Annexin-V staining (FITC conjugated, Thermo Fisher, catalog #A13199), 1E6 edited cells were harvested and washed once with PBS and once with Annexin-V binding buffer (Thermo Fisher, catalog #V13246) and resuspended in 100 µL Annexin-V binding buffer. Staining was performed as per manufacturers protocol. Briefly, 1 µL of FITC-conjugated Annexin-V was added to the cell suspension and was incubated for 15 min at room temperature, protected from light. 2 mL of binding buffer was added and cells were centrifuged at 500 x g for 5 min at room temperature. Cells were resuspended in 200 µL of binding buffer and analyzed by flow cytometry using BD LSRFortessa.

5.9 Genome editing HPV18+ HeLa cells

2.5E5 HeLa cells were seeded per well in 6-well plates containing 2 mL complete media. The following day, 100 µl of Cas9 and E6 sgRNA or Cas9 with scrambled sgRNA containing VLPs was added to cells in media supplemented with 0.8 µg/mL polybrene (Millipore Sigma, catalog # TR-1003-G).

5.10 Colony forming assay

VLP-treated HEK 293T expressing eGFP cells or edited Hela cells were trypsinized 24 h post-VLP delivery. Cells were seeded at 250 cells/well in a 12-well plate (n=12/condition). After one

week, colony formation was first assessed by light microscopy, and then colonies were stained with crystal violet and counted.

5.11 TIDE analysis

Forward and reverse primers flanking 500 bp upstream and downstream of HPV 18 E6 sgRNA recognition sites were designed and ordered from IDT **(see Table 2 for primer sequences**). Following editing, genomic DNA was extracted using Quick Extract. PCR was performed using CloneAmp master mix (Takara, catalog #: 639298) as follows (based on manufacturers protocol):

Temperature	Time	
98 °C	10 sec	
55 °C	15 sec	30 cycles
72 °C	10 sec	

Amplicons were sent for Sanger sequencing at the OHRI StemCore sequencing facility. The raw trace files (.ab1 format) were then uploaded into the TIDE NKI web tool for analysis.

5.12 Cloning and construction of plasmids

5.12.1 Generation of Gag fusion proteins

To clone Gag-eGFP and Gag-Nanoluciferase plasmids, the coding sequences for eGFP and Nanoluciferase were ordered as geneblock fragments from IDT flanked by AgeI and KpnI restriction sites. 1 µg Gag-Cas9 vector was digested with AgeI and KpnI. A 6470 bp fragment was gel purified and ligated with eGFP or Nanoluciferase fragments digested with AgeI and KpnI using T4 DNA ligase (New England Biolabs, catalog #:M0202S). The mCherry-Gag fusion construct

design was generated as described (except that Cas9 was replaced with the mCherry coding sequence)[106].

5.12.2 Lentivirus plasmids for insertion into VV

The lentivirus genome containing eGFP as a transgene was designed from plasmid pLenti-CMV-eGFP-Puro (a gift from Eric Campeau & Paul Kaufman, Addgene plasmid # 17448). The RSV promoter was replaced with a synthetic VV early-late promoter followed by nucleotides 2448 to 7582 from the plasmid. A VV transcription termination signal (sequence: TTTTTNT) was added to the end of the construct. The construct (5208 bp) was ordered as a geneblock fragment from Thermo Fisher Scientific and cloned into a VV plasmid containing homology arms to the thymidine kinase locus with mCherry as a selection marker (previously generated by members of the Bell lab) using restriction enzymes XhoI and NotI. The VSV-G coding sequence was inserted into a plasmid containing homology arms to the B8R locus of VV with eGFP as a selection marker and was designed and cloned by former Bell lab post-doctoral fellow Dr. Nikolas Tim Martin.

For insertion of Gag-Pol into VV A56R locus, nucleotides 1809 to 7715 (5907 in total) were taken from pSPAX2 (a gift from Didier Trono, Addgene plasmid # 12260) and a VV early-late promoter (sequence: AAAATTGAAATTTTATTTTTTTTTTTTGGAATATAAATA) was placed upstream of the construct. The resulting fragment was ordered from Synbio Technologies and cloned into A56R homology arm containing plasmid with BFP as a selection marker, designed by previous members of the Bell lab, with AflII and SalI restriction enzymes.

5.13 Engineering VV by infection-transfection

1E5 U2OS cells stably expressing Cas9 were plated one day prior to infections in 24-well plates, per well. Cells were infected with VV (MOI of 0.5) for 2 h in 1 mL SFM. Following infection, the media was changed to 1 mL complete media and cells were transfected with 800 ng of linearized template plasmid and 1.3 μL of 3 μM sgRNA stock (Synthego) targeting the locus of interest,

using 1.5 µL JetPrime transfection reagent (Polyplus, catalog #: 101000046) in 50 µL JetPrime buffer, as per manufacturers instructions. After 48 h, cells were subjected to 3 cycles of freezing and thawing to release virus to begin virus rescue (by plaque purification, single cell sorting or puromycin-based selection).

5.14 Generating VV H5R driven puromycin resistance gene (with eGFP as a LV transgene)

To replace the PGK promoter with the VV early-late H5R promoter for selection of VV under puromycin-mediated selective pressure, a gene-block fragment was designed and ordered from Thermo Fisher Scientific, consisting of VV H5R promoter (sequence: 5' TTAAAGTTACAAACAACTAGGAAATTGGTTTATGATGTATAATTTTTTTAGTTTTTAT AGATTCTTTATTCTATACTTAAAAAATGAAAATAAATACAAAGGTTCTTGAGGGTTG TGTTAAATTGAAAGCGAGAAATAATCATAAATTATTTCATTATCGCGATATCCGTTA AGTTTGTAT 3') placed upstream of a short fragment of the puromycin resistance gene (sequence:

5'ACCTGCAGCCCAAGCTTACCATGACCGAGTACAAGCCCACGGTGCGCCTCGCCAC CCGCGACGACGTCCCCAGGGCCGTACGCACCCTCGCCGCCGCGTTCGCCGACTACCC CGCCACGCGCCACACCGTCGATCCGGACCGCCA 3') flanked by EcoRI and RsrII unique restriction enzyme sites. 1 µg of the original vector and 1 µg of the newly designed fragment were digested with EcoRI and RsrII. An 8357 bp band resulting from digestion of the original vector and a 2371 bp fragment from H5R-puro digestion were gel purified and ligated using T4 DNA ligase.

5.15 Single cell sorting of virally infected cells

Infected cells were washed with PBS once, trypsinized and neutralization of trypsin was performed with complete media. Cells were centrifuged at 1500 rpm for 5 min, after which they were resuspended in 500 µl PBS supplemented with EDTA. A SONY MA900 was used for sorting.

Cells were first gated for BFP and eGFP, followed by mCherry, and cells were then sorted into a 96 well pre-seeded with 1.2E4 U2OS cells per well.

5.16 Genomic DNA extraction, PCR screening and gel electrophoresis

U2OS cells were seeded at 1.2E4 cells per well in a 96 well plate the day prior to infection. ~15µL/virus clone was used to infect cells in 100 µL complete media. Once infection reached complete spread (based on expression of mCherry as assessed by EVOS M5000 microscope), samples were collected in 36 µL Quick Extract (Lucigen, QE09050) and incubated at the following settings:

	Temperature	Time
1.	68 °C	15 minutes
2.	95 °C	10 minutes

Following incubation, PCR was performed using CloneAmp master mix (Takara, catalog #: 639298) consisting of 7.5 µL CloneAmp, 1.5µl of each forward and reverse primers and 3 µL of extracted DNA (total volume of 16.5 µL in multiplexed PCRs). PCR was conducted with the following settings:

	Temperature	Time	
1.	98 °C	10 sec	
2.	98 °C	15 sec	34 cycles
3.	62 °C	15 sec	

4. 72 °C 30 sec

5. 72 °C 1 min 30 sec

Agarose gel electrophoresis: Amplicons generated by PCR were analyzed on 1% agarose gels at 45 Volts for 45 minutes.

5.17 VV plaque assay

10-fold serial dilutions of each virus were prepared in serum free media (SFM, DMEM) and confluent 6-well plates (seeded at 1E6 overnight) were infected in a volume of 800 µL. Infected cells were incubated at 37°C, 5% CO^2 for 2 h to allow virus attachment, after which the inoculum was removed and replaced with 1.5% carboxymethyl-cellulose overlay. Cells were then incubated for 48 h at 37 °C and then stained with crystal violet to count plaques. Titers were quantified using the following formula:

$$Titer\left(\frac{plaque\ forming\ units\ (pfu)}{mL}\right) = \frac{Plaque\ Count * Dilution\ Factor}{Inoculum\ Volume\ (mL)}$$

5.18 Multi-step virus growth curves

3E5 U2OS cells were seeded per well in 12-well plates the day prior to infections. 1 mL of SFM was added to each well. Cells were infected with each virus at an MOI of 0.01 for 1 h after which media was replaced with 1 mL complete media. Samples were collected at 0, 24, 48 and 72 h for titering. For the 0 h time-point, contents of the well were collected immediately after removing virus.

5.19 Purification of VV and isolation of viral DNA for Nanopore sequencing

Purified viral pellet was resuspended in 200 µL PBS. Purelink viral DNA/RNA kit was used for DNA isolation as per manufacturers protocol (Thermo Fisher, Catalog number #12280050).

Whole genome sequencing was performed by Plasmidsaurus using Nanopore sequencing technology.

For subsequent studies involving passaging VV in the presence of puromycin, 48 h prior to infection, 2 roller bottles were seeded with 9.6E7 CV-1 cells per bottle (cell density of 3E4/cm^2) in 200 mL of DMEM supplemented with 10% FBS buffered with HEPES. The day of infection, media was replaced with DMEM 10% FBS+ HEPES. Cells were infected at an MOI of 0.02 with VV-lenti-eGFP (or with VV-lenti-Cre). 2 h post-infection, media was supplemented with 1.5 µg/mL puromycin. 48 h post-infection, when all cells had detached, virus was harvested. The contents of the roller bottles were pooled in 500 mL spin capsules and centrifuged for 3000 rpm for 10 minutes at room temperature to pellet the cells. The supernatant was discarded and the resulting cell pellet was resuspended in 25 mL 1mM Tris/HCL pH 9. The cell pellet was stored at -80^{O}C. To continue with virus purification, the suspension was thawed in a 37^{O}C water bath and centrifuged at 3000 x rpm for 10 min to pellet cell debris. Supernatant was carefully placed in a 50 mL falcon tube (Corning, catalog #: 1443222). 2 mM $MgCl_2$ and 150 U/mL Benzonase were added and incubated at room temperature for 10 min, followed by addition of 1X TrypLE and another incubation at room temperature for 10 min. The virus suspension was transferred into two new Beckman-Coulter centrifuge tubes (Beckman Coulter, catalog #: C14292). Tubes were filled to the top with sterile 1 mM Tris pH 9, and were weighed in their buckets for balancing (range must be within 0.05 g). Samples were centrifuged at 20 666 x g for 1h30 min at 4^{O}C (rotor SW32). Supernatant was aspirated and pellet was re-suspended in 1 mL of 1 mM Tris pH 9. Once pellet was well re-suspended, an addition 24 mL of 1 mM Tris pH 9. In a new centrifuge tube (Beckman Coulter, catalog #: C14292), a sucrose cushion was prepared by adding 12 mL of 36% sucrose to the bottom of the tube. The volume was then completed to the top by addition of 1 mL of 1 mM

Tris pH 9. Tubes were once again weighed and centrifuged at 20 666 x g for 1h30 min at 4^{O}C (rotor SW32). The final pellet was resuspended in 1 mL of 1 mM Tris pH 9 and was aliquotted frozen at -80^{O}C. Virus was tittered by plaque assay.

5.20 Quality control for purified VV maintained under puromycin selection

CV-1 cells were seeded at 1E4 cells per well in a 96 well plate. Tittered virus was diluted 1:10000 (1E9 PFU/ mL diluted to 1E5 PFU/mL) and 1 µL, 3 µL or 5 µL of virus was used to infect CV-1 cells. After 2 h, virus was removed and media containing puromycin at a dose of 1 µg/mL was added. 24 h post-infection, all cells were infected and were collected in 36 µL of Quick extract solution. PCR analysis was conducted as previously described.

5.21 Immunoblotting and immunofluorescence staining

Immunoblotting: Cells were washed with cold PBS once, and were lysed in 100 µL RIPA buffer (for VLP transduced cells or VV infected cells) or in 500 µl RIPA buffer (VLP producer cells) containing protease inhibitor cocktail (Thermo Fisher, catalog number 78440). Cells were harvested by scraping them off plates, contents were collected in 1.5 mL micro-centrifuge tubes and incubated on ice for 20 min. The contents were centrifuged for 20 min at 11 000 g at 4^{o}C. Protein containing supernatants were transferred to new micro-centrifuge tubes. Protein concentration was estimated using the Pierce BCA protein assay (Thermo Fisher, catalog # 23227). For each condition, 10 µg of protein was resolved by polyacrylamide gel electrophoresis under denaturing conditions (45 min to 1 h, 100V at room temperature), followed by wet transfer to 0.2 µm Nitrocellulose membrane (1 h, 0.45 mA at 4^{o}C with ice packs). The membranes were blocked in 5% milk (in TBS-T buffer) for 1 h at room temperature. All primary antibodies were diluted in 5% milk (in TBS-T buffer) and incubated overnight at 4^{o}C. Blots were rinsed three times for 10 min with TBS-T buffer, secondary antibodies were incubated at room temperature for 30 min and blots were rinsed three times for 10 min with TBS-T buffer once again. Blots were imaged using

ChemiDoc Imaging System (Biorad, catalog #: 12003153). Primary antibodies used were: anti-Cas9 (Diagenode, catalog #: C15200203 1:1000), anti-p53 (Santa Cruz, # sc-47698, 1:500), anti-p21 (Santa Cruz, sc-397, 1:500), anti-HIV-1 p24 (to probe for Gag-Pol, Abcam, #ab63913, 1:1000), anti-β-Actin (Rabbit mAb, #4970, 1:1000). VSV-G was detected by probing the membrane using an Ilkow lab in-house generated polyclonal anti-VSV antibody (1:1000). Secondary antibodies used were: horseradish-peroxidase conjugated anti-rabbit (ThermoFisher, catalog #: 31460, 1:5000) or anti-mouse (ThermoFisher, catalog #: 31430, 1:5000).

Immunofluorescence staining: 2.5E5 HeLa cells were plated per well on sterile glass coverslips in 6-well plates and incubated overnight at 37ºC in a 5% CO^2 humidified incubator. Cells were then treated with 100 µL of VLPs containing Cas9 + sgRNA targeting E6 or control VLPs. 120 h post- transduction, coverslips were fixed with 4 % paraformaldehyde, quenched with 100mM glycine in PBS * (with 1 mM $CaCl_2$ and 0.5 mM $MgCl_2$), permeabilized with 0.1 % Triton X-100, then blocked in 5 % BSA in PBS* for 2 h at room temperature. Coverslips were incubated overnight at 4ºC with anti-p53 (Santa Cruz, # sc-47698, 1:200), followed by goat anti-mouse AlexaFluor 488 (Invitrogen, catalog #: A-11029, 1:400). Coverslips were washed and mounted using ProLong Gold Antifade with DAPI (Invitrogen, catalog #: P36930). Images were acquired with EVOS M5000.

5.22 Transduction of cells with Cre expressing lentivirus

HEK 293T and MC38 Cre reporter cells were a gift from Peivand Sadat Mousavi and Duncan Mackenzie. 1E6 cells were seeded in 6-well plates the day prior to transduction, and cells were transduced with 100 µL of Lenti-X concentrated lentivirus produced from VV-lenti-Cre infected cells, in 1 mL complete media supplemented with 0.8 µg/mL polybrene (Millipore Sigma, catalog # TR-1003-G). Fluorescence microscopy images were taken at 20X magnification with EVOS M5000.

5.23 Infection of CHO cells

8E5 CHO cells per well were seeded in 6-well plates the day prior to infection. Cells infected with VV-lenti GFP at an MOI of 0.5 in 2 mL complete media. Cells were monitored based on fluorescence daily and imaged using EVOS M5000 microscope on days 2, 7 and 11 post-infection.

5.24 Electron microscopy

1E6 U2OS cells were seeded per well in 6-well plates the day prior to infections. Media was replaced with 1.5 mL fresh complete media. Cells were then infected with either VV-lenti-eGFP at an MOI 0.5 or WT VV WR at an MOI 0.5, or they were transfected with lentivirus producer plasmids; 1.5 µg pSPAX2 (a gift from Didier Trono, Addgene plasmid # 12260), 0.5 µg pMD2.G (a gift from Didier Trono, Addgene plasmid # 12259) and 1 µg pLenti CMV GFP Puro (a gift from Eric Campeau & Paul Kaufman, Addgene plasmid # 17448) using Jetprime (Polyplus, catalog #: 101000046) following manufacturers protocol. Each condition was performed in triplicate. 24 h post-infection or transfection, the supernatants were harvested and pooled (total pooled volume of media=4.5 mL) and concentrated by ultracentrifugation at 20 000 x g for 1 h and 30 min at 4^{o}C. The final pellet was resuspended in 100 µL complete media. 30 µL of clarified supernatant was diluted with 30 µL fixative (5% glutaraldehyde + 4% paraformaldehyde in 0.1M cacodylate buffer) and was incubated for 60 minutes at room temperature. For collection of cellular samples, cells were trypsinized and washed with PBS twice. The cell pellet was fixed overnight at 4^{o}C with gentle agitation, in a final volume of 0.5 mL fixative (2.5% glutaraldehyde + 2% paraformaldehyde in 0.1M sodium cacodylate buffer). Grid preparation, sample deposition onto the grid, agarose embedding and sectioning (for cellular samples), negative staining and imaging was performed by the University of Ottawa EM core facility. Samples were imaged with the JEOL JEM-1400Flash.

5.25 Statistical analysis

Statistical analysis was performed using Prism v.10. Means of two groups were compared using two-tailed Student's unpaired *t*-test. Means of more than two groups were compared using one-way ANOVA with Tukey's multiple correction test, $p<0.05$.

5.26 List of tables

Table 2: Primer sequences for TIDE analysis of CRISPR-Cas9 based targeting of eGFP and E6

Target amplification	Forward sequence	Reverse sequence
eGFP	tcatatgccaagtacgcccc	ttctgcttgtcggccatgat
E6	aaatcactatgcgccaacgc	cagctgggtttctctacgtgt

Table 3: sgRNA targeting sequences for HPV18 E6 or E7

sgRNA candidate # and target gene	Sequence (excluding PAM)
NTC	cgaggagctgttcaccgggg
E6 0	cgcgctttgaggatccaaca
E6 1	acaagctacctgatctgtgc
E6 2	acacggcgaccctacaagct
E6 3	aagctacctgatctgtgca
E7 1	gagcaattaagcgactcag
E7 2	gttgaccttctatgtcacga

Table 4: Primer sequences to detect lentiviral genome from VV

Primer pair to detect lentivirus genome from VV	Forward sequence	Reverse sequence	Expected band length (bp)
1	cgtgggtcattgttatgaatctc	ttaactgcgaatcgttctagctc	**1109**
2	ttaactgcgaatcgttctagctc	aatcgaatggatctgtctctgtc	**1191**
3	agagttaggcagggatattcacc	gatcttgaagttcaccttgatgc	**1401**
4	ggcacaagctggagtacaactac	ggagatgaggaagaggagaacag	**1412**
		Modified sequence with VV H5R driven puromycin resistance: gttcttgcagctcggtga	
5	Caatagcagctttgctccttc	tcaccatcctaggttagaagctg	**1335**
	Modified sequence with VV H5R driven puromycin resistance: ccgcctggaattcttaaagttacaaacaac		
6	tctaacctaggatggtgagcaag	ccgggagcagatcctatatacac	**1283**

Table 5: sgRNA sequences targeting VV loci for insertion of transgenes

sgRNA target gene	Sequence (excluding PAM)
B8R	gagaattataatatatctca
J2R (TK)	tgttgaattctgtgagcgta
A56R	tgtatttacaatcaactctg

References

1 Luo, Q. & Smith, D. P. Global cancer burden: progress, projections, and challenges. *The Lancet* **406**, 1536-1537 (2025). https://doi.org:10.1016/S0140-6736(25)01570-3

2 Brenner, D. R. *et al.* Projected estimates of cancer in Canada in 2022. *Cmaj* **194**, E601-e607 (2022). https://doi.org:10.1503/cmaj.212097

3 Hanahan, D. Hallmarks of cancer—Then and now, and beyond. *Cell* **189**, 2254-2277 (2026). https://doi.org:10.1016/j.cell.2025.12.049

4 Kaviarasan, V., Ragunath, B. & Veerabathiran, R. in *Oncogenic Viruses* (ed Moulay Mustapha Ennaji) 61-80 (Academic Press, 2023).

5 Robert, J., De Jesús Andino, F., Banach, M., Hyoe Rhoo, K. & Edholm, E.-S. in *Ecology and Evolution of Cancer* (eds Beata Ujvari, Benjamin Roche, & Frédéric Thomas) 119-135 (Academic Press, 2017).

6 Tufail, M., Jiang, C.-H. & Li, N. Immune evasion in cancer: mechanisms and cutting-edge therapeutic approaches. *Signal Transduction and Targeted Therapy* **10**, 227 (2025). https://doi.org:10.1038/s41392-025-02280-1

7 Ostrand-Rosenberg, S. & Sinha, P. Myeloid-derived suppressor cells: linking inflammation and cancer. *J Immunol* **182**, 4499-4506 (2009). https://doi.org:10.4049/jimmunol.0802740

8 Beury, D. W. *et al.* Cross-talk among myeloid-derived suppressor cells, macrophages, and tumor cells impacts the inflammatory milieu of solid tumors. *J Leukoc Biol* **96**, 1109-1118 (2014). https://doi.org:10.1189/jlb.3A0414-210R

9 Etxeberria, I. *et al.* Engineering bionic T cells: signal 1, signal 2, signal 3, reprogramming and the removal of inhibitory mechanisms. *Cell Mol Immunol* **17**, 576-586 (2020). https://doi.org:10.1038/s41423-020-0464-1

10 Hossen, M. M. *et al.* Current understanding of CTLA-4: from mechanism to autoimmune diseases. *Frontiers in Immunology* **Volume 14 - 2023** (2023). https://doi.org:10.3389/fimmu.2023.1198365

11 Xu, Y., Xiong, J., Sun, X. & Gao, H. Targeted nanomedicines remodeling immunosuppressive tumor microenvironment for enhanced cancer immunotherapy. *Acta Pharmaceutica Sinica B* **12**, 4327-4347 (2022). https://doi.org:https://doi.org/10.1016/j.apsb.2022.11.001

12 Hanahan, D. Hallmarks of Cancer: New Dimensions. *Cancer Discov* **12**, 31-46 (2022). https://doi.org:10.1158/2159-8290.Cd-21-1059

13 Ashworth, A., Lord, Christopher J. & Reis-Filho, Jorge S. Genetic Interactions in Cancer Progression and Treatment. *Cell* **145**, 30-38 (2011). https://doi.org:https://doi.org/10.1016/j.cell.2011.03.020

14 Lane, D. P. p53, guardian of the genome. *Nature* **358**, 15-16 (1992). https://doi.org:10.1038/358015a0

15 Hamzehloie, T., Mojarrad, M., Hasanzadeh Nazarabadi, M. & Shekouhi, S. The role of tumor protein 53 mutations in common human cancers and targeting the murine double minute 2-p53 interaction for cancer therapy. *Iran J Med Sci* **37**, 3-8 (2012).

16 Cruz-Gálvez, C. C., Ordaz-Favila, J. C., Villar-Calvo, V. M., Cancino-Marentes, M. E. & Bosch-Canto, V. Retinoblastoma: Review and new insights. *Front Oncol* **12**, 963780 (2022). https://doi.org:10.3389/fonc.2022.963780

17 Hanahan, D. & Weinberg, Robert A. Hallmarks of Cancer: The Next Generation. *Cell* **144**, 646-674 (2011). https://doi.org:10.1016/j.cell.2011.02.013

18 Bister, K. Discovery of oncogenes: The advent of molecular cancer research. *Proc Natl Acad Sci U S A* **112**, 15259-15260 (2015). https://doi.org:10.1073/pnas.1521145112

19 Blackadar, C. B. Historical review of the causes of cancer. *World J Clin Oncol* **7**, 54-86 (2016). https://doi.org:10.5306/wjco.v7.i1.54

20 Muijlwijk, T. *et al*. Hallmarks of a genomically distinct subclass of head and neck cancer. *Nature Communications* **15**, 9060 (2024). https://doi.org:10.1038/s41467-024-53390-3

21 Suh, Y., Amelio, I., Guerrero Urbano, T. & Tavassoli, M. Clinical update on cancer: molecular oncology of head and neck cancer. *Cell Death Dis* **5**, e1018 (2014). https://doi.org:10.1038/cddis.2013.548

22 Ruttkay-Nedecky, B. *et al*. Relevance of infection with human papillomavirus: The role of the p53 tumor suppressor protein and E6/E7 zinc finger proteins (Review). *Int J Oncol* **43**, 1754-1762 (2013). https://doi.org:10.3892/ijo.2013.2105

23 Molina, M. A., Steenbergen, R. D. M., Pumpe, A., Kenyon, A. N. & Melchers, W. J. G. HPV integration and cervical cancer: a failed evolutionary viral trait. *Trends in Molecular Medicine* **30**, 890-902 (2024). https://doi.org:10.1016/j.molmed.2024.05.009

24 Horner, S. M., DeFilippis, R. A., Manuelidis, L. & DiMaio, D. Repression of the human papillomavirus E6 gene initiates p53-dependent, telomerase-independent senescence and apoptosis in HeLa cervical carcinoma cells. *J Virol* **78**, 4063-4073 (2004). https://doi.org:10.1128/jvi.78.8.4063-4073.2004

25 Shamanna, R. A., Hoque, M., Pe'ery, T. & Mathews, M. B. Induction of p53, p21 and apoptosis by silencing the NF90/NF45 complex in human papilloma virus-transformed cervical carcinoma cells. *Oncogene* **32**, 5176-5185 (2013). https://doi.org:10.1038/onc.2012.533

26 DeFilippis, R. A., Goodwin, E. C., Wu, L. & DiMaio, D. Endogenous human papillomavirus E6 and E7 proteins differentially regulate proliferation, senescence, and apoptosis in HeLa cervical carcinoma cells. *J Virol* **77**, 1551-1563 (2003). https://doi.org:10.1128/jvi.77.2.1551-1563.2003

27 James, C. D. *et al.* Human Papillomavirus 16 E6 and E7 Synergistically Repress Innate Immune Gene Transcription. *mSphere* **5**, e00828-00819 (2020). https://doi.org:10.1128/mSphere.00828-19

28 Ruttkay-Nedecky, B. *et al.* Relevance of infection with human papillomavirus: the role of the p53 tumor suppressor protein and E6/E7 zinc finger proteins (Review). *International journal of oncology* **43 6**, 1754-1762 (2013).

29 Xu, Y. & Li, Z. CRISPR-Cas systems: Overview, innovations and applications in human disease research and gene therapy. *Comput Struct Biotechnol J* **18**, 2401-2415 (2020). https://doi.org:10.1016/j.csbj.2020.08.031

30 Ran, F. A. *et al.* Genome engineering using the CRISPR-Cas9 system. *Nat Protoc* **8**, 2281-2308 (2013). https://doi.org:10.1038/nprot.2013.143

31 Li, T. *et al.* CRISPR/Cas9 therapeutics: progress and prospects. *Signal Transduction and Targeted Therapy* **8**, 36 (2023). https://doi.org:10.1038/s41392-023-01309-7

32 Zafar, A., Khatoon, S., Khan, M. J., Abu, J. & Naeem, A. Advancements and limitations in traditional anti-cancer therapies: a comprehensive review of surgery, chemotherapy, radiation therapy, and hormonal therapy. *Discov Oncol* **16**, 607 (2025). https://doi.org:10.1007/s12672-025-02198-8

33 Fallarino, F. & Blank, C. U. Lessons from neoadjuvant immunotherapy in melanoma: understanding antitumour immunity and tumour escape. *Nature Reviews Immunology* **26**, 152-162 (2026). https://doi.org:10.1038/s41577-025-01222-w

34 Patel, K. K., Tariveranmoshabad, M., Kadu, S., Shobaki, N. & June, C. From concept to cure: The evolution of CAR-T cell therapy. *Molecular Therapy* **33**, 2123-2140 (2025). https://doi.org:10.1016/j.ymthe.2025.03.005

35 McCarthy, E. F. The toxins of William B. Coley and the treatment of bone and soft-tissue sarcomas. *Iowa Orthop J* **26**, 154-158 (2006).

36 Carlson, R. D., Flickinger, J. C., Jr. & Snook, A. E. Talkin' Toxins: From Coley's to Modern Cancer Immunotherapy. *Toxins (Basel)* **12** (2020). https://doi.org:10.3390/toxins12040241

37 Li, Z., Song, W., Rubinstein, M. & Liu, D. Recent updates in cancer immunotherapy: a comprehensive review and perspective of the 2018 China Cancer Immunotherapy Workshop in Beijing. *J Hematol Oncol* **11**, 142 (2018). https://doi.org:10.1186/s13045-018-0684-3

38 Liu, S., Sun, Q. & Ren, X. Novel strategies for cancer immunotherapy: counter-immunoediting therapy. *J Hematol Oncol* **16**, 38 (2023). https://doi.org:10.1186/s13045-023-01430-8

39 Gao, Z., Ling, X., Shi, C., Wang, Y. & Lin, A. Tumor immune checkpoints and their associated inhibitors. *J Zhejiang Univ Sci B* **23**, 823-843 (2022). https://doi.org:10.1631/jzus.B2200195

40 Sobhani, N. *et al.* CTLA-4 in Regulatory T Cells for Cancer Immunotherapy. *Cancers (Basel)* **13** (2021). https://doi.org:10.3390/cancers13061440

41 Jia, L., Zhang, Q. & Zhang, R. PD-1/PD-L1 pathway blockade works as an effective and practical therapy for cancer immunotherapy. *Cancer Biol Med* **15**, 116-123 (2018). https://doi.org:10.20892/j.issn.2095-3941.2017.0086

42 Chen, R., Johnson, J., Rezazadeh, A. & Dudek, A. Z. Tumour-infiltrating lymphocyte therapy landscape: prospects and challenges. *BMJ Oncology* **4**, e000566 (2025). https://doi.org:10.1136/bmjonc-2024-000566

43 Parums, D. V. Editorial: First Regulatory Approval for Adoptive Cell Therapy with Autologous Tumor-Infiltrating Lymphocytes (TILs) - Lifileucel (Amtagvi). *Med Sci Monit* **30**, e944927 (2024). https://doi.org:10.12659/msm.944927

44 Zugasti, I. *et al.* CAR-T cell therapy for cancer: current challenges and future directions. *Signal Transduction and Targeted Therapy* **10**, 210 (2025). https://doi.org:10.1038/s41392-025-02269-w

45 Waldman, A. D., Fritz, J. M. & Lenardo, M. J. A guide to cancer immunotherapy: from T cell basic science to clinical practice. *Nature Reviews Immunology* **20**, 651-668 (2020). https://doi.org:10.1038/s41577-020-0306-5

46 Rosa, R. *et al.* Current state of CAR-T cell therapies for solid tumors. *Med* https://doi.org:10.1016/j.medj.2026.101028

47 Collins, S. A., Shah, A. H., Ostertag, D., Kasahara, N. & Jolly, D. J. Clinical development of retroviral replicating vector Toca 511 for gene therapy of cancer. *Expert Opin Biol Ther* **21**, 1199-1214 (2021). https://doi.org:10.1080/14712598.2021.1902982

48 Xiao, D. *et al.* Oncolytic viruses: advanced strategies in cancer therapy. *Signal Transduction and Targeted Therapy* **11**, 45 (2026). https://doi.org:10.1038/s41392-025-02343-3

49 Lemos de Matos, A., Franco, L. S. & McFadden, G. Oncolytic Viruses and the Immune System: The Dynamic Duo. *Mol Ther Methods Clin Dev* **17**, 349-358 (2020). https://doi.org:10.1016/j.omtm.2020.01.001

50 Cao, G., Ding, C., Dai, J. & Qiu, X. Oncolytic virus and immunogenic cell death in cancer therapy. *Tumour Virus Research* **20**, 200333 (2025). https://doi.org:https://doi.org/10.1016/j.tvr.2025.200333

51 Palmer, N., Khakoo, S., Sanchez-Elsner, T. & Vallejo, A. F. Enhancing natural killer cell anti-tumour activity through macrophage manipulation. *Frontiers in Immunology* **Volume 16 - 2025** (2025). https://doi.org:10.3389/fimmu.2025.1656925

52 Breitbach, C. J. *et al.* Targeting Tumor Vasculature With an Oncolytic Virus. *Molecular Therapy* **19**, 886-894 (2011). https://doi.org:https://doi.org/10.1038/mt.2011.26

53 Macedo, N., Miller, D. M., Haq, R. & Kaufman, H. L. Clinical landscape of oncolytic virus research in 2020. *J Immunother Cancer* **8** (2020). https://doi.org:10.1136/jitc-2020-001486

54 Maruyama, Y. *et al.* Regulatory Issues: PMDA - Review of Sakigake Designation Products: Oncolytic Virus Therapy with Delytact Injection (Teserpaturev) for Malignant Glioma. *Oncologist* **28**, 664-670 (2023). https://doi.org:10.1093/oncolo/oyad041

55 Pelin, A., Boulton, S., Tamming, L. A., Bell, J. C. & Singaravelu, R. Engineering vaccinia virus as an immunotherapeutic battleship to overcome tumor heterogeneity. *Expert Opinion on Biological Therapy* **20**, 1083-1097 (2020). https://doi.org:10.1080/14712598.2020.1757066

56 Samson, A. *et al.* Neoadjuvant Intravenous Oncolytic Vaccinia Virus Therapy Promotes Anticancer Immunity in Patients. *Cancer Immunol Res* **10**, 745-756 (2022). https://doi.org:10.1158/2326-6066.Cir-21-0171

57 Park, A. K. *et al.* Effective combination immunotherapy using oncolytic viruses to deliver CAR targets to solid tumors. *Sci Transl Med* **12** (2020). https://doi.org:10.1126/scitranslmed.aaz1863

58 Taha, Z. *et al.* Complementary dual-virus strategy drives synthetic target and cognate T-cell engager expression for endogenous-antigen agnostic immunotherapy. *Nature Communications* **15**, 7267 (2024). https://doi.org:10.1038/s41467-024-51498-0

59 Gammon, D. B. & Evans, D. H. The 3'-to-5' exonuclease activity of vaccinia virus DNA polymerase is essential and plays a role in promoting virus genetic recombination. *J Virol* **83**, 4236-4250 (2009). https://doi.org:10.1128/jvi.02255-08

60 Greseth, M. D. & Traktman, P. The Life Cycle of the Vaccinia Virus Genome. *Annu Rev Virol* **9**, 239-259 (2022). https://doi.org:10.1146/annurev-virology-091919-104752

61 Moss, B. Genetically engineered poxviruses for recombinant gene expression, vaccination, and safety. *Proc Natl Acad Sci U S A* **93**, 11341-11348 (1996). https://doi.org:10.1073/pnas.93.21.11341

62 Stawowczyk, M., Ye, Y. & Chen, N. G. Vaccinia Virus—A Swiss Army Knife Against Cancer. *Cancers* **17**, 2324 (2025).

63 Kieser, Q., Noyce, R. S., Shenouda, M., Lin, Y. J. & Evans, D. H. Cytoplasmic factories, virus assembly, and DNA replication kinetics collectively constrain the formation of poxvirus recombinants. *PLoS One* **15**, e0228028 (2020). https://doi.org:10.1371/journal.pone.0228028

64 Howard, A. R., Senkevich, T. G. & Moss, B. Vaccinia virus A26 and A27 proteins form a stable complex tethered to mature virions by association with the A17 transmembrane protein. *J Virol* **82**, 12384-12391 (2008). https://doi.org:10.1128/jvi.01524-08

65 Roberts, K. L. & Smith, G. L. Vaccinia virus morphogenesis and dissemination. *Trends in Microbiology* **16**, 472-479 (2008). https://doi.org:10.1016/j.tim.2008.07.009

66 Laudermilch, E. & Chandran, K. MAVERICC: Marker-free Vaccinia Virus Engineering of Recombinants through in vitro CRISPR/Cas9 Cleavage. *Journal of Molecular Biology* **433**, 166896 (2021). https://doi.org:https://doi.org/10.1016/j.jmb.2021.166896

67 Evans, D. H. Poxvirus Recombination. *Pathogens* **11** (2022). https://doi.org:10.3390/pathogens11080896

68 Wyatt, L. S., Earl, P. L. & Moss, B. Generation of Recombinant Vaccinia Viruses. *Current Protocols in Protein Science* **89**, 5.13.11-15.13.18 (2017). https://doi.org:https://doi.org/10.1002/cpps.33

69 Breitbach, C. J. *et al.* Intravenous delivery of a multi-mechanistic cancer-targeted oncolytic poxvirus in humans. *Nature* **477**, 99-102 (2011). https://doi.org:10.1038/nature10358

70 Crupi, M. J. F. *et al.* Oncolytic virus driven T-cell-based combination immunotherapy platform for colorectal cancer. *Front Immunol* **13**, 1029269 (2022). https://doi.org:10.3389/fimmu.2022.1029269

71 Martin, N. T. *et al.* Engineering Rapalog-Inducible Genetic Switches Based on Split-T7 Polymerase to Regulate Oncolytic Virus-Driven Production of Tumour-Localized IL-12 for Anti-Cancer Immunotherapy. *Pharmaceuticals (Basel)* **16** (2023). https://doi.org:10.3390/ph16050709

72 Laudermilch, E. & Chandran, K. MAVERICC: Marker-free Vaccinia Virus Engineering of Recombinants through in vitro CRISPR/Cas9 Cleavage. *J Mol Biol* **433**, 166896 (2021). https://doi.org:10.1016/j.jmb.2021.166896

73 Whelan, J. T. *et al.* CRISPR-mediated rapid arming of poxvirus vectors enables facile generation of the novel immunotherapeutic STINGPOX. *Front Immunol* **13**, 1050250 (2022). https://doi.org:10.3389/fimmu.2022.1050250

74 Rezaei, R. *et al.* Antibiotic-mediated selection of randomly mutagenized and cytokine-expressing oncolytic viruses. *Nature Biomedical Engineering* **9**, 822-835 (2025). https://doi.org:10.1038/s41551-024-01259-7

75 Mirbahari, S. N. *et al.* Recent progress in combination therapy of oncolytic vaccinia virus. *Frontiers in Immunology* **Volume 15 - 2024** (2024).

76 Heo, J. *et al.* A phase II trial of JX-594, a targeted multimechanistic oncolytic vaccinia virus, followed by sorafenib in patients with advanced hepatocellular carcinoma (HCC). *Journal of Clinical Oncology* **30**, e14566-e14566 https://doi.org:10.1200/jco.2012.30.15_suppl.e14566

77 Smith, G. L. & Moss, B. Infectious poxvirus vectors have capacity for at least 25 000 base pairs of foreign DNA. *Gene* **25**, 21-28 (1983). https://doi.org:10.1016/0378-1119(83)90163-4

78 Hruby, D. E. & Ball, L. A. Mapping and identification of the vaccinia virus thymidine kinase gene. *J Virol* **43**, 403-409 (1982). https://doi.org:10.1128/jvi.43.2.403-409.1982

79 Potts, K. G. *et al.* Deletion of F4L (ribonucleotide reductase) in vaccinia virus produces a selective oncolytic virus and promotes anti-tumor immunity with superior safety in bladder cancer models. *EMBO Mol Med* **9**, 638-654 (2017). https://doi.org:10.15252/emmm.201607296

80 DeHaven, B. C., Gupta, K. & Isaacs, S. N. The vaccinia virus A56 protein: a multifunctional transmembrane glycoprotein that anchors two secreted viral proteins. *J Gen Virol* **92**, 1971-1980 (2011). https://doi.org:10.1099/vir.0.030460-0

81 Kelly, K. J. *et al.* Novel oncolytic agent GLV-1h68 is effective against malignant pleural mesothelioma. *Hum Gene Ther* **19**, 774-782 (2008). https://doi.org:10.1089/hum.2008.036

82 Verardi, P. H., Jones, L. A., Aziz, F. H., Ahmad, S. & Yilma, T. D. Vaccinia virus vectors with an inactivated gamma interferon receptor homolog gene (B8R) are attenuated In vivo without a concomitant reduction in immunogenicity. *J Virol* **75**, 11-18 (2001). https://doi.org:10.1128/jvi.75.1.11-18.2001

83 Banskota, S. *et al.* Engineered virus-like particles for efficient in vivo delivery of therapeutic proteins. *Cell* **185**, 250-265.e216 (2022). https://doi.org:https://doi.org/10.1016/j.cell.2021.12.021

84 Rein, A. Murine leukemia viruses: objects and organisms. *Adv Virol* **2011**, 403419 (2011). https://doi.org:10.1155/2011/403419

85 An, M. *et al.* Engineered virus-like particles for transient delivery of prime editor ribonucleoprotein complexes in vivo. *Nature Biotechnology* **42**, 1526-1537 (2024). https://doi.org:10.1038/s41587-023-02078-y

86 Kaczmarczyk, S. J., Sitaraman, K., Young, H. A., Hughes, S. H. & Chatterjee, D. K. Protein delivery using engineered virus-like particles. *Proc Natl Acad Sci U S A* **108**, 16998-17003 (2011). https://doi.org:10.1073/pnas.1101874108

87 Wu, D. T. & Roth, M. J. MLV based viral-like-particles for delivery of toxic proteins and nuclear transcription factors. *Biomaterials* **35**, 8416-8426 (2014). https://doi.org:10.1016/j.biomaterials.2014.06.006

88 Mangeot, P. E. *et al.* Genome editing in primary cells and in vivo using viral-derived Nanoblades loaded with Cas9-sgRNA ribonucleoproteins. *Nature Communications* **10**, 45 (2019). https://doi.org:10.1038/s41467-018-07845-z

89 Wolff, J. H. & Mikkelsen, J. G. Delivering genes with human immunodeficiency virus-derived vehicles: still state-of-the-art after 25 years. *Journal of Biomedical Science* **29**, 79 (2022). https://doi.org:10.1186/s12929-022-00865-4

90 Zufferey, R. *et al.* Self-inactivating lentivirus vector for safe and efficient in vivo gene delivery. *J Virol* **72**, 9873-9880 (1998). https://doi.org:10.1128/jvi.72.12.9873-9880.1998

91 Zufferey, R. *et al.* Self-Inactivating Lentivirus Vector for Safe and Efficient In Vivo Gene Delivery. *Journal of Virology* **72**, 9873-9880 (1998). https://doi.org:10.1128/jvi.72.12.9873-9880.1998

92 Liechtenstein, T., Perez-Janices, N. & Escors, D. Lentiviral vectors for cancer immunotherapy and clinical applications. *Cancers (Basel)* **5**, 815-837 (2013). https://doi.org:10.3390/cancers5030815

93 Deng, L., Liang, P. & Cui, H. Pseudotyped lentiviral vectors: Ready for translation into targeted cancer gene therapy? *Genes & Diseases* **10**, 1937-1955 (2023). https://doi.org:https://doi.org/10.1016/j.gendis.2022.03.007

94 Muul, L. M. *et al.* Persistence and expression of the adenosine deaminase gene for 12 years and immune reaction to gene transfer components: long-term results of the first clinical gene therapy trial. *Blood* **101**, 2563-2569 (2003). https://doi.org:10.1182/blood-2002-09-2800

95 Cavazzana-Calvo, M. *et al.* Gene Therapy of Human Severe Combined Immunodeficiency (SCID)-X1 Disease. *Science* **288**, 669-672 (2000). https://doi.org:doi:10.1126/science.288.5466.669

96 Schröder, A. R. W. *et al.* HIV-1 Integration in the Human Genome Favors Active Genes and Local Hotspots. *Cell* **110**, 521-529 (2002). https://doi.org:10.1016/S0092-8674(02)00864-4

97 Duvergé, A. & Negroni, M. Pseudotyping Lentiviral Vectors: When the Clothes Make the Virus. *Viruses* **12**, 1311 (2020).

98 Holzer, G. W., Mayrhofer, J. A., Gritschenberger, W., Dorner, F. & Falkner, F. G. Poxviral/retroviral chimeric vectors allow cytoplasmic production of transducing defective retroviral particles. *Virology* **253**, 107-114 (1999). https://doi.org:10.1006/viro.1998.9496

99 Konetschny, C., Holzer, G. W. & Falkner, F. G. Retroviral vectors produced in the cytoplasmic vaccinia virus system transduce intron-containing genes. *J Virol* **76**, 1236-1243 (2002). https://doi.org:10.1128/jvi.76.3.1236-1243.2002

100 Konetschny, C. *et al.* Generation of transduction-competent retroviral vectors by infection with a single hybrid vaccinia virus. *J Virol* **77**, 7017-7025 (2003). https://doi.org:10.1128/jvi.77.12.7017-7025.2003

101 Hertig, C., Coupar, B. E., Gould, A. R. & Boyle, D. B. Field and vaccine strains of fowlpox virus carry integrated sequences from the avian retrovirus, reticuloendotheliosis virus. *Virology* **235**, 367-376 (1997). https://doi.org:10.1006/viro.1997.8691

102 Maricarmen, G., Neelam, N., Willie, M. R. & Aly, M. F. Molecular Characterization of Reticuloendotheliosis Virus Insertions in the Genome of Field and Vaccine Strains of Fowl Poxvirus. *Avian Diseases* **47**, 343-354 (2003). https://doi.org:10.1637/0005-2086(2003)047[0343:MCORVI]2.0.CO;2

103 Carson, S., Miller, H. B. & Witherow, D. S. in *Molecular Biology Techniques (Third Edition)* (eds Susan Carson, Heather B. Miller, & D. Scott Witherow) 21-29 (Academic Press, 2012).

104 Qian, Y. *et al.* Transduction of Lentiviral Vectors and ADORA3 in HEK293T Cells Modulated in Gene Expression and Alternative Splicing. *Int J Mol Sci* **26** (2025). https://doi.org:10.3390/ijms26094431

105 Xiong, Y. *et al.* Engineered Amber-Emitting Nano Luciferase and Its Use for Immunobioluminescence Imaging In Vivo. *Journal of the American Chemical Society* **144**, 14101-14111 (2022). https://doi.org:10.1021/jacs.2c02320

106 Choi, J. G. *et al.* Lentivirus pre-packed with Cas9 protein for safer gene editing. *Gene Ther* **23**, 627-633 (2016). https://doi.org:10.1038/gt.2016.27

107 Hehmann-Titt, G., Schiffer, S., Berges, N., Melmer, G. & Barth, S. Improving the Therapeutic Potential of Human Granzyme B for Targeted Cancer Therapy. *Antibodies* **2**, 19-49 (2013).

108 Chen, M. & Qi, L. S. Repurposing CRISPR System for Transcriptional Activation. *Adv Exp Med Biol* **983**, 147-157 (2017). https://doi.org:10.1007/978-981-10-4310-9_10

109 Chen, S. T., Iida, A., Guo, L., Friedmann, T. & Yee, J. K. Generation of packaging cell lines for pseudotyped retroviral vectors of the G protein of vesicular stomatitis virus by using a modified tetracycline inducible system. *Proc Natl Acad Sci U S A* **93**, 10057-10062 (1996). https://doi.org:10.1073/pnas.93.19.10057

110 Tolonen, N., Doglio, L., Schleich, S. & Krijnse Locker, J. Vaccinia virus DNA replication occurs in endoplasmic reticulum-enclosed cytoplasmic mini-nuclei. *Mol Biol Cell* **12**, 2031-2046 (2001). https://doi.org:10.1091/mbc.12.7.2031

111 Chakrabarti, S., Sisler, J. R. & Moss, B. Compact, Synthetic, Vaccinia Virus Early/Late Promoter for Protein Expression. *BioTechniques* **23**, 1094-1097 (1997). https://doi.org:10.2144/97236st07

112 Lustig, S. *et al.* Effective post-exposure protection against lethal orthopoxviruses infection by vaccinia immune globulin involves induction of adaptive immune response. *Vaccine* **27**, 1691-1699 (2009). https://doi.org:https://doi.org/10.1016/j.vaccine.2009.01.038

113 Bell, N. M. & Lever, A. M. L. HIV Gag polyprotein: processing and early viral particle assembly. *Trends in Microbiology* **21**, 136-144 (2013). https://doi.org:https://doi.org/10.1016/j.tim.2012.11.006

114 Smith, G. L., Vanderplasschen, A. & Law, M. The formation and function of extracellular enveloped vaccinia virus. *J Gen Virol* **83**, 2915-2931 (2002). https://doi.org:10.1099/0022-1317-83-12-2915

115 Brennan, G. *et al.* Molecular Mechanisms of Poxvirus Evolution. *mBio* **14**, e0152622 (2023). https://doi.org:10.1128/mbio.01526-22

116 Ramsey-Ewing, A. & Moss, B. Restriction of vaccinia virus replication in CHO cells occurs at the stage of viral intermediate protein synthesis. *Virology* **206**, 984-993 (1995). https://doi.org:10.1006/viro.1995.1021

117 Hsiao, J.-C. *et al.* A Poxvirus Host Range Protein, CP77, Binds to a Cellular Protein, HMG20A, and Regulates Its Dissociation from the Vaccinia Virus Genome in CHO-K1 Cells. *Journal of Virology* **80**, 7714-7728 (2006). https://doi.org:10.1128/jvi.00207-06

118 Ottolino-Perry, K., Diallo, J. S., Lichty, B. D., Bell, J. C. & McCart, J. A. Intelligent design: combination therapy with oncolytic viruses. *Mol Ther* **18**, 251-263 (2010). https://doi.org:10.1038/mt.2009.283

119 Richert-Pöggeler, K. R., Franzke, K., Hipp, K. & Kleespies, R. G. Electron Microscopy Methods for Virus Diagnosis and High Resolution Analysis of Viruses. *Front Microbiol* **9**, 3255 (2018). https://doi.org:10.3389/fmicb.2018.03255

120 Griffiths, G., Roos, N., Schleich, S. & Locker, J. K. Structure and assembly of intracellular mature vaccinia virus: thin-section analyses. *J Virol* **75**, 11056-11070 (2001). https://doi.org:10.1128/jvi.75.22.11056-11070.2001

121 Hollinshead, M., Vanderplasschen, A., Smith, G. L. & Vaux, D. J. Vaccinia virus intracellular mature virions contain only one lipid membrane. *J Virol* **73**, 1503-1517 (1999). https://doi.org:10.1128/jvi.73.2.1503-1517.1999

122 Tajima, M., Nakajima, H. & Ito, Y. Electron microscopy of equine infectious anemia virus. *J Virol* **4**, 521-527 (1969). https://doi.org:10.1128/JVI.4.4.521-527.1969

123 Fuentes, D. R., Swigut, T. & Wysocka, J. Systematic perturbation of retroviral LTRs reveals widespread long-range effects on human gene regulation. *Elife* **7** (2018). https://doi.org:10.7554/eLife.35989

124 Chen, M. *et al.* Endogenous retroviral solo-LTRs in human genome. *Front Genet* **15**, 1358078 (2024). https://doi.org:10.3389/fgene.2024.1358078

125 Falkner, F. G. & Moss, B. Escherichia coli gpt gene provides dominant selection for vaccinia virus open reading frame expression vectors. *J Virol* **62**, 1849-1854 (1988). https://doi.org:10.1128/jvi.62.6.1849-1854.1988

126 Dobson, B. M. & Tscharke, D. C. Redundancy complicates the definition of essential genes for vaccinia virus. *J Gen Virol* **96**, 3326-3337 (2015). https://doi.org:10.1099/jgv.0.000266

127 Qin, L. & Evans, D. H. Genome scale patterns of recombination between coinfecting vaccinia viruses. *J Virol* **88**, 5277-5286 (2014). https://doi.org:10.1128/jvi.00022-14

128 Ma, H. & Kafri, T. A single-LTR HIV-1 vector optimized for functional genomics applications. *Mol Ther* **10**, 139-149 (2004). https://doi.org:10.1016/j.ymthe.2004.04.012

129 Maeder, M. L. *et al.* CRISPR RNA-guided activation of endogenous human genes. *Nat Methods* **10**, 977-979 (2013). https://doi.org:10.1038/nmeth.2598

130 Idres, Y. M., Lai, A. J., McMillan, N. A. J. & Idris, A. Hyperactivation of p53 using CRISPRa kills human papillomavirus-driven cervical cancer cells. *Virus Genes* **59**, 312-316 (2023). https://doi.org:10.1007/s11262-022-01960-2

131 Pal, M. & Herold, M. J. CRISPR base editing applications for identifying cancer-driving mutations. *Biochem Soc Trans* **49**, 269-280 (2021). https://doi.org:10.1042/bst20200550

132 Gehrke, J. M. *et al.* An APOBEC3A-Cas9 base editor with minimized bystander and off-target activities. *Nat Biotechnol* **36**, 977-982 (2018). https://doi.org:10.1038/nbt.4199

133 Nyberg, W. A. *et al.* In vivo site-specific engineering to reprogram T cells. *Nature* **652**, 712-721 (2026). https://doi.org:10.1038/s41586-026-10235-x

134 Schrörs, B. *et al.* MC38 colorectal tumor cell lines from two different sources display substantial differences in transcriptome, mutanome and neoantigen expression. *Front Immunol* **14**, 1102282 (2023). https://doi.org:10.3389/fimmu.2023.1102282

135 Boulton, S. *et al.* Oncolytic vaccinia virus encoding constitutively active EPAC remodels the tumor microenvironment to enhance therapeutic efficacy with chemotherapy and surgery. *J Immunother Cancer* **14** (2026). https://doi.org:10.1136/jitc-2025-013832

136 de Visser, K. E. & Joyce, J. A. The evolving tumor microenvironment: From cancer initiation to metastatic outgrowth. *Cancer Cell* **41**, 374-403 (2023). https://doi.org:10.1016/j.ccell.2023.02.016

137 Lickefett, B. *et al.* Lymphodepletion - an essential but undervalued part of the chimeric antigen receptor T-cell therapy cycle. *Front Immunol* **14**, 1303935 (2023). https://doi.org:10.3389/fimmu.2023.1303935

138 Chen, A. J., Zhang, J., Agarwal, A. & Lakdawalla, D. N. Value of Reducing Wait Times for Chimeric Antigen Receptor T-Cell Treatment: Evidence From Randomized Controlled Trial Data on Tisagenlecleucel for Diffuse Large B-Cell Lymphoma. *Value in Health* **25**, 1344-1351 (2022). https://doi.org:https://doi.org/10.1016/j.jval.2022.02.007

139 Agliardi, G., Dias, J., Rampotas, A., Garcia, J. & Roddie, C. Accelerating and optimising CAR T-cell manufacture to deliver better patient products. *The Lancet Haematology* **12**, e57-e67 (2025). https://doi.org:https://doi.org/10.1016/S2352-3026(24)00273-4

140 Kekre, N. *et al.* CLIC-01: Manufacture and distribution of non-cryopreserved CAR-T cells for patients with CD19 positive hematologic malignancies. *Front Immunol* **13**, 1074740 (2022). https://doi.org:10.3389/fimmu.2022.1074740

141 Marshall, A. In vivo CAR-Ts captivate big pharma. *Nature Biotechnology* **43**, 1893-1896 (2025). https://doi.org:10.1038/s41587-025-02955-8

142 Li, Y.-R., Zhu, Y., Halladay, T. & Yang, L. In vivo CAR engineering for immunotherapy. *Nature Reviews Immunology* **25**, 725-744 (2025). https://doi.org:10.1038/s41577-025-01174-1

143 Andorko, J. I. *et al.* Targeted In Vivo Generation of CAR T and NK Cells Utilizing an Engineered Lentiviral Vector Platform. *Blood* **142**, 763 (2023). https://doi.org:https://doi.org/10.1182/blood-2023-189087

144 Rabinowich, H., Pricop, L., Herberman, R. B. & Whiteside, T. L. Expression and function of CD7 molecule on human natural killer cells. *J Immunol* **152**, 517-526 (1994).

145 Alrehaili, M., Couto, P. S., Khalife, R. & Rafiq, Q. A. CAR-macrophages in solid tumors: promise, progress, and prospects. *npj Precision Oncology* **9**, 382 (2025). https://doi.org:10.1038/s41698-025-01170-7

146 Roerden, M. & Spranger, S. Cancer immune evasion, immunoediting and intratumour heterogeneity. *Nature Reviews Immunology* **25**, 353-369 (2025). https://doi.org:10.1038/s41577-024-01111-8

147 Garcia-Lora, A., Algarra, I. & Garrido, F. MHC class I antigens, immune surveillance, and tumor immune escape. *J Cell Physiol* **195**, 346-355 (2003). https://doi.org:10.1002/jcp.10290

148 Rodriguez, G. M. *et al.* NLRC5 elicits antitumor immunity by enhancing processing and presentation of tumor antigens to CD8(+) T lymphocytes. *Oncoimmunology* **5**, e1151593 (2016). https://doi.org:10.1080/2162402x.2016.1151593

149 McCart, J. A. *et al.* Complex interactions between the replicating oncolytic effect and the enzyme/prodrug effect of vaccinia-mediated tumor regression. *Gene Ther* **7**, 1217-1223 (2000). https://doi.org:10.1038/sj.gt.3301237

150 Frank, A. M. *et al.* Combining T-cell-specific activation and in vivo gene delivery through CD3-targeted lentiviral vectors. *Blood Adv* **4**, 5702-5715 (2020). https://doi.org:10.1182/bloodadvances.2020002229

151 Zhou, Q. *et al.* Exclusive Transduction of Human CD4+ T Cells upon Systemic Delivery of CD4-Targeted Lentiviral Vectors. *J Immunol* **195**, 2493-2501 (2015). https://doi.org:10.4049/jimmunol.1500956

152 Xu, E. J. K. *et al.* Peptide-MHC-targeted retroviruses enable in vivo expansion and gene delivery to tumor-specific T cells. *Sci Adv* **11**, eadv2331 (2025). https://doi.org:10.1126/sciadv.adv2331

153 Sadelain, M., Rivière, I. & Riddell, S. Therapeutic T cell engineering. *Nature* **545**, 423-431 (2017). https://doi.org:10.1038/nature22395

154 Alwithenani, A., Hengswat, P. & Chiocca, E. A. Oncolytic viruses as cancer therapeutics: From mechanistic insights to clinical translation. *Mol Ther* **33**, 2217-2228 (2025). https://doi.org:10.1016/j.ymthe.2025.03.035

155 Rama, A. R., Aguilera, A., Melguizo, C., Caba, O. & Prados, J. Tissue Specific Promoters in Colorectal Cancer. *Dis Markers* **2015**, 390161 (2015). https://doi.org:10.1155/2015/390161

156 Kyo, S., Takakura, M., Fujiwara, T. & Inoue, M. Understanding and exploiting hTERT promoter regulation for diagnosis and treatment of human cancers. *Cancer Sci* **99**, 1528-1538 (2008). https://doi.org:10.1111/j.1349-7006.2008.00878.x

157 Azad, T. *et al.* Synthetic virology approaches to improve the safety and efficacy of oncolytic virus therapies. *Nat Commun* **14**, 3035 (2023). https://doi.org:10.1038/s41467-023-38651-x

158 Stavrakaki, E., Everts, A., van den Hoogen, B. G. & Lamfers, M. L. M. The 16th International Oncolytic Virus Conference: Advancing oncolytic virotherapy by balancing anti-tumor and anti-viral immunity. *Molecular Therapy Oncology* **33** (2025). https://doi.org:10.1016/j.omton.2025.200950

159 Çuburu, N. *et al.* Harnessing anti-cytomegalovirus immunity for local immunotherapy against solid tumors. *Proceedings of the National Academy of Sciences* **119**, e2116738119 (2022). https://doi.org:doi:10.1073/pnas.2116738119

160 Greco, B., Doglio, M. & Casucci, M. Engineering in vivo CAR-T cells. *Nature Medicine* **32**, 1194-1195 (2026). https://doi.org:10.1038/s41591-026-04296-8

Appendix

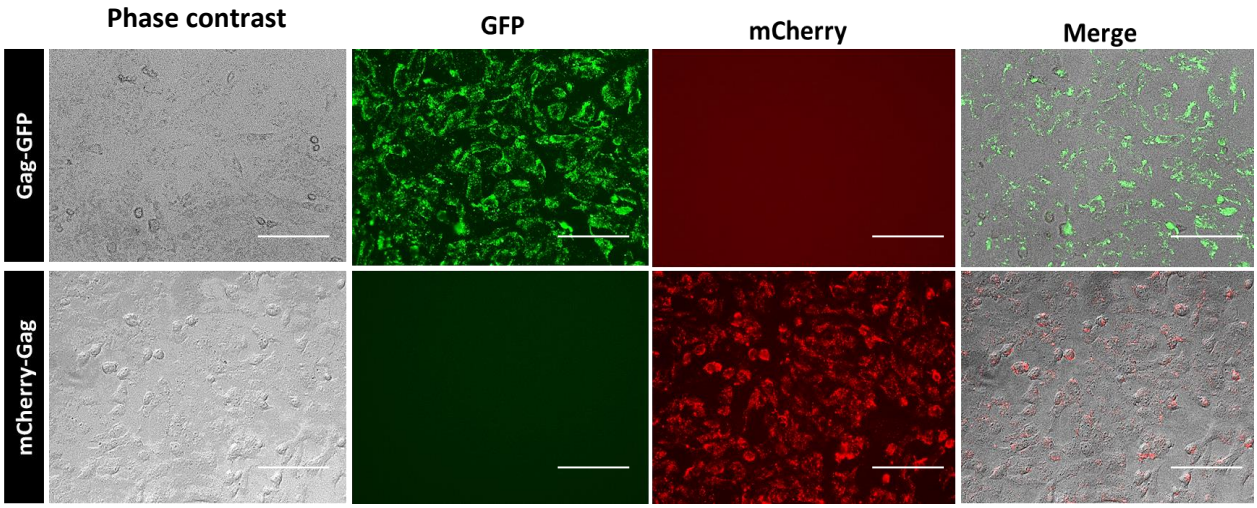

Appendix Figure 1: Evaluating VLP-mediated delivery of N or C-terminal fusion constructs. VERO cells were transduced with 100 µl of concentrated VLPs produced with Gag-eGFP or mCherry-Gag fusion constructs. Fluorescent microscopy images taken at 10X magnification by EVOS M5000 24 h post-transduction, scale bar= 150 µm.

A.

sgRNA	Probability of insertions (%)			
	A	T	C	G
E6 0	61	14.6	24.4	0
E6 1	4.1	65.4	8.7	21.7
E6 2	0	17.1	82.9	0
E6 3	5.8	83.1	4.1	6.9
E7 1	-	-	-	-
E7 2	17	3.3	79.7	0

B.

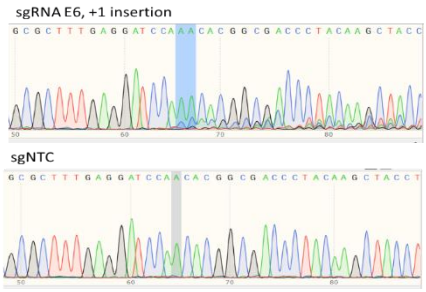

C.

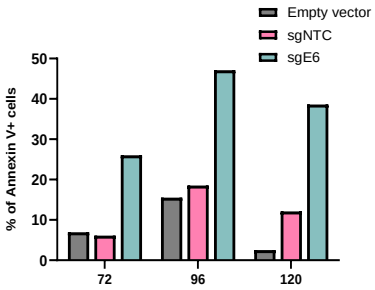

Appendix Figure 2: TIDE analysis following VLP-based CRISPR-Cas9 editing of oncogenic HPV 18 E6 or E7 in HeLa cells. A. The probability of base insertions for each candidate sgRNA. **B.** Chromatogram showing a +1 insertion of adenine (A) (shown in blue) at the editing site for candidate sgRNA E6 0 following TIDE analysis, aligning with a 61% probability of insertion shown in panel **A**. **C**. Flow cytometric assessment of Annexin-V+ cellular frequencies (%) at 72 h, 96 h or 120 h after delivery of VLPs loaded with Cas9 and sgE6 0, sgNTC or empty particles (containing Cas9 but no sgRNA).

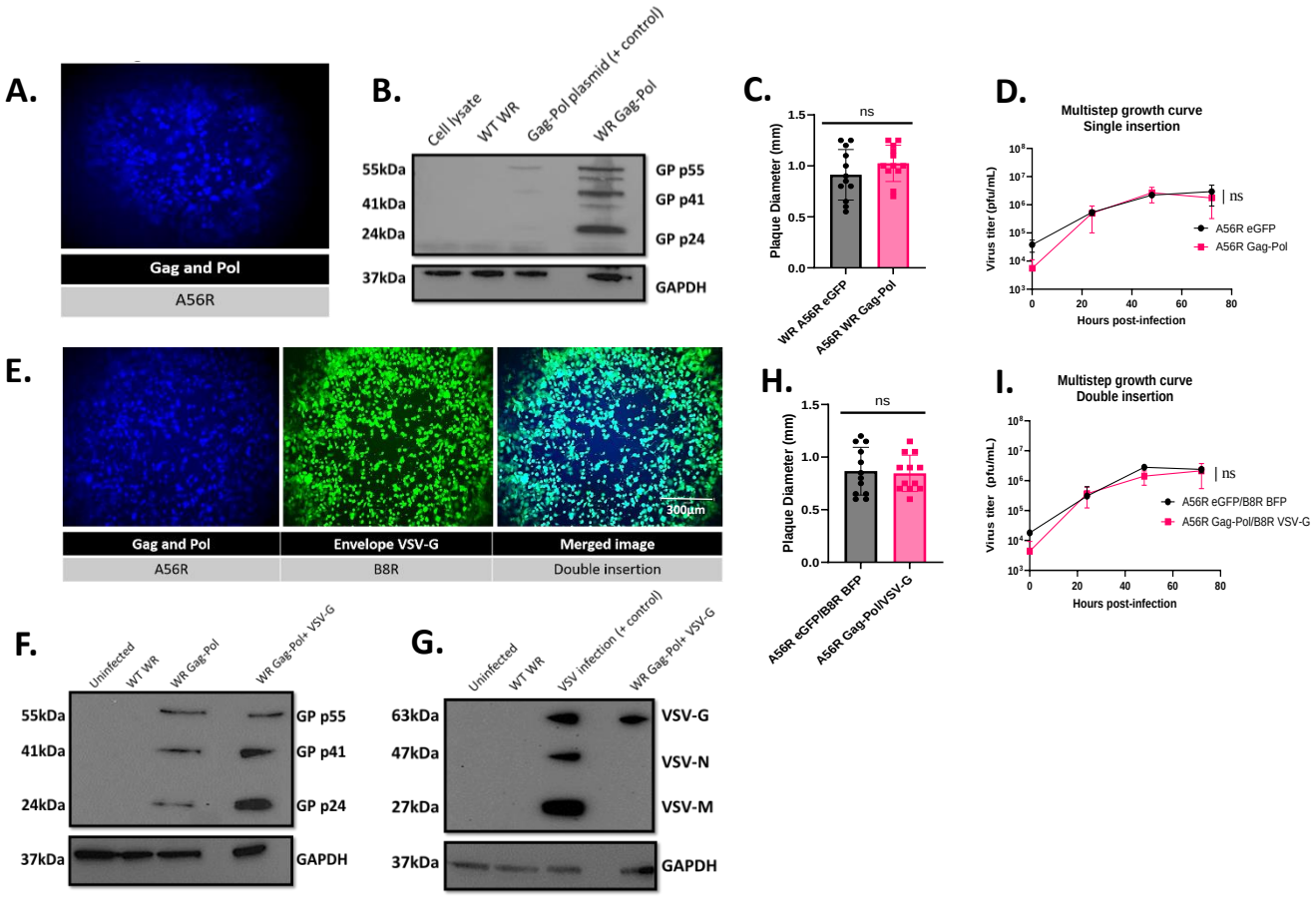

Appendix Figure 3: Generation and characterization of single and double engineered VV encoding lentiviral packaging and envelope glycoprotein components. A. Fluorescence microscopy image of a BFP expressing plaque following plaque purification to rescue VV engineered to encode Gag-Pol. **B.** Immunoblot of HIV p24 expression from whole cell lysates of U2OS cells infected with single recombinant virus. pSPAX plasmid DNA transfected into U2OS was used as positive control (lane 3). GAPDH was used as a loading control. **C.** Plaque diameters for VV encoding Gag-Pol in A56R and VV encoding BFP in A56R measured at 10X magnification 48 h post-infection (n=12). Shown is the mean ± SD, p-value computed using unpaired t-test. **D.** Multistep growth curves comparing viruses from C (n=3). Shown is the mean ± SEM, p-value computed using unpaired Student's t-test. **E.** Representative fluorescence microscopy images of BFP+ (left image) and eGFP+ (middle image) plaques 48 h post-infection following plaque purification to rescue double VV, captured at 10X magnification. Merged image shows overlapping BFP and eGFP (right image), scale bar= 300µm. **F.** Immunoblotting of HIV p24 expression from whole cell lysates of U2OS cells infected with double engineered WR. VV encoding Gag-Pol (single insertion) was used as a positive control (lane 3). GAPDH was used as a loading control. **G.** Western blot analysis of VSV-G expression from whole cell lysates of U2OS

cells infected with double recombinant VV. U2OS cells infected with VSV were used as a positive control (lane 3). GAPDH was used as a loading control. **H**. Plaque diameters of VV encoding Gag-Pol and VSV-G compared to VV encoding fluorophores in A56R and B8R, measured at 10X magnification 48 h post-infection (n=12). Shown is the mean ± SD, p-value computed using unpaired Student's t-test. **I.** Multistep growth curves comparing viruses described in H. Shown is the mean ± SEM, p-value computed using unpaired Student's t-test.

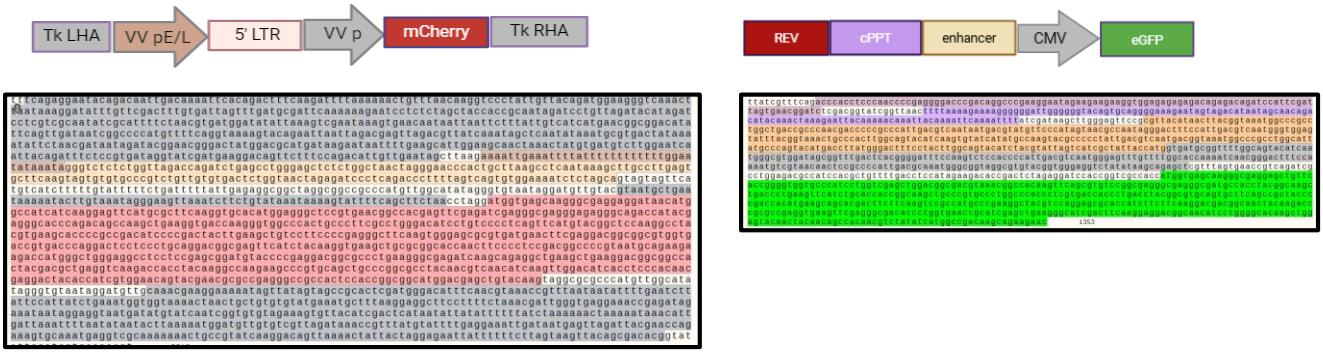

Appendix Figure 4: Sequencing of PCR amplicons to detect the presence of intact or recombined lentivirus genome from VV. Multiplexed PCR was conducted with primer pairs 1F+6R and 3F+3R. Left side shows sequencing of upper band (2265 bp amplicon). Right side shows sequencing of lower amplicon (1401 bp).

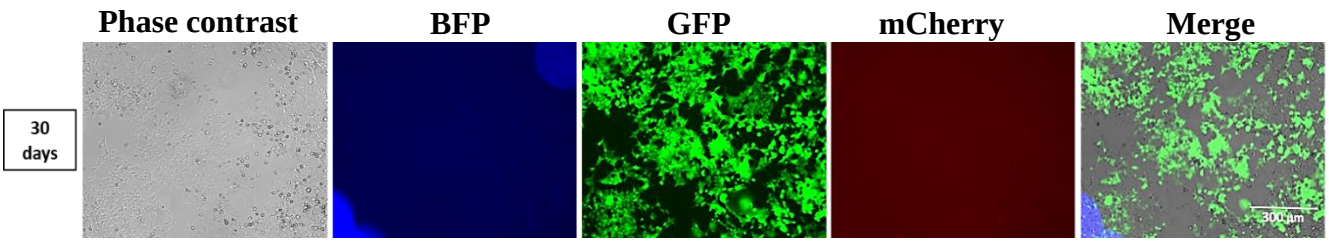

Appendix Figure 5: Production of lentivirus particles from a mixed population of VV. HEK 293T cells were transduced with eGFP encoding lentivirus particles produced from cells infected with a mixed population of VV. Following transduction, cells were subjected to puromycin selection (1 µg/mL) to enrich for successfully transduced cells. Fluorescence in the BFP and mCherry channels is shown to confirm absence of VV infection in the transduced population. Image was taken 30 days post-transduction, using EVOS M5000 at 10X magnification, scale bar= 300µm.

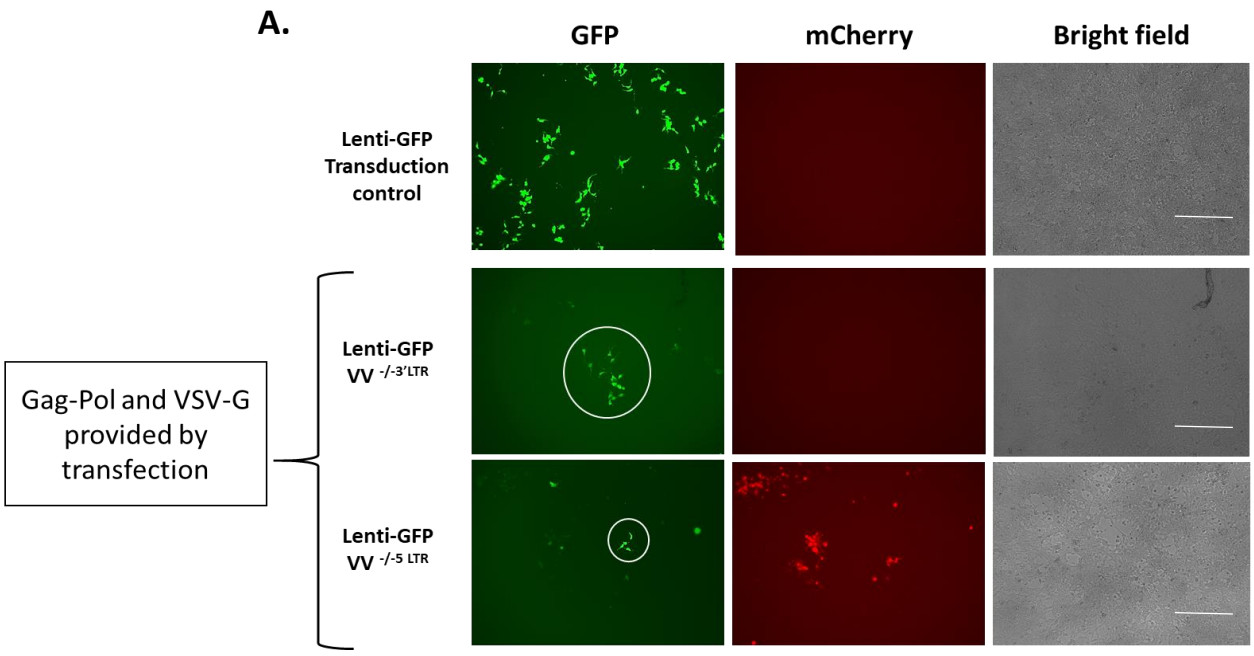

Appendix Figure 6: Solo-LTR containing vectors have potential for lentivirus production. A. HEK 293T cells were infected with VV-lenti -/-3'LTR or VV-lenti -/-5'LTR (both encoding mCherry), while Gag-Pol and VSV-G were provided by transient plasmid transfection. 48 h post-transfection, the supernatant was harvested, filtered by 0.1 µm, concentrated and used to transduce HEK 293T cells. The top most panel shows transduction of HEK 293T cells with conventionally produced lentivirus as a transduction control. In both VV-lenti -/-3'LTR or VV-lenti -/-5'LTR conditions, eGFP+ cells were observed 48 h post-transduction (circled in white). Notably, despite filtration, in the VV-/-5'LTR condition, VV escaped filtration, as seen with fluorescence in the mCherry channel. Images were acquired using EVOS M500 at 10X magnification, scale bar= 300 µm.

Curriculum Vitae

EDUCATION
PhD Candidate- Ottawa Hospital Research Institute/ University of Ottawa
Research supervisors: Dr. John Bell and Dr. Carolina Ilkow
January 2021- July 2026

- Engineered an oncolytic vaccinia virus platform to encode lentiviral vectors components, for tumor-localized transgene delivery
- Assessed transduction of lentivirus particles in mammalian cells
- Developed and optimized analytical assays to characterize viral replication and transgene expression (Fluorescense-based assays, multiplex PCR, Immunoblotting, plaque assay)

Msc. – Ottawa Hospital Research Institute/ University of Ottawa
2019-2020

- Developed and validated a retroviral-derived virus-like-particle platform for transient intracellular protein delivery with a focus on CRISPR-Cas9 for transient genome editing
- Evaluated genome editing efficiency

Bsc. McGill University- Microbiology and Immunology
2016-2019

EMPLOYMENT EXPERIENCE
Student analyst - Public Health Agency of Canada, Centre for Communicable Diseases and Infection Control
2021

Florist/Customer service representative at Les Jardins du Marché
2016

RESEARCH EXPERIENCE
Research Intern – National Research Council Canada
Supervisors: Louis-Patrick Gagnon, Dr. Joseph Schrag and Dr. Mauro Acchione
2019

- Contributed to therapeutic protein characterization within the Protein Quality Attributes and Characterization group
- Applied analytical approaches to assess protein quality
- Supported development of quality-by-design frameworks for biologics

Research Intern - Goodman Cancer Research Centre
Supervisor: Dr. Jose Teodoro
2018

- Investigated the role of GOS2 in lipid metabolism

Research Intern- HMR Research Center
Supervisor: Dr. Denis-Claude Roy
2017 and 2018

- Ex vivo T cell expansion against minor histocompatibility antigens (MiHAs)
- Identification of antigen specific T cells upon exposure to multiple MiHA peptides using Dextramer staining

AWARDS/PRIZES

1. Best poster presentation award at HMR Summer Student Research Symposium, August 2017
2. BioCanRX Summer Student Scholarship, Summer 2018, May-August, 6000$
    a. News letter feature: https://biocanrx.com/biocanrx-summer-students-tell
3. 1st place prize for best oral presentation at the Ontario Quebec Undergraduate Immunology Conference (OQUIC), May 2019, 500$
4. 2nd place prize for Human Health Therapeutics Summer Student 3MT Competition, August 2019, 50$
5. Admission Scholarship, University of Ottawa, 2019
6. MITACS Accelerate CanPRIME studentship, September 2019- September 2020
7. FRQS graduate fellowship, May 2021-May 2024, 21 000$/year
8. Judith R. Raymond scholarship in cancer research, May 2021, 5000$
9. Queen Elizabeth II Scholarship in Science and Technology, May 2021, 15 000$
10. 1st place prize for best poster presentation at 21st Annual OHRI Research Day, November 2021, 250$
11. Queen Elizabeth II Scholarship in Science and Technology, May 2022, 15 000$
12. BioCanRx Travel award, Summit 4CI, Montreal, QC (October 2022)
13. Awarded 6000$ from CIHR to host a Café Scientifique for cancer patients and their families, on behalf of the OHRI Cancer Research Program trainee committee
    a. CIHR interview feature : https://cihr-irsc.gc.ca/e/54009.html
14. Third place prize for best seminar, University of Ottawa BMI Seminar Day, February 2023, 75$
15. Top graduate poster, BioCanRx Summit4CI, October 2023, 500$
16. Second place prize for best poster presentation at 23rd Annual OHRI Research Day, November 2023, 200$
17. People's choice poster award, 23rd Annual OHRI Research Day, November 2023
18. Second place prize for best poster presentation at 24th Annual OHRI Research Day, November 2024, 200$
19. BioCanRx Travel award, Summit 4CI, Toronto, ON (April 2025)
20. Honourable mention for PhD poster category, 25th Annual OHRI Research Day, November 2025, 125$
21. BioCanRx Travel award to attend AACR Immuno-oncology conference in Los Angeles, February 2026, 1200$
22. BioCanRx Travel award, Summit 4CI, Vancouver, BC (March 2026)
23. Top graduate poster, BioCanRx Summit4CI, March 2026, 500$

LEADERSHIP, OUTREACH and VOLUNTEERING

The Ottawa Hospital Research Institute – Cancer Therapeutics program trainee committee
Graduate student member

- Organize and plan lab tours for community engagement
- Successfully awarded funding from CIHR to host Café Scientifique

Biochemistry, Microbiology and Immunology Graduate Student Association (BMI GSA)
Council Member
University of Ottawa | September 2022 – September 2023

- Represented graduate student interests and contributed to discussions regarding student initiatives and academic community engagement
- Participated in planning and supporting graduate student events and activities

Canadian Cancer Society
Research Information Outreach Team (RIOT) Volunteer
Ottawa, ON | September 2020 – September 2023

- Promoted awareness of advances in cancer research through outreach and educational initiatives
- Assisted in organizing laboratory tours for students and sponsors
- Created educational content, including short videos and blog posts related to cancer research and ongoing projects

University of Ottawa Journal of Medicine (UOJM)
Reviewer and Copy Editor
Ottawa, ON | October 2020 – December 2021

- Reviewed scientific manuscripts and provided constructive feedback on article strengths and areas for improvement
- Assisted with copy editing to ensure clarity, accuracy, and consistency in published articles

Ottawa Hospital Research Institute (OHRI)
Research Day Organizing Committee Member
Ottawa, ON | October 2019 – Present

- Contributed to planning and execution of the annual OHRI Research Day as a trainee representative
- Compiled poster and oral presentation guidelines for trainees
- Prepared trainee award presentation slideshows and coordinated with IT teams for virtual events
- Participated in monthly committee meetings to provide updates and support event organization

Let's Talk Science (LTS)
Outreach Volunteer and OSIC Judge
Ottawa, ON | September 2019 – September 2020

- Delivered hands-on science demonstrations and educational activities in elementary and high school classrooms
- Served as a judge for the Ontario Science Innovation Challenge (OSIC)
- Evaluated high school grant proposals in both English and French and assessed finalist poster presentations

National Research Council Canada (NRC)
Student Outreach Volunteer
Royalmount Campus, Montreal, QC | June 2019 – August 2019

- Guided high school students through laboratory tours and demonstrations
- Taught laboratory safety and etiquette and explained scientific techniques through interactive demonstrations
- Encouraged scientific discussion and answered student questions about research and laboratory work

Royalmount Research Day
Event Volunteer
Montreal, QC | June 2019 – August 2019

- Assisted with event setup and venue organization for annual research presentations
- Guided presenters and attendees to poster and oral presentation locations

Hôpital Maisonneuve-Rosemont
Physician Shadowing Experience
Montreal, QC | May 2018 – August 2018

- Observed clinical interactions involving leukemia and lymphoma patients
- Gained exposure to cancer therapeutics, patient examinations, and clinical healthcare practices
- Developed a deeper interest in oncology and translational medicine

McGill Campus Life and Engagement
Orientation Day Volunteer
Montreal, QC | June 2016

- Guided incoming students around campus and answered questions regarding university resources and student life
- Assisted with event setup, signage placement, and distribution of food items during orientation activities

Lakeshore General Hospital
Volunteer
Montreal, QC | June 2015 – August 2015

- Assisted with food preparation and service in the hospital coffee shop
- Supported patient meal assistance by helping patients eat comfortably and at an appropriate pace

Multicultural Committee, John Abbott College
Student Representative (for India)
Montreal, QC | April 2015

- Represented India on the multicultural committee and collaborated with a team of five students
- Assisted with budget allocation, guest coordination, venue decoration, and event planning for multicultural activities

UNDERGRADUATE LAB MENTORSHIP

- BioCanRx funded summer student (2021), Nils Nordstrom
- BioTalent funded summer student (2022), Jamie Asselin
- Two Honours students from UOttawa Biomedical sciences program, Wagma Safi and Claudia Santos-Saenz

LIST OF PUBLICATIONS

1 **Neutrophil Plasticity is Important for Oncolytic Vaccinia Virus Therapy**, **Jaahnavi Dave*,** Stephen Boulton*, Siddharth Singh, Carolina S. Ilkow, John C. Bell
1.1 manuscript in preparation,
1.2 *co-first authorship

2 Boulton S, Singh S, Organ B, Thomas J, Rezaei R, Gill R, Vallati S, Guo Q, **Dave J,** Petryk J, De Souza CT, Austin B, He X, Gingrich A, Crupi MJF, Singaravelu R, Ilkow C, Bell JC. Oncolytic vaccinia virus encoding constitutively active EPAC remodels the tumor microenvironment to enhance therapeutic efficacy with chemotherapy and surgery. J Immunother Cancer. 2026 Jan 22;14(1):e013832. doi: 10.1136/jitc-2025-013832. PMID: 41571294; PMCID: PMC12829389.

3 Stephen Boulton, Mathieu J.F. Crupi, Siddharth Singh, Madalina E. Carter-Timofte, Taha Azad, Bailey C. Organ, Xiaohong He, Rida Gill, Serge Neault, Taylor Jamieson, **Jaahnavi Dave**, Naziia Kurmasheva, Bradley Austin, Julia Petryk, Ragunath Singaravelu, Ben Zhen Huang, Noah Franco, Kaaviya Babu, Robin J. Parks, Carolina S. Ilkow, David Olagnier, John C. Bell, Inhibition of exchange proteins directly activated by cAMP as a strategy for broad-spectrum antiviral development, Journal of Biological Chemistry, 2023

4 Surendran A, Jamalkhah M, Poutou J, Birtch R, Lawson C, **Dave J**, Crupi MJF, Mayer J, Taylor V, Petryk J, de Souza CT, Moodie N, Billingsley JL, Austin B, Cormack N, Blamey N, Rezaei R, McCloskey CW, Fekete EEF, Birdi HK, Neault S, Jamieson TR, Wylie B, Tucker S, Azad T, Vanderhyden B, Tai LH, Bell JC, Ilkow CS. Fatty acid transport protein inhibition sensitizes breast and ovarian cancers to oncolytic virus therapy *via* lipid modulation of the tumor microenvironment. Front Immunol. 2023 Mar 10;14:1099459. doi: 10.3389/fimmu.2023.1099459. PMID: 36969187; PMCID: PMC10036842.

5 Boulton S, Poutou J, Martin NT, Azad T, Singaravelu R, Crupi MJ, Jamieson T, He X, Marius R, Petryk J, de Souza CT, Austin B, Taha Z, Whelan J, Khan ST, Pelin A, Rezaei R, Surendran S, Tucker S, Brown EEF, **Dave J,** Diallo JS, Auer R, Angel JB, Cameron W, Cailhier JF, Lapointe R, Potts K, Mahoney DJ, Bell JC, Ilkow CS. Single-dose replicating poxvirus vector-based RBD vaccine drives robust humoral and T cell immune response against SARS-CoV-2 infection. Molecular Therapy. 2021 Oct 20

6 Azad T, Rezaei R, Surendran A, Singaravelu R, Boulton S, **Dave J**, Bell JC, Ilkow CS. Hippo Signaling Pathway as a Central Mediator of Receptors Tyrosine Kinases (RTKs) in Tumorigenesis. Cancers (Basel). 2020 Jul 24;12(8):2042. doi: 10.3390/cancers12082042. PMID: 32722184; PMCID: PMC7463967.

7 Azad T, Singaravelu R, Crupi MJF, Jamieson T, **Dave J,** Brown EEF, Rezaei R, Taha Z, Boulton S, Martin NT, Surendran A, Poutou J, Ghahremani M, Nouri K, Whelan JT, Duong J, Tucker S, Diallo JS, Bell JC, Ilkow CS. Implications for SARS-CoV-2 Vaccine Design: Fusion of Spike Glycoprotein Transmembrane Domain to Receptor-Binding Domain Induces Trimerization. Membranes (Basel). 2020 Aug 30;10(9):E215. doi: 10.3390/membranes10090215. PMID: 32872641.

8 Brown EEF, Rezaei R, Jamieson TR, **Dave J**, Martin NT, Singaravelu R, Crupi MJF, Boulton S, Tucker S, Duong J, Poutou J, Pelin A, Yasavoli-Sharahi H, Taha Z, Arulanandam R, Surendran A, Ghahremani M, Austin B, Matar C, Diallo JS, Bell JC, Ilkow CS, Azad T. Characterization of Critical Determinants of ACE2-SARS CoV-2 RBD Interaction. Int J Mol Sci. 2021 Feb 25;22(5):2268. doi: 10.3390/ijms22052268. PMID: 33668756; PMCID: PMC7956771.